STUDIES ON CATALYTIC HYDROGEN GENERATION FROM SODIUM BOROHYDRIDE

A thesis submitted in partial fulfillment of the requirements for the Degree of

DOCTOR OF PHILOSOPHY

By

ARSHDEEP KAUR
Registration Number: 901201002

Under the supervision of

Dr. D. Ganagacharyulu

Professor

and

Dr. Pramod K. Bajpai

Distinguised Professor

DEPARTMENT OF CHEMICAL ENGINEERING
THAPAR UNIVERSITY
PATIALA-147004, PUNJAB, INDIA

August 2017

CERTIFICATE

Certified that the thesis entitled **"Studies on catalytic hydrogen generation from sodium borohydride"** being submitted by Ms. Arshdeep Kaur for the award of Degree of **Doctor of Philosophy** to the Department of Chemical Engineering, Thapar University, Patiala (INDIA), is a record of bonafide research work carried out by her under our supervision and guidance and has fulfilled the requirements for the submission of this thesis, which to our knowledge has reached the requisite standard.

The matter embodied in the thesis has not being submitted in the part or full to any other University or Institution for the award of any degree or diploma.

(D. Gangacharyulu)
Professor
Department of Chemical Engineering
Thapar University, Patiala

(Pramod K. Bajpai)
Distinguished Professor
Department of Chemical Engineering
Thapar University, Patiala

DECLARATION

I, **Arshdeep Kaur,** hereby declare that the thesis, entitled, **"STUDIES ON CATALYTIC HYDROGEN GENERATION FROM SODIUM BOROHYDRIDE"**, submitted to the **Thapar University**, in partial fulfillment of the requirements for the award of the Degree of Doctor of Philosophy in Chemical Engineering is a record of original and independent research work done by me during the period 2013 – 2017, under the supervision and guidance of **Prof. D. Gangacharyulu**, Professor and **Prof. Pramod K. Bajpai**, Distinguished Professor, Department of Chemical Engineering, Thapar University. The work contained in this thesis has not been previously submitted to meet the requirements for a degree or diploma at this or any other higher education institution.

(Arshdeep Kaur)

Registration No: 901201002

ACKNOWLEDGEMENTS

First and foremost, praises and thanks to the God, the Almighty, for His showers of blessings to complete the research successfully.

I would like to extend my sincere gratitude to my research guides **Prof. D. Gangacharyulu**, Professor and **Prof. Pramod K. Bajpai**, Distinguished Professor, Department of Chemical Engineering, Thapar University for giving me the opportunity to carry out research and providing invaluable guidance throughout this research. Their understanding and encouragement have provided good and smooth basis for my Ph. D. tenure. Their dynamism, vision and sincerity have deeply inspired me. Without their patience, guidance and effort this work would not have been possible.

I am extremely thankful to **Dr. Raj K. Gupta**, Head, Department of Chemical Engineering, Thapar University for extending the opportunity to undertake this doctoral research.

I am also thankful to my doctoral committee members **Prof. Kulvir Singh**, Professor, School of Physics, Thapar University**, Dr. Vijaya Kumar Bulasara**, Assistant Professor, Department of Chemical Engineering and **Dr. S.K. Singh**, Assistant Professor, Department of Chemical Engineering, Thapar University for advising and guiding me right throughout my research work. I appreciate the liberal support of all the staff members of Department of Chemical Engineering, Thapar University.

I am indebted to my colleagues and friends for their constant support and help during my research. I am grateful to my father **Dr. Darshan Singh**, mother **Mrs. Ashadeep Kaur** and my whole family. Without their everlasting desire, affectionate blessings and help it would not have been possible for me to complete my studies.

I would like to greatly acknowledge the financial support from **Rajiv Gandhi Fellowship Scheme** under **University Grants Commission (UGC)**, Government of India to carry doctoral studies.

Date: 31st August, 2017

Arshdeep Kaur

(Arshdeep Kaur)

ABSTRACT

Solid-state hydrogen storage has acknowledged substantial concern as a potential for hydrogen source for portable fuel cell applications. This method involves storage of hydrogen in complex chemical hydrides. These hydrides have high hydrogen content and hydrogen can be released through several chemical pathways. Sodium borohydride ($NaBH_4$) stands out as preeminent among chemical hydrides owing to its high hydrogen storage capacity (10.8 wt%) and potentially safe operational uses. However, $NaBH_4$ hydrolysis system also suffers from some major drawbacks: variance between theoretical and practical gravimetric hydrogen storage densities, solubility of residue ($NaBO_2$ based by-products) and cost of $NaBH_4$.

This study basically focuses on reducing the gap between theoretical and experimental hydrogen storage densities that increases the overall efficiency of $NaBH_4$ based hydrogen generation (HG) system. Solubility of $NaBO_2$ is the major hindrance that repels in globalizing the use of $NaBH_4$ based HG system. Therefore, present study also highlights the analysis of residue by various characterization techniques. These techniques assist in determining various reactions that could occur in the system and that effect hydrogen generation rate (HGR). Considering the cost of $NaBH_4$, this work is based on combining $NaBH_4$ with appropriate catalyst promoter that additionally promotes HGR of the system. This combined dual-solid-fuel system is highly efficient in terms of hydrogen storage capacities compared with single hydride based system. It effectively decreases the use of $NaBH_4$ and reduces its cost.

Kinetics of $NaBH_4$ hydrolysis reaction without addition of catalyst is poor and slow therefore an appropriate catalyst is required to improve the reaction kinetics. Consequently, after the selection of catalyst, parameters that affect the rate of reaction like concentrations of all the reactants and temperature are studied and kinetic parameters are determined. Therefore, in the present work detailed kinetic study is carried out on two hydrogen generation systems (with and without addition of catalyst promoter).

Cobalt chloride hexahydrate ($CoCl_2.6H_2O$) is chosen as a most efficient and low cost catalyst for $NaBH_4/H_2O$ system, compared with various platinum and ruthenium based catalysts that are not suitable for long term use due to the cost issues. Moreover, strong cationic charge on cobalt and high solubility of chlorine are the reasons behind high reactivity of $CoCl_2$ for $NaBH_4$ hydrolysis as compared to other Co based salts.

The reaction rate of $NaBH_4$ hydrolysis is affected by the concentrations of reactant ($NaBH_4$), stabilizer (NaOH), catalyst ($CoCl_2.6H_2O$) and reaction temperature. All these factors are observed and it is concluded that HGR increases with increase concentration of each factor. After observing these parameters, the kinetic studies are performed using power law kinetic model. The order and individual rate constants for each reactant are calculated. HGR is also investigated at different temperatures (293, 303, 313 and 323 K) using Arrhenius equation, at constant $NaBH_4$ (1.25 moles/L), NaOH (1.6 moles/L) and $CoCl_2$ (0.02 moles/L) concentrations. The activation energy is calculated for this system is 46 kJ/moles.

Hydrogen generation densities at different $NaBH_4$ concentrations are compared. For example, experimental hydrogen density of 7.9 wt% and theoretical hydrogen density of 10.8 wt% is observed for $NaBH_4$ at room temperature and atmospheric pressure. The overall efficiency at this $NaBH_4$ concentration is 73%. It is observed that experimental hydrogen density is quite lower as compared to the theoretical one. Thus, to make the system more competent and proficient improvement in terms of overall efficiency is required. The next section of the work deals with addition of catalyst promoter in the solution to increase the overall efficiency of the system.

The concept to enhance hydrogen storage densities through coupling reactions or by using dual-solids for hydrogen generation is further studied in this work. Various catalyst promoting materials like γ-Al_2O_3 nanoparticles, γ-Al_2O_3 particles, CNT, MMT clay, SiO_2, zeolite and zirconia sand are compared with respect to hydrogen generation rate (HGR). Maximum HGR is obtained on addition of Al_2O_3 nanoparticles (20 nm) in $NaBH_4/H_2O$ system with $CoCl_2$ as catalyst. Maximum HGR obtained is 19.47 moles/L.sec for $NaBH_4$ (1.26 moles/L), Al_2O_3 nanoparticles (0.12 moles/L) and $CoCl_2.6H_2O$ (0.02 moles/L) as catalyst at room temperature and atmospheric pressure. Due to the high surface to volume ratio of alumina nanoparticles hydrogen desorption rates are enhanced from the reactants. Additionally, owing to reactive nature of alumina nanoparticles and its hydrophilic and amphoteric nature, it is selected as catalyst promoter for $NaBH_4$/ H_2O based HG system.

For $NaBH_4$/γ-Al_2O_3 nanoparticles/H_2O based HG system, various catalysts like $CoCl_2.6H_2O$, $CoSO_4.7H_2O$, $(CH_3COO)_2Co.4H_2O$, $Co(NO_3)_2.H_2O$, $CdSO_4$ and $CuSO_4.5H_2O$ are evaluated in terms of HG and HGR. Following order for maximum and overall HGR is observed: $CoCl_2.6H_2O$ > $CoSO_4.7H_2O$ > $(CH_3COO)_2Co.4H_2O$ > $Co(NO_3)_2.H_2O$ for $NaBH_4$ (1.26 moles/L)/Al_2O_3 nanoparticles (0.12 moles/L)/H_2O and catalyst (0.02 moles/L) at room temperature and atmospheric pressure. Nil amount of hydrogen evolved with $CdSO_4$ and

$CuSO_4.5H_2O$. Comparative studies are also performed between γ-Al_2O_3 (100-200 μm) and γ-Al_2O_3 (20 nm) to observe the difference in hydrogen generation (HG) with respect to particle size.

Higher HG is observed with γ-Al_2O_3 having particle size of 20 nm than γ-Al_2O_3 having particle size of 100-200 μm, therefore, it is selected as promoter for the present $NaBH_4/H_2O$ system with $CoCl_2$ as catalyst.

Hydrogen generation rate is monitored with change in concentration of $NaBH_4$, γ-Al_2O_3 nanoparticles, $CoCl_2$ and NaOH. It is concluded that hydrogen generation rate increases with increases in NaOH, Al_2O_3, $NaBH_4$ and $CoCl_2$ concentrations. After observing each parameter individually, the order for each component is calculated.

Hydrogen generation rate is investigated at different temperatures (303, 313, 323 and 333 K) for constant $NaBH_4$ (1.25 moles/L), NaOH (1.4 moles/L), $CoCl_2$ (0.02 moles/L) and Al_2O_3 (0.09 moles/L) concentrations. Thus activation energy is calculated is 29 kJ/moles and A is 18.62×10^8 $(sec)^{-1}(L/moles)^{2.15}$. This value is less than activation energy calculated for $NaBH_4/H_2O$ system without addition of γ-Al_2O_3 nanoparticles.

Maximum hydrogen generation efficiencies are calculated at different mass ratios of $Al_2O_3/NaBH_4$. Very high efficiency of 99.34% is achieved at mass ratio of 0.09 : 0.7 for Al_2O_3 : $NaBH_4$ with theoretical hydrogen density of 10.76 wt% and experimental hydrogen density of 10.69 wt%. Therefore, it is observed that efficiency with addition of γ-Al_2O_3 nanoparticles is higher compared with the efficiency of previous HG ($NaBH_4/H_2O$) system.

The residue obtained from the optimum system consisting of $NaBH_4$ (1.26 moles/L), Al_2O_3 (0.12 moles/L), NaOH (0.93 moles/L), and $CoCl_2$ aqueous solution (0.02 moles/L) is analyzed. The residue is characterized using EDS, XRD and FTIR to predict the possible reactions that could occur between different reactants.

The work is extensive study of two different HG systems ($NaBH_4$/γ-Al_2O_3 nanoparticles/H_2O & $NaBH_4/H_2O$) including optimization of catalyst, operating parameters followed by kinetic studies and analysis of residue obtained of both the HG systems. On account of HGR, activation energy and efficiency, $NaBH_4$/γ-Al_2O_3 nanoparticles/H_2O based HG system with $CoCl_2$ as catalyst is better than $NaBH_4/H_2O$ based hydrogen generation and therefore, it can be considered as an efficient system to be used in practical application for hydrogen generation and storage.

TABLE OF CONTENTS

LIST OF FIGURES

LIST OF TABLES

LIST OF SYMBOLS

Item	Item Description	Unit
A	Pre exponential factor	$(sec)^{-1}$
A	Order with respect to $NaBH_4$	-
BH_4^-	Borohydride ions	-
B	Order with respect to $CoCl_2$	-
b_1	Order with respect to Al_2O_3	-
Co_xB	Cobalt boride species	-
$[CoCl_2]$	Concentration of cobalt chloride	moles/L
C	Order with respect to NaOH	-
E	Activation energy	kJ/moles
H	Hydrogen atoms	-
H_2	Hydrogen molecules	-
$H^{\delta-}$	Ionic form of hydride	-
k_1	Rate constant with respect to $NaBH_4$	-
k_2	Rate constant with respect to $CoCl_2$	-
k_3	Rate constant with respect to NaOH	-
k_a	Rate constant with respect to Al_2O_3	-
$k_{overall}$	Overall hydrogen generation rate constant	-
R	Universal gas constant	J/(moles.K)
$r_{H_2[NaBH_4]}$	Rate of hydrogen generation with $NaBH_4$	moles/(L.sec)
$r_{H_2[CoCl_2]}$	Rate of hydrogen generation with $CoCl_2$	moles/(L.sec)
$r_{H_2[NaOH]}$	Rate of hydrogen generation with NaOH	moles/(L.sec)
$r_{H_2[Al_2O_3]}$	Rate of hydrogen generation with Al_2O_3	moles/(L.sec)
T	Absolute temperature	Kelvin

LIST OF ABBREVIATIONS

Abbreviations	Item Description
CNT	Carbon nano tubes
FTIR	Fourier transform infrared spectroscopy
GHSC	Gravimetric hydrogen storage capacity
HG	Hydrogen generation
HGR	Hydrogen generation rate
MOF’s	Metal organic frameworks
N–H	Nitrogen and hydrogen bonding
NTP	Normal temperature and pressure
SB	Sodium borohydride
SDD	Silicon drift detector
SEM	Scanning electron microscopy
STP	Standard temperature and pressure
TCD	Thermal conductivity detector
XRD	X-ray diffraction

CHAPTER 1

Introduction

Extensive use of fossil fuels has given rise to major climatic concern that is liberation of carbon dioxide in to the atmosphere thus imposing adverse climatic effect which may impose serious health concerns to mankind. Additionally, probable reduction in availability of fossil energy sources is expected due to expansion of world's population and industrialization by 75% in the next 20-30 years (Ley et al., 2014).

Hydrogen (H_2) has a great potential as an energy carrier, specifically as fuel for fuel cell applications. It is environmental friendly, regenerative fuel with very high calorific value. It has energy density of 142 MJ/kg that is three times higher than petroleum (47 MJ/kg). Therefore, hydrogen is probable source to replace petroleum from its vehicular and other applications as it can form higher efficiency fuel cells than combustion engines. The hydrogen based economy gives the vision to present era to reach all the global energy demands and reduce the reliability on fossil fuels, thus moving towards clean and green future (Muir and Yao, 2011) and has the potential to substitute the present energy dependency on fossil fuels. Carbon cycle (blue arrows) hydrocarbons undergo combustion and the process is energy consuming as shown in Figure 1.1. CO_2 produced after the reaction is released into the atmosphere that causes global warming (black arrow). Green arrows present hydrogen cycle that present green and renewable energy source.

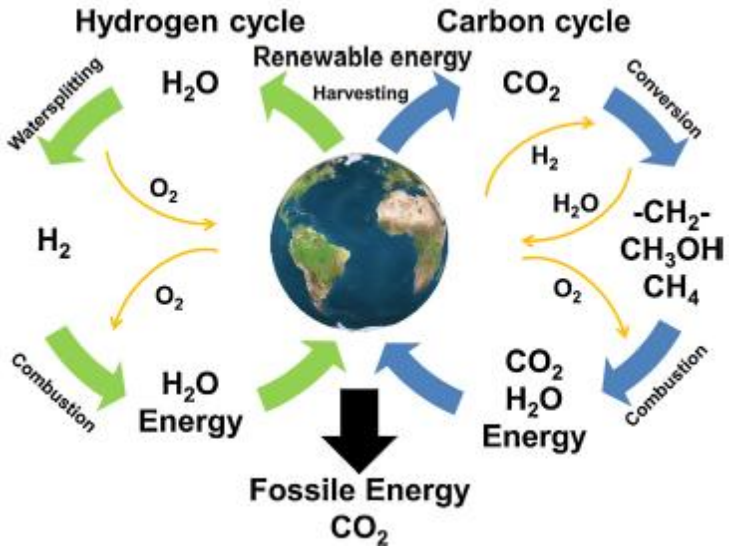

Figure 1.1: Carbon cycle and hydrogen cycle (Muir and Yao, 2011)

Hydrogen energy is also been projected as extensive resolution for a secure energy future for increasing energy security and strengthening the developing countries economy (Alfonso et al., 2009). Before the ultimate implementation of hydrogen as clean source of fuel and the transition from carbon based fossil fuel energy system to hydrogen based economy, it involves various technological, significant scientific and economic barriers (Shashikala, 2012).

In transportation sector, hydrogen storage technologies must be highly efficient. Many advances in hydrogen production and storage have been made and implemented (Shang and Chen, 2006). High volumetric and gravimetric storage capacity, good mechanical, thermal stability and cost of operating system are few criteria for hydrogen storage (Shashikala, 2012).

1.1. Hydrogen storage methods

There are three conventional ways to store hydrogen as these are (i) in the form of compressed gas, (ii) as cryogenic liquid hydrogen (LH_2) and (iii) solid-state hydrogen storage.

1.1.1. Compressed hydrogen storage

Hydrogen can be stored in the form of compressed gas at high pressures of 150-200 atm. Special hydrogen cylinders like carbon fiber reinforced cylinders are available to withstand very high pressures up to 700 atm. Compressed hydrogen storage technique deals with low volumetric density of hydrogen, high pressure requirements, weight of cylinder and energy required to compress hydrogen adds cost to the whole process.

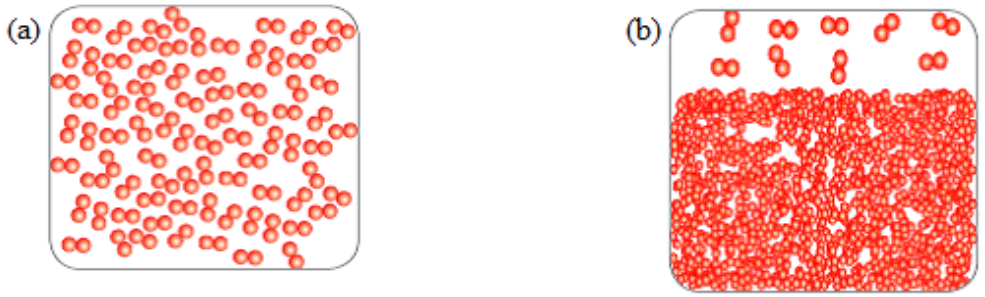

Compressed hydrogen gas

Hydrogen gas in the form of cryogenic liquid

Figure 1.2 (a & b): Compressed hydrogen gas storage and cryo-compressed hydrogen gas storage (Sakintuna et al., 2007)

As a solution, volumetric storage capacity could be further increased by cryo-compressed hydrogen storage that is by cooling the hydrogen gas to −253°C. By cryo-compressed technique, volumetric capacity could be increased by factor of four. This system deals with energy requirement to compress and liquefy hydrogen gas, making the process energy intensive. Liquid hydrogen is highly volatile and evaporated hydrogen gas could form an explosive mixture with air. Hence, the main drawback of these methods is the low volume density of the system and sophisticated technologies with various safety concerns (Sakintuna et al., 2007). Hydrogen molecules in form of compressed gas and cryogenic liquid are shown in Figure 1.2 (a & b).

1.1.2. Material based hydrogen storage

There are three general mechanisms known for storing hydrogen in materials: absorption, adsorption and chemical reaction. Hydrogen is stored on the surfaces of solids by adsorption and within solids by absorption as shown in Figure 1.3 (a & b). Density of hydrogen increases in moving from adsorption to absorption. Adsorption may be subdivided into physisorption and chemisorption, based on the adsorption mechanism. In this phenomenon, hydrogen attaches to the surface of a material either as hydrogen molecules (H_2) or hydrogen atoms (H). Physisorbed hydrogen is more weakly energetically bound to the material than is chemisorbed hydrogen. These processes usually require highly porous materials to maximize the surface area available for hydrogen adsorption to occur and to allow easy uptake and release of hydrogen from the material. Example for material based hydrogen storage with adsorption phenomenon is metal hydrides hydrogen storage.

Surface adsorption Surface absorption

Figure 1.3 (a & b): Surface adsorption hydrogen bonding and surface absorption hydrogen bonding (Klanchar et al., 2004)

In absorption, hydrogen molecules detach into hydrogen atoms that are included into the solid lattice framework. With this method it is possible to store larger quantities of hydrogen in smaller volumes at low pressure and temperatures. In absorptive hydrogen storage, hydrogen

is absorbed directly into the bulk of the material. Example of material based hydrogen storage with absorption phenomenon is complex and chemical hydrides (Klanchar et al., 2004).

1.2. Chemical hydrogen storage pathway

Storage technology in which hydrogen is generated or released through a chemical reaction defines the term chemical hydrogen storage. Common reactions involve chemical hydrides with water or alcohols. Typically, these reactions are not easily reversible on-board a vehicle. Hence, the spent fuel and byproducts must be removed from the vehicle and regenerated off-board. Hydrogen is strongly bound within molecular structures in chemical compounds containing hydrogen atoms as shown in Figure 1.4 (a & b). Thus, the chemical reaction path for hydrogen storage involves chemical reactions for both hydrogen generation and hydrogen storage (Klanchar and Lloyd, 2000).

Figure 1.4 (a & b): Absorption of hydrogen molecules in complex chemical hydrides (Klanchar and Lloyd, 2000)

As reported by Klanchar et al. (2004) solid state or material based hydrogen storage involves storing hydrogen in complex chemical hydrides. These hydrides have high gravimetric and volumetric densities and hydrogen can be released with chemical reactions. In addition, hydrolysis of chemical hydrides takes place at relatively low temperatures and gives promising theoretical hydrogen storage efficiencies. Some familiar chemical hydride materials are sodium hydride (NaH), lithium hydride (LiH), magnesium hydride (MgH_2), calcium hydride (CaH_2), titanium hydride (TiH_2) and complex chemical hydride materials are lithium aluminum hydride ($LiAlH_4$), sodium borohydride ($NaBH_4$) and lithium borohydride ($LiBH_4$).

Volumetric hydrogen densities for various methods of hydrogen storage are shown in Figure 1.5. Lowest density is observed for pressurized hydrogen storage methods. In metal organic frameworks (MOFs), hydrogen is weekly bonded on the surface of material by physisorption. In complex chemical hydrides like $LiBH_4$, $NaAlH_4$, $LiAlH_4$, $NaBH_4$ and chemical hydride

AlH_3, hydrogen is strongly bonded via chemical bond to the material. As shown, hydrogen bonded through chemical hydrides has higher volumetric hydrogen density (Garetz, 2012).

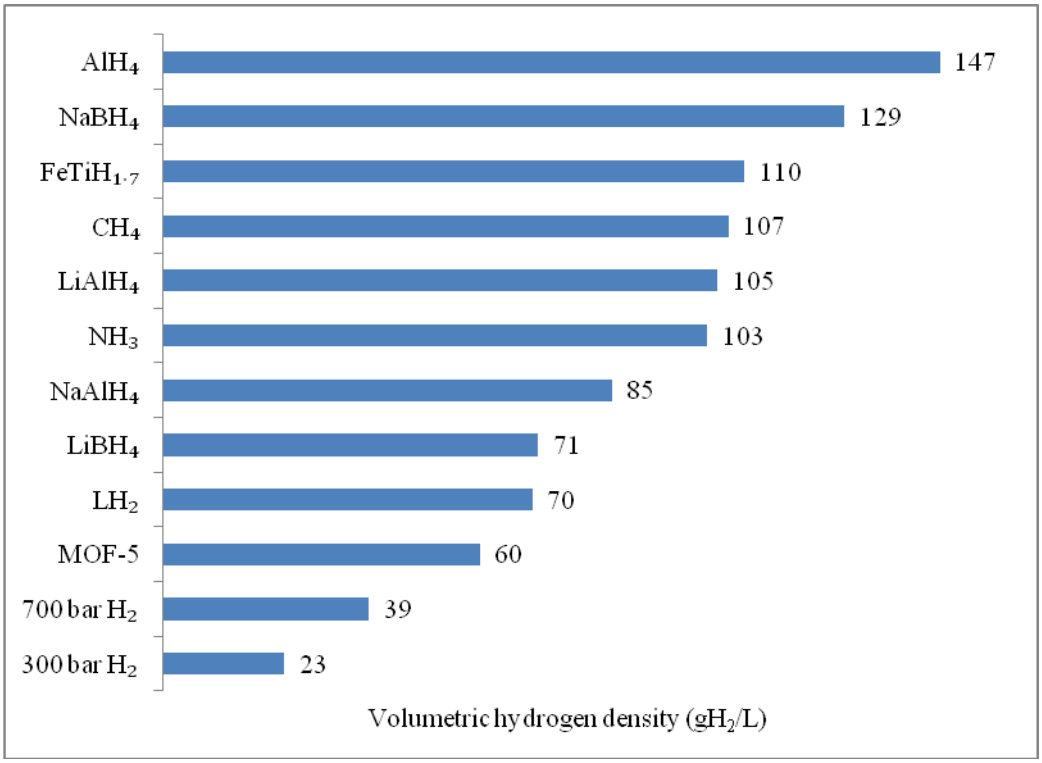

Figure 1.5: Volumetric hydrogen density of variety of hydrogen storage methods (Garetz, 2012).

Among above chemical hydrides, sodium borohydride ($NaBH_4$) has been considered as the most attractive hydrogen storage material, as it provides a safe and practical mean of producing hydrogen and has high hydrogen content. It undergoes hydrolysis reaction like other hydrides and forms the byproduct sodium metaborate ($NaBO_2$). By dissolving sodium borohydride in a basic solution, a highly stable aqueous solution is formed and further in $NaBH_4$ hydrolysis reaction hydrogen release could be initiated with active catalyst. Reaction stoichiometry states that 1g of $NaBH_4$ solution will produce 2.4 L of hydrogen at normal temperature and pressure (NTP). On this basis, it gives gravimetric storage capacity of 10.8 wt%. Moreover, storing hydrogen in the form of aqueous solutions has many advantages.

Hydrogen with $NaBH_4$ could be released at ambient conditions, thus increasing its application for portable fuel cells. Sodium borohydride based hydrogen storage is compared with other chemical hydrides are shown in Table 1.1. $NaBH_4$ based system is much safer and stable due to its low heat of hydrolysis. Millenium Cell is first portable hydrogen storage system with aqueous $NaBH_4$ solutions that stimulated the research in this field.

As the practical gravimetric hydrogen storage capacity (GHSC) of $NaBH_4$ is less than that of the theoretical GHSC (10.8 wt%), in 2007 Department of Energy (US-DOE), USA published no-go recommendation for $NaBH_4$ based hydrogen storage system (Muir and Yao, 2011).

Table 1.1: Comparison of chemical hydrides with heat of hydrolysis reaction (Demirci and Mieli, 2009)

S. No.	Name of hydride	H_2 (wt%)	% H_2 in stoichiometric mixture	Heat of hydrolysis reaction (kJ/mole H_2)
1.	$LiBH_4$	18	8.5	−90
2.	LiH	13	8	−145
3.	$NaBH_4$	10.5	7.5	−80
4.	$LiAlH_4$	10.5	7.5	−150
5.	AlH_3	10	7	−158
6.	MgH_2	7.5	6.4	−161
7.	$NaAlH_2$	7.2	6	−140
8.	CaH_2	4.9	5.1	−140
9.	NaH	4.9	4	−150

1.3. Coupling reactions

A concept to improve hydrogen storage capacities in $NaBH_4$ based hydrogen storage system is through coupling reactions, for example, $NaBH_4$/Al with cobalt-molybdenum-boron as catalyst (Zhuang et al., 2013), $NaBH_4$/Al with Al-Li-Co/$NaBH_4$ in pure water (Wang et al., 2013), $CoCl_2$ as catalyst (Dai et al., 2011), Al-Li/$NaBH_4$ mixture in water activated by nickel (Shu et al., 2012) and Al/$NaBH_4$ activated by lanthanum metal and $CoCl_2$ as catalyst (Jianbo et al., 2012). All the above hydrogen generation systems resulted in high hydrogen storage efficiencies and faster kinetic rates.

1.4. Nanoparticles for hydrogen generation

Physicochemical properties of materials change if the particle size is reduced to low nanometers range. Nanoparticle materials can improve the economics of hydride based storage systems. Due to the high surface to volume ratio of nanoparticles hydrogen desorption rates are enhanced. It reduces the hydride weight (volume per unit of stored hydrogen) thus augmenting the range of materials and enhancing the performance characteristics (Snow, 2003).

1.5. Catalyst for $NaBH_4$ hydrogen storage system

A significant research towards synthesizing an active catalyst is a step forward for development of $NaBH_4$ based on-board HG systems. Cobalt(II) chloride, nickel(II) chloride, iron(II) chloride, copper(II) chloride and manganese(II) chloride are non-noble catalysts that are investigated with time for $NaBH_4$ hydrolysis. Out of all above, cobalt(II) chloride is found to be highly active. Besides this, noble metal catalysts like ruthenium and platinum with different supporting materials as platinum loaded on $LiCoO_2$ or ruthenium loaded on TiO_2 are also studied. Due to cost factors, it is not feasible to make use of noble metal catalysts for widespread applications in hydrogen storage systems (Muir and Yao, 2011).

1.6. Continuous flow hydrogen generation system for hydrogen storage and generation applications

Continuous flow hydrogen generation system as reported by Demirci and Miele (2009) is shown in Figure 1.6.

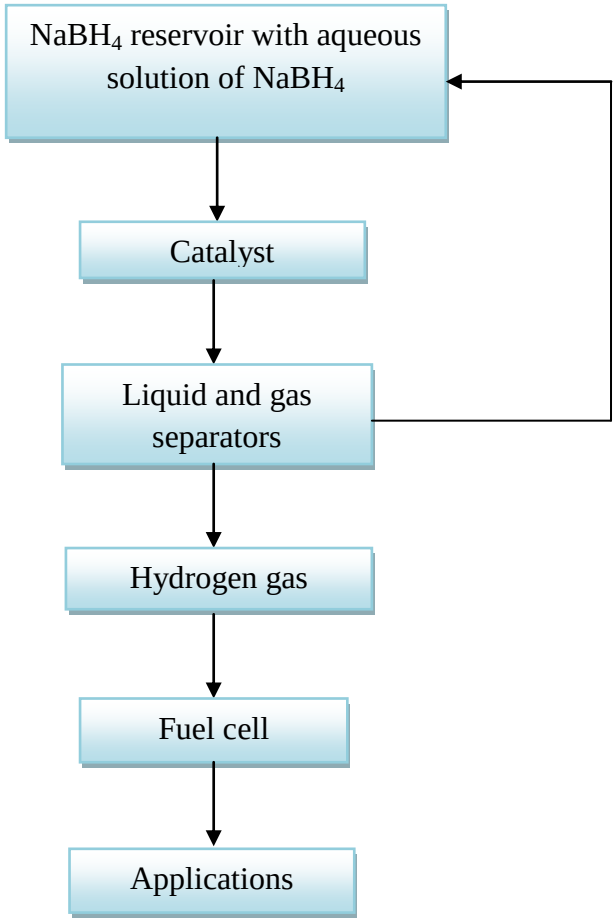

Figure 1.6: Continuous flow hydrogen generation system

Liquid reservoir containing aqueous solution of $NaBH_4$ is supplied with the catalyst for the reaction. The solution is fed to the liquid and gas separator from which pure hydrogen gas is recovered. The pure hydrogen gas is fed to the fuel cell for further applications. The byproduct after recycling is again sent to the liquid reservoir so that could be used again.

1.7. Scope of work

It has been found that storing and delivering pure H_2 gas is major technological challenge and conventional hydrogen storage methods deals with various safety concerns therefore, could not be considered for long term H_2 storage technique. Recently developed technologies include material based H_2 storage like chemical hydrides. Of all the chemical hydride materials $NaBH_4$ is most probable hydrogen storage material due to high H_2 storage capacities.

The scope of the work is to couple $NaBH_4$ with other credible H_2 storage material for high H_2 storage densities. Recently many materials are coupled with $NaBH_4$ like Si, clay, CNT, Al or Al_2O_3 etc. that enhances the overall efficiency of the system. We aim to find the most suitable and effective H_2 storage material to pair with $NaBH_4$ for high hydrogen generates rate, efficient H_2 storage and generation system.

CHAPTER 2

Literature Review

2.1. Introduction

Technologies for hydrogen storage should be considerably advanced if hydrogen based energy system, particularly in the transportation sector is to be established (Marrero et al., 2009). Storing hydrogen is relatively difficult because of its low density and critical temperature. As discussed in Chapter 1, there are three ways to store hydrogen; (a) compressed gas, (b) cryogenic liquid hydrogen (LH_2) and (c) solid-state hydrogen storage (Moussa et al., 2013 and Eberle et al., 2009). The main disadvantage of compressed gas and cryogenic liquid hydrogen storage is low volumetric density of the system. Hydrogen can only be stored in pressurized form (up to 700 bar) or cryo-compressed form (−253°C). Various safety concerns and sophisticated technologies are required to adopt this method of hydrogen storage. Many novel concepts of hydrogen storage had emerged in past decades like chemical hydrogen storage or material based hydrogen storage (Demirci and Miele, 2009). Solid-state hydrogen storage involves storage of hydrogen in complex chemical hydrides. These hydrides have high hydrogen content and hydrogen can be released through several chemical pathways. Hydrolysis of chemical hydrides takes place at comparatively moderate temperatures and gives promising theoretical hydrogen storage efficiencies (Sakintuna et al., 2007 & Demirci and Mieli, 2009).

Complex hydrides as $LiBH_4$, NH_3BH_3, $NaBH_4$ and $NaAlH_4$ have theoretical hydrogen storage densities of 18.5 wt%, 19.4 wt%, 10.8 wt% and 7.8 wt%, respectively (Ritter et al., 2003). Moreover, carbon-based materials such as single and multi-walled nanotubes, fibers and activated carbon are also widely studied as hydrogen storage materials (Dillon and Heben, 2001). Among the above given technologies, chemical hydrides are considered as most potential hydrogen storage materials. The above discussed hydrides are boron based materials with 4(B-H) bonds and hydrogen in the form of hydrides $H^{\delta-}$. The hydrogen bonded to boron in the form of hydrides is prime reason behind high hydrogen densities (Moussa et al., 2013; Akdim et al., 2011; Retnamma et al., 2011 and Ritter et al., 2003).

Recycling of the spent fuel is another area in the use of chemical hydrides as hydrogen storage material that is considered as a major drawback of this system. Thus, to build hydrogen economy based on chemical hydrides, hydrogen generation and spent fuel recycling should be taken as key areas of development (Dai et al., 2011 a).

2.2. Chemical hydrogen storage in hydrides

The term 'chemical hydrogen storage' is used to describe storage technologies in which hydrogen is generated through a chemical reaction. Hydrogen is evolved either by breaking the hydride thermally at higher temperature (thermolysis) or by reaction with water (hydrolysis).

2.2.1. Hydrogen generation by thermolysis

Hydrogen generation through thermolysis is due to change in temperature and pressure to release hydrogen. In thermolysis, rehydrogenation of hydrogen is possible but these hydrides have low hydrogen densities and hydrogen is released at high temperatures (Hordeski, 2008). Following are few chemical hydrides in which hydrogen is released through thermolysis.

Magnesium borohydride

With hydrogen content of 14.9 wt%, volumetric density 147 kg/m^3 and low enthalpy of formation 40 kJ/mole, magnesium hydride has high potential to become one of the most important hydrogen storage materials (Ronnebro, 2011 and Li et al., 2011). The disadvantage of using magnesium hydride as hydrogen storage material is that speed of hydrogen release/uptake is excessively slow and reaction operates only at higher temperatures (Hou, 2006)

Considering the above disadvantage, addition of NbF_5 improves the extent of hydrogen release as well as the kinetics of the reaction because pure $Mg(BH_4)_2$ releases hydrogen at temperature greater than 270^{o}C. Mg $(BH_4)_2$ with NbF_5 begins hydrogen release at ≈75^{o}C (Ahmad et al., 2012).

Calcium borohydride

Calcium borohydride ($Ca(BH_4)_2$) has theoretical hydrogen storage of 9.6 wt% and releases hydrogen according to the following reaction (Miwa et al., 2006),

$$Ca(BH_4)_2 \rightarrow 2/3CaH_2 + 1/3CaB_6 + 10/3H_2 \qquad (2.1)$$

Kim et al. (2008) and Mao et al. (2010) found experimentally that approximately 9.0 wt% of hydrogen is released when $Ca(BH_4)_2$ is heated to 527^{o}C. This value shows good potential of calcium hydride to store hydrogen. $Ca(BH_4)_2$ has been predicted theoretically to have limited feasibility as a reversible storage material for on-board storage due to the formation of a stable intermediate compound of $CaB_{12}H_{12}$ (Wang et al., 2009).

Sodium alanates

Bogdanovic et al. (2000) & Jensen and Gross, (2001) stated that sodium alanate ($NaAlH_4$) have good hydrogen storage capacity of 7.4 wt%. However, the release of hydrogen does not occur in a single step reaction, decomposition of $NaAlH_4$ proceeds as follows:

$$3NaAlH_4 \rightleftharpoons Na_3AlH_6 + 2Al + 3H_2 \quad (2.2)$$

$$Na_3AlH_6 \rightleftharpoons 3NaH + Al + 3/2H_2 \quad (2.3)$$

$$NaH \rightleftharpoons Na + 1/2H_2 \quad (2.4)$$

The operating temperatures are between 185^{o}C and 260^{o}C for the first and the second reaction, respectively. The major drawback is that reactions is slow and have poor kinetics. Sodium alanate when catalysed by titanium ($NaAlH_4$ + 2% Ti) shows twice the reversible capacity than any other chemical hydride (Bogdanovic and Schwickardi, 1997).

Lithium alanates

Lithium alanates are very attractive for hydrogen storage, because of their high hydrogen content. The total hydrogen content is 10.5 and 11.2 wt% for $LiAlH_4$ and Li_3AlH_6, respectively. But $LiAlH_4$ has an extremely high equilibrium pressure of hydrogen, even at room temperature. $LiAlH_4$ is an example of an unstable hydride, which decomposes easily and cannot be re-hydrogenated (Zaluski et al., 1999)

The decomposition process of $LiAlH_4$ occurs in two steps:

$$3LiAlH_4 \rightarrow Li_3AlH_6 + 2Al + 3H_2 \quad (2.5)$$

$$Li_3AlH_6 \rightarrow 3LiH + Al + 3/2H_2 \quad (2.6)$$

Although $LiAlH_4$ contains over 40% more hydrogen by weight than $NaAlH_4$, it is not used for reversible hydrogen storage (Jang et al., 2006).

Lithium nitride

Lithium nitride (Li_3N) has theoretical hydrogen storage capacity of more than 10 wt% (Hu and Ruckenstien, 2003). Metal (N–H) system could prove to be a promising route for reversible solid hydrogen storage. Although the temperature required to release the hydrogen is too high for hydrogen storage.

$$Li_3N + 2H_2 \rightarrow LiNH_2 + 2LiH \quad (2.7)$$

Over a temperature range from 100^{o}C to 250^{o}C, 9.3 wt% of hydrogen storage can be achieved. A serious probable issue regarding nitride based storage material is the generation

of NH_3, which consumes some H_2 and also poisons the downstream processes (Chen et al., 2002).

Lithium borohydride

Hydrogen released by decomposition of lithium borohydride ($LiBH_4$) is 13.8 wt% (Zuttel et al., 2003). According to Fakioglu et al. (2004) hydrogen desorbs from $LiBH_4$ at temperatures greater than 470^oC. It is reported that $LiBH_4$ can reversibly store 8–10 wt% hydrogen at temperature range 315-400^oC by addition of MgH_2 and $TiCl_3$. However, the kinetics is too slow for practical applications. In addition, $LiBH_4$ is an expensive compound (Vajo et al., 2005).

2.2.2. Hydrogen generation by hydrolysis

Nonreversible hydrides or chemical release of hydrogen is through hydrolysis. Hydrides have high weight percent of hydrogen. Hydrides, such as sodium and lithium borohydride, also have high weight densities and have been proposed efficient for hydrogen storage (Chandra, 2008).

Table 2.1: Hydrogen storage properties of hydrides (Klanchar et al., 2000).

Hydride Reactions and Hydrogen Storage Properties of Hydrides	Fraction Hydrogen	Hydrogen Specific Mass (kg H_2/ kg of hydride)	Hydrogen Density (kg H_2/ L)
$LiH + H_2O \rightarrow LiOH + H_2$	0.126	0.252	0.122
$NaH + H_2O \rightarrow NaOH + H_2$	0.042	0.083	0.106
$CaH_2 + 2H_2O \rightarrow Ca(OH)_2 + 2H_2$	0.048	0.095	0.121
$MgH_2 \rightarrow Mg + H_2$	0.076	0.076	0.110
$LiAlH_4 + H_2O \rightarrow LiOH + Al + 2.5H_2$	0.105	0.132	0.121
$TiH_2 \rightarrow Ti + H_2$	0.040	0.040	0.152
$LiBH_4 + H_2O \rightarrow LiOH + HBO_2 + 4H_2$	0.184	0.367	0.235
$NaBH_4 + 2H_2O \rightarrow NaBO_2 + 4H_2$	0.105	0.211	0.226
Millennium fuel cell 35% solution $NaBH_4 + 4H_2O \rightarrow NaBO_2 + 4H_2 + 2H_2O$	---	0.077	0.77

Reaction equations and associated hydrogen storage properties of some eminent chemical hydride materials like LiH, NaH, CaH_2, MgH_2 etc. are shown in Table 2.1. Fraction H gives the number of hydrogen atoms in the hydride divided by the molecular weight of the hydride.

Hydrogen specific mass is defined as the mass (kg) of H_2 produced per unit mass of original hydride material (kg H_2/kg material) and hydrogen density is determined from the mass of hydrogen produced per unit volume of hydride (kg H_2/L) (Klanchar et al., 2004).

The physical, chemical and safety properties of these reactants and products propose that they could be used in a complete hydride based storage system. Typically, hydrogen can be generated from chemical hydrides through a direct reaction with water. Below are few chemical hydrides in which hydrogen is released through hydrolysis.

Lithium borohydride

Lithium borohydride and other lithium based hydrides are sensitive towards moisture in environment under standard temperature and pressure (STP) conditions. These hydrides react vigorously with water giving an exothermic reaction. Due to these concerns storing, processing, handling and manufacturing of these materials is a big concern. They have to be kept under special dry air conditions to avoid dehydrogenation if used for on-board hydrogen storage applications. Due to largest hydrogen content in lithium borohydride, it is also a major area of interest in HG. The hydrolysis reaction of lithium borohydride is as follows:

$$LiBH_4 + 2H_2O \rightarrow LiBO_2 + 4H_2 \qquad (2.8)$$

It has high hydrogen gravimetric capacity among other chemical hydrides i.e. (18.4 wt%) and very high volumetric hydrogen density (121 kg H_2/m^3). (Mitrofanova et al., 1989; Arkhipov, 1967; Kojima et al., 2007 and Aiello et al., 1999).

Lithium hydride

Lithium hydride reacts easily with water at ambient temperatures and pressures and releases hydrogen as:

$$LiH + H_2O \rightarrow LiOH + H_2 \qquad (2.9)$$

The reaction gives very high hydrogen density. Every 8 g of lithium hydride produces 2 g of hydrogen gas with hydrogen capacity of 25 wt % (Chandra, 2008 and Hordeski, 2008). Major drawback in lithium hydride hydrolysis is the formation of byproduct lithium hydroxide. Lithium hydroxide forms a thick layer on the LiH and prevents diffusion of water with lithium hydride and reduces HG. This effectively slows the reaction before all LiH is used (Pitcher and Kavarnos, 1997).

Lithium aluminium hydride

Lithium aluminium hydride reacts violently with water. Therefore, all reactions are carried in inert and dry conditions. It had highest heat of hydrolysis compared with other hydrides therefore, unstable to work at room temperature and pressure (Jensen and Takara, 2000).

$$LiAlH_4 + 4H_2O \rightarrow LiOH + Al(OH)_3 + 4H_2 \quad (2.10)$$

Sodium borohydride

Boron hydrides are most prominent hydrogen storage systems due to its high volumetric and gravimetric densities, sodium borohydride is widely studied among other boron hydrides. Sodium borohydride (SB) was discovered in 1940. It was highly studied during 1990's because hydrogen was considered as only efficient renewable energy carrier. For fuel cell applications, extensive studies were carried on sodium borohydride and many papers on sodium borohydride have been published. SB is a versatile hydride with wide applications, as a reducing agent in industrial processes, during waste water treatment, pharmaceutical and paper industry. Due to its high hydrogen content of 10.8 wt %, it is been suggested as promising source of hydrogen. (Demirci and Miele, 2009).

Chemical formula of sodium borohydride is $NaBH_4$. It is white colored powder and is soluble in water. Sodium metaborate is formed as a byproduct after the hydrolysis of $NaBH_4$. The hydrolysis reaction of $NaBH_4$ is expressed in equation 2.11,

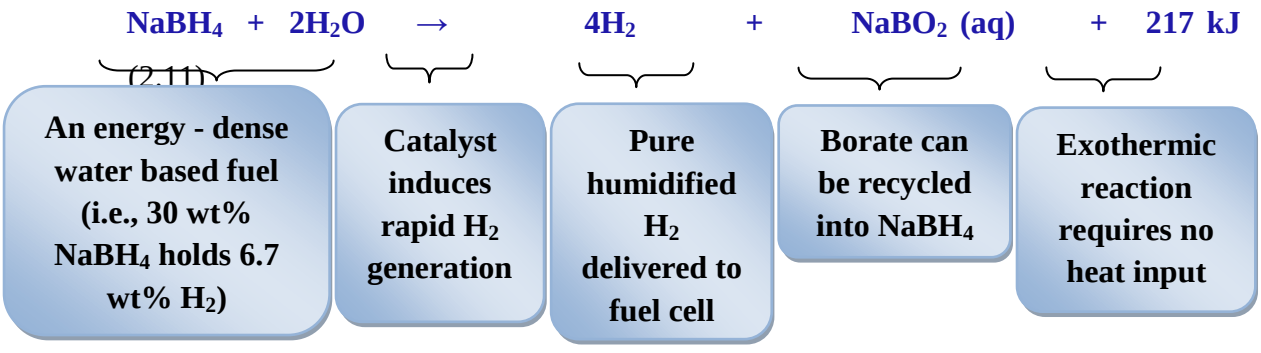

The hydrolysis reaction of sodium borohydride is studied mainly because of its high hydrogen density and low heat of hydrolysis as compared to other hydrides shown in Table 1.1. The hydrolysis reaction is spontaneous and exothermic, that is no external heat is required to carry the reaction. The reaction can be accelerated with the use of potential catalyst. Pure hydrogen is produced at low temperatures (0-25°C) and the byproducts produced are environmental friendly.

Approximately, 1g of $NaBH_4$ gives about 2.4 L of hydrogen at normal temperature and pressure (NTP). Therefore, large quantities of hydrogen could be obtained with small quantities of sodium borohydride (Murooka et al., 2012). Chemical properties of $NaBH_4$ are given in Table 2.2.

Table 2.2: Safety concerns and chemical properties of sodium borohydride:

S. No.	Properties	Sodium Borohydride
1.	Molecular formula	$NaBH_4$
2.	State at room temperature	Solid
3.	Molecular weight (g/moles)	37.8
4.	H_2 storage capacity (gH_2/L)	133
5.	Density (g/cm^3)	1.07
6.	Solubility (g/100 g of H_2O)	55
7.	Melting point (°C)	505
8.	Decomposition temperature (°C)	565
9.	Stability	Moisture sensitive
10.	Stability in aqueous solutions	Self-hydrolysis
11.	Chemicals to avoid	Acids and oxidizing agents

As shown in Figure 2.1, as volume of solution increases, $NaBH_4$ requirement decreases, 9 kg of H_2 is produced from 40 wt% $NaBH_4$ with 28 gallons (106 L) of solution.

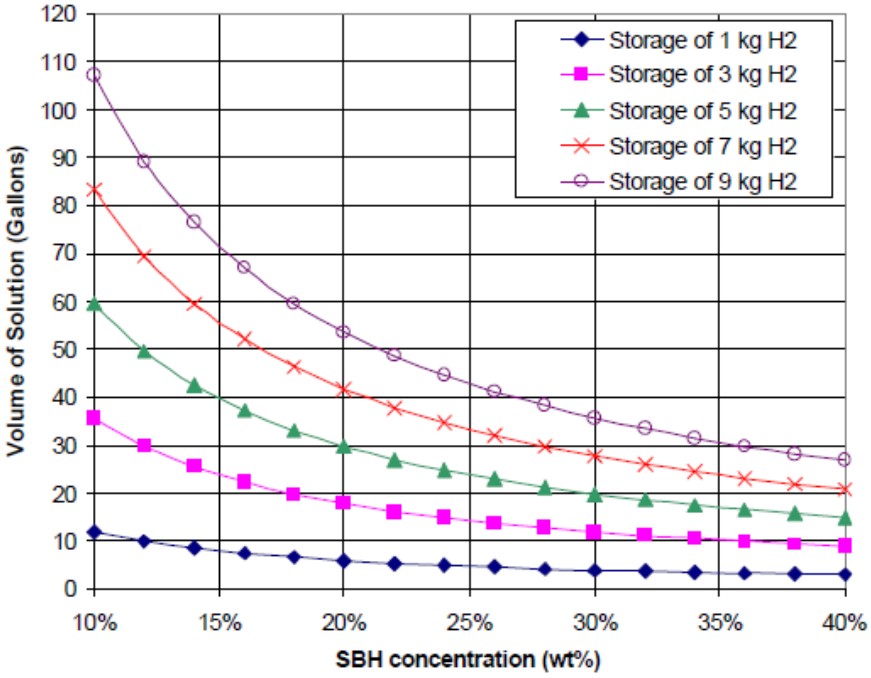

Figure 2.1: Volumetric storage efficiency of $NaBH_4$ (Ying, 2003)

Similarly, gives gravimetric storage efficiency of $NaBH_4$ is given in Figure 2.2. It is observed that as wt% of $NaBH_4$ increases gravimetric hydrogen storage density increases (Ying, 2003).

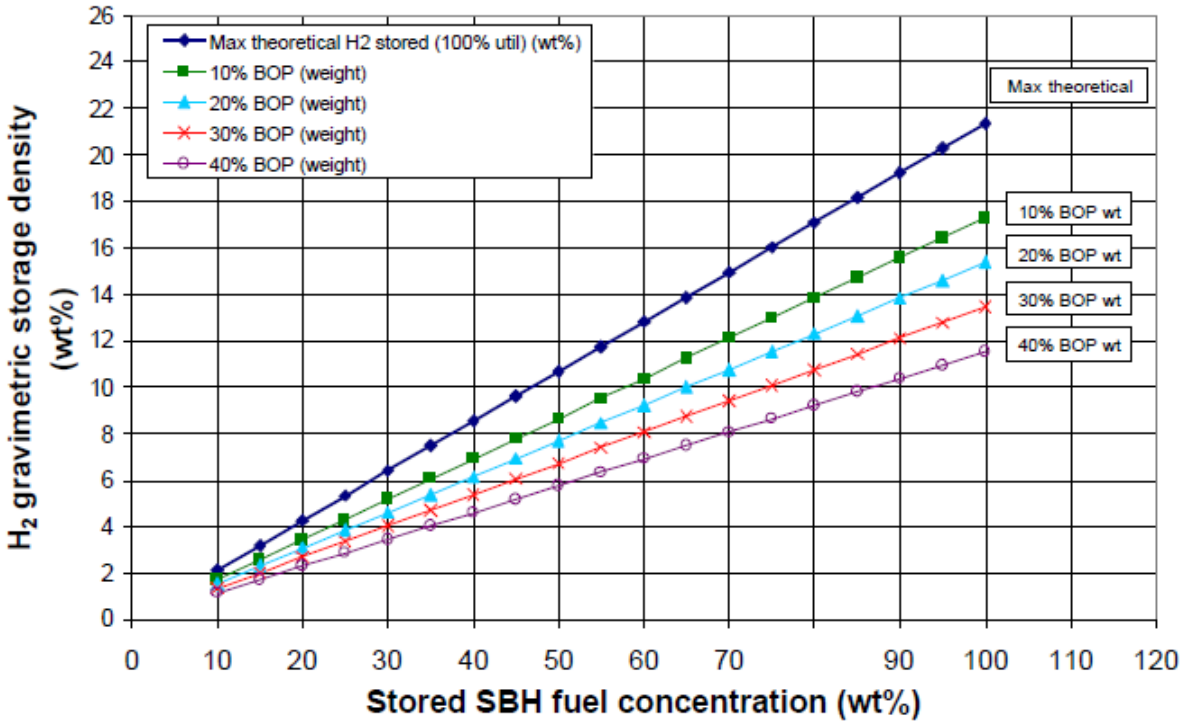

Figure 2.2: Gravimetric storage efficiency of $NaBH_4$ (Ying, 2003)

Possible storage of aqueous solution of $NaBH_4$ is proposed by Akdim et al. (2009) for portable applications as given in Figure 2.3.

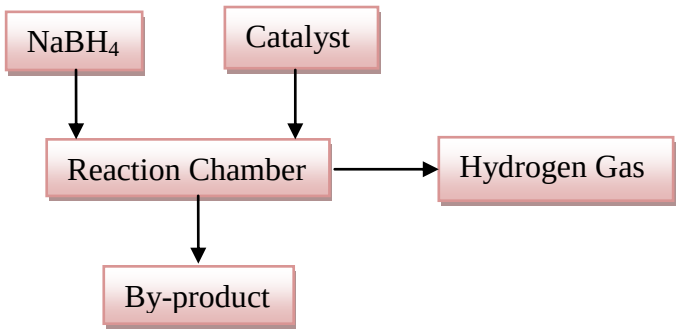

Figure 2.3: Schematic diagram for possible storage of aqueous $NaBH_4$ (Akdim et al., 2009)

Besides its all advantages, department of energy (DOE) USA recommended "no-go" for the aqueous solution of sodium borohydride as hydrogen storage medium for vehicular applications. This decision is mainly because of its major disadvantages like solubility of byproduct $NaBO_2$ that requires significant amount of water for completion of reaction, recycling of $NaBO_2$ and cost of sodium borohydride. Considering all the above factors and

disadvantages related to sodium borohydride as hydrogen storage material, the concept of use of dual solid for hydrogen generation is in process and it is discussed in section 2.4.

2.3. Aluminium/H_2O reactions for hydrogen generation

Hydrogen production from aluminium can be achieved under mild conditions of temperature and pressure. Commercially available aluminium or aluminium alloys could reduce hydrogen production costs when combined with other hydrides for example sodium borohydride. At room temperature, the reaction between aluminium metal and water forms aluminium hydroxide and hydrogen (Hou, 2006 & Smith 1972), as per following reaction.

$$2Al + 6H_2O \rightarrow 2Al(OH)_3 + 3H_2 \qquad (2.12)$$

Gutbier and Hohne (1976) revealed that the gravimetric hydrogen capacity from the above reaction is 3.7 wt%. The major drawback in this reaction is formation of oxide passivation layer on aluminium surface. This prevents water to react with aluminium metal and further release of hydrogen. For maintaining the reaction of aluminium with water, continual removal and disruption of this aluminium oxide layer is required (Smith, 1972).

Oxides of alumina like γ-Al_2O_3 and α-Al_2O_3 are also used for hydrogen generation. Aluminium is also used as a support for the catalyst or as promoting material with other hydrides. This novel concept of coupling reactions is discussed in the next section (2.4).

2.4. Coupling reactions

In comparison with the conventional hydride based hydrogen storage systems, newly developed dual-solid−fuel system demonstrates distinct advantages in hydrogen storage densities (volumetric and gravimetric) and high hydrogen generation rate.

2.4.1. Hydrogen generation from ($NaBH_4$/Al) with $CoCl_2$ as catalyst

Dai et al. (2011 b) investigated chemical hydrogen storage system composed of $NaBH_4$/Al (100-200µm)/NaOH solid powder mixture with aqueous solution of $CoCl_2$ as catalyst. Rapid hydrogen release is observed as soon as aqueous solution of $CoCl_2$ comes in contact with $NaBH_4$/Al/NaOH powder mixture and 90% fuel conversion is observed after 3 minutes.

2.4.2. Hydrogen generation from (Al, Li, Co/$NaBH_4$) with pure water

Composite of Al (10µm), Li, Co and $NaBH_4$ as given by Wang et al. (2013) gives 100% hydrogen yield and good hydrogen generation at 50^oC.

The combined effect of Li and Co on $Al/NaBH_4$ hydrolysis results in the formation of alkaline solution and stable $Co/LiAl_2(OH)_7$ catalyst, and its catalytic activity is further increased by hydrolysis of byproducts $Al(OH)_3/NaBO_2$. The optimized compound could be potentially applied as hydrogen source for portable fuel cell applications.

2.4.3. Hydrogen generation from $Al/NaBH_4$ composite activated by lanthanum (La) metal and $CoCl_2$ salt in pure water

Composition of Al(10μm)/$NaBH_4$ mixture activated by La and $CoCl_2$ in water for hydrogen generation is investigated by Jianbo et al. (2012). Al, La, $CoCl_2/NaBH_4$ mixture (mass ratio of 1:1) yielded 1664 ml/g hydrogen with 100% efficiency within 60min at 60^{o}C. The hydrogen generation rate and amount could be regulated by varying composition of materials.

2.4.4. Hydrogen generation from Al, $Li/NaBH_4$ mixture in water activated by nickel (Ni) powder

As stated by Shu et al. (2012), Al (10μm) $Li/NaBH_4$ mixture activated by Ni powder in water for hydrogen generation gives high hydrogen generation at an optimized Al, Li, $Ni/NaBH_4$ mixture (mass ratio of 3:1). The mixture generates 1540 mL/g hydrogen with 96% efficiency at 60^{o}C. Ni powder shows dual catalytic effects on the hydrolysis of Al $Li/NaBH_4$ mixture due to the formation of Ni_2B in the hydrolysis process.

2.4.5. Hydrogen generation form cobalt-molybdenum-boron catalyst with alkaline $NaBH_4$ solution and Al powder

According to Zhuang et al. (2013), catalyst study is a major issue in the development of $NaBH_4$ based hydrogen generation systems. Co–Mo–B as a catalyst display extremely higher catalytic activity. Combined usage of concentrated $NaBH_4$ solution and Co–Mo–B catalyst with small amount of Al powder (325 μm) yields 6 wt% hydrogen capacity with fast kinetics.

2.5. Selection of catalyst

Theoretical yield of hydrogen is too low when sodium borohydride reacts with water. This is mainly due to the anion BO_2^- (from byproduct $NaBO_2$). This increases the pH of solution and effects hydrolysis of $NaBH_4$. According to Schlesinger et al. (1953), the pH of the solution could be lowered by either adding a strong acid or by adding some catalyst. The latter method is a solution for long term hydrogen storage. Therefore, widespread studies are carried out on highly active and low cost $NaBH_4$ catalyst for portable and practical hydrogen storage system (Muir and Yao, 2011).

2.5.1. Noble metal catalysts

Since 2000, various noble metal catalysts were used and studied for hydrolysis of $NaBH_4$ like platinum, ruthenium and rhodium that exhibit very high catalytic activity. Some of the reported catalysts consist of noble metal loaded on support material. For example, ruthenium (Ru) loaded on ion exchange resin IRA-400 (Amendola et al., 2000), activated carbon, titania and $LiCoO_2$. Platinum (Pt) catalyst is loaded on $LiCoO_2$ and Ru loaded on TiO_2 is also used (Muir and Yao, 2011). The major drawback in the use of ruthenium catalyst is that its activity decreases in alkaline solution or its activity is affected by NaOH in solution. These catalysts suffer cost issues for extensive use in hydrogen storage system (Water et al., 2008).

2.5.2. Non noble catalysts

Schlesinger et al. (1953) reported many non-noble metal catalysts like nickel(II) chloride, iron(II) chloride, copper(II) chloride, manganese(II) chloride and cobalt(II) chloride. These non-noble metal catalysts were preferred over noble metal catalysts as low cost alternatives. Of all the above catalysts, cobalt(II) chloride is most reactive.

Demirci et al. (2010) investigated cobalt in its various forms like chloride, metallic, boride, metal oxides etc. Further, Akdim et al. (2009) observed cobalt chloride as most reactive among its other cobalt based salts like $Co(CH_3COO)_2$, $CoSO_4$, CoF_2, $Co(NO_3)_2$.

The highest reactivity of $CoCl_2$ is due to electrophilic nature of Co^{+2} ions which are strongly attracted towards BH_4^- ions from $NaBH_4$, thus enhancing the hydrolysis of $NaBH_4$ (Akdim et al., 2011). The major drawback of cobalt based catalysts is that they lose their reactivity. For this reason, to increase the catalyst stability and reactivity, it is supported over some support like, active carbon, CNT, alumina etc. Supports increase dispersion of cobalt on its surface and increase catalytic sites of catalyst (Demirci and Miele, 2014).

2.6. Summary of literature

Following is the summary of literature studies presenting comparison among various chemical hydrides for HG system.

Table 2.3: Chemical hydrogen storage in hydrides by thermolysis

S. No.	Hydrogen storage materials	H_2 content (wt%)	Temperature (^oC)	Limitations	Reference
1.	MgH_2	14.9	270	Slow and poor kinetics, reaction initiation at higher temperature.	Harder, 2011
2.	$Ca(BH_4)_2$	9.6	527	Same as above	Wang et al., 2009
3.	$NaAlH_4$	7.4	185-260	Same as above	Bogdanovic et al., (2000) & Jensen and Gross, (2001)
4.	$LiAlH_4$	10.5	160-200	Same as above	Jang et al., 2006
5.	$LiNH_2$	10.4	230	Generation of NH_3, consumes H_2 and poisonous in downstream processes.	Chen et al., 2002
6.	$LiBH_4$	18	470	Expensive, kinetics is too slow	Vajo et al., 2005

Table 2.4: Chemical hydrogen storage in hydrides by hydrolysis

S. No.	Hydrogen storage materials	H_2 content (wt%)	Temperature (^oC)	Limitations	Advantages	Reference
1.	LiH	25	Room temperature	Formation of LiH lowers HGR	High hydrogen density	Pitcher and Kavarnos, 1997
2.	$LiBH_4$	18	Same	Unstable hydride	Same	Kojima et al., 2007
3.	$LiAlH_4$		Same	Unstable hydride	Same	Jang et al., 2006
4.	$NaBH_4$	10	Room temperature	Expensive	Fast kinetics and reaction initiates at room temperature.	Dai et al., 2011
5.	Al and Al alloys (Powder)	3.7	Room temperature	Highly exothermic reaction, presence of coherent layer.	Can reduce production cost due to easy availability.	Hou, 2006
6.	$NaBH_4$/Al	5.4	Room temperature	–	Faster kinetics, reaction initiation at room temperature, production cost is reduced.	Dai et al., 2011 a

Tables 2.3 and 2.4 indicate various hydrogen storage materials, their reaction initiation temperature, hydrogen content and advantages & limitations.

It can be concluded form literature review that chemical hydrogen storage in hydrides, based on hydrolysis, is more effective than thermolysis pathway. In thermolysis, slow and poor kinetics is observed whereas in hydrolysis faster kinetics and high hydrogen capacities are observed. Reaction initiates at higher temperature in thermolysis whereas in hydrolysis reaction initiates at room temperature. Efficiency of system could be increased in hydrolysis by combining the H_2 storage material with other potential hydrogen storage material.

The constituted dual fuel system exhibits complimentary attributes, such as eminent hydrogen density, reduced material cost and adequate controllability of reactions at moderate temperatures, making it promising for mobile and portable hydrogen source applications.

Work needs to be carried out to study all the factors that could affect hydrogen generation after the selection of most proficient hydrogen generation materials. Kinetic studies are required supporting the study for efficient hydrogen generation system to observe the factors that could cause variation in hydrogen generation rate. Studies on operating parameters like temperature, pressure and concentrations of all the materials are required. Extensive kinetics studies should be carried out on combination of a catalyst promoter, active catalyst and chemical hydride with high hydrogen storage capacity that could constitute as effective hydrogen generation system for various applications.

2.7. Gaps identified

- No work has been done, to our best knowledge, on utilization of nanoparticles of aluminium oxide/aluminium in combination with chemical hydrides for hydrogen generation, which can result in faster kinetics of hydrolysis reaction at lower temperatures.
- Studies on operating parameters like temperature, pressure and pH of alumina and aluminium nanoparticles with chemical hydrides are not being reported.
- Extensive kinetic studies are not reported on combination of alumina and aluminium nanoparticles with various hydrides which can further result in optimising operating conditions for high hydrogen generation rate.

2.8. Objectives

The objectives of the thesis are as follows:

- To study hydrogen generation from sodium borohydride with and without catalyst.
- To study the effect of various operating parameters for hydrogen generation system.
- To study the kinetics of hydrogen generation from sodium borohydride.

CHAPTER 3

Experimental

3.1. Introduction

This chapter presents the materials procured and experimental setup prepared to perform kinetic studies that is to observe change in kinetic data by variation in parameters like concentration of the materials and with temperature. Method for quantitative analysis of hydrogen gas and characterization of residual material is also discussed.

3.2. Materials

Materials used in the study are sodium borohydride ($NaBH_4$) (97% purity) and cobalt chloride hexahydrate ($CoCl_2.6H_2O$) (98% purity) procured from M/s Loba Chemie Ltd., sodium hydroxide pellets (NaOH) (97% purity) and cobalt acetate tetrahydrate $(CH_3COO)_2Co.4H_2O$) purchased from Central Drug House Pvt. Ltd., γ-alumina (Al_2O_3) (20nm, 99% purity), γ-alumina (Al_2O_3) (100-200µm, 99% purity) and montmorillonite (MMT) clay obtained from M/s Sigma Aldrich Chemicals Pvt. Ltd., copper sulphate penta hydrate ($CuSO_4.5H_2O$) (99% purity) and zeolite 13X (99% purity) obtained from Merck Ltd, carbon nano tubes (CNT) purchased from Nanoshell Ltd. Chemicals like cobalt sulphate heptahydrate ($CoSO_4.7H_2O$) (99% purity), silicon oxide (SiO_2) (99% purity), cobalt tri nitrate ($Co(NO_3)_2.3H_2O$) (97% purity), cadmium sulphate ($CdSO_4$) (99% purity) and zirconium sand (ZrO_2 66 %, SiO_2 32.54 %, Al_2O_3 1.15 %, TiO_2 0.27 %, Fe_2O_3 0.04 %) were purchased from SD Fine Chemicals Ltd.

3.3. Experimental setup

The experimental arrangement as shown in Figure 3.1 mainly consists of:

Three-port reactor: A three port reactor having capacity of 250 mL is used to carry the experimental reactions. The left-hand port is equipped with thermowell to continuously monitor the temperature of the reactor. Middle port is connected to pressure equalizing funnel and the right-hand port guides the generated hydrogen to water replacement system.

Heating Mantle: The reaction temperature is controlled by using heating mantle.

Pressure equalizing funnel: Dropping funnel is used to equalize pressure for air-sensitive materials and to provide inert gas environment to the reaction. In this study it is used to add aqueous NaOH solution to the reactor and further helps in equalizing the pressure during $NaBH_4$ hydrolysis reaction.

Water container: To submerge the inverted cylinder in the water replacement system with capacity of 4 L.

Measuring Cylinder: Hydrogen generated is measured in inverted measuring cylinder with capacity of 3 L.

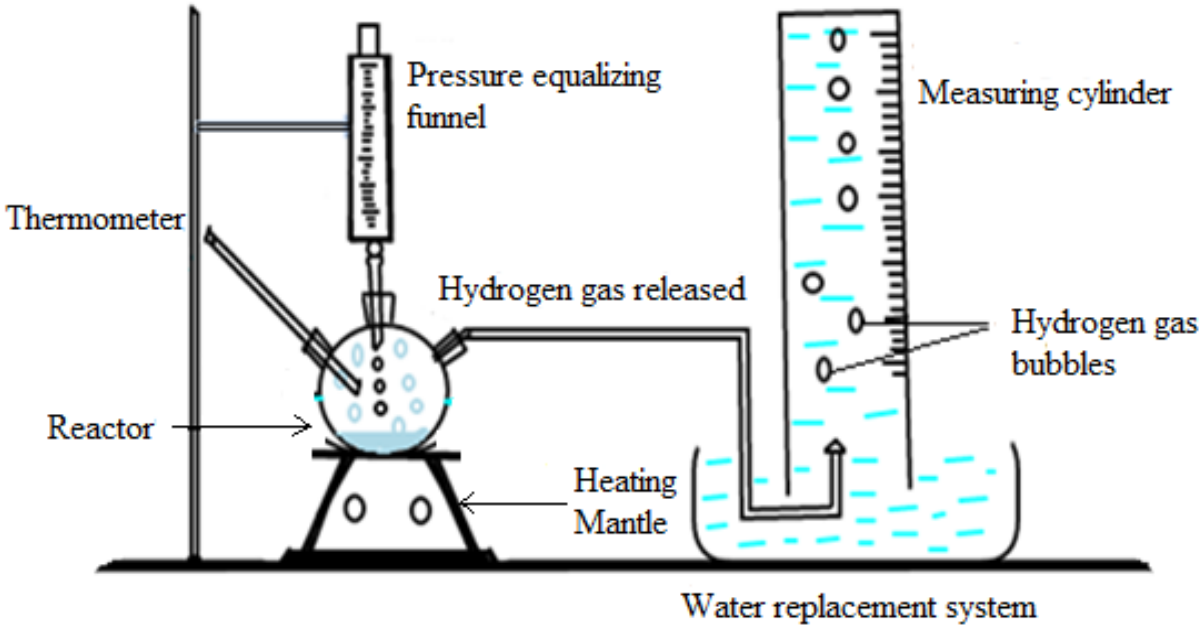

Figure 3.1: Schematic diagram of experimental set up

According to the above schematic diagram shown in Figure 3.1, experimental facility is created in laboratory to carry out the experiments as shown in Figure 3.2, 3.3 (a) and (b).

3.4. Experimental procedure

Experiments are carried out in a 250 mL three neck round bottom reaction flask under isothermal conditions. The reactor is cleaned and dried before starting the experiment. Predetermined amount (given in relevant chapters) of reactants is added in the reactor that is attached to pressure equalizing funnel from the middle port.

Aqueous solution of NaOH of amount 10 mL is added drop wise to the reactor by dropping funnel. Hydrogen gas is evolved as soon as aqueous solution of NaOH comes in contact with reactants. Hydrogen generation is measured by displaced water volumes in measuring cylinder as a function of time and corrected to the values at 298 K and 1 atm.

Figure 3.2: Experimental Setup

Figure 3.3(a): Three port reactor

Figure 3.3(b): Water displacement system

Hydrogen measuring cylinder is attached to water replacement system as shown in Figure 3.1. Homogeneous dispersion of catalyst is achieved in short period of time due to stirring action by evolved hydrogen gas bubbles. Evolved hydrogen gas is collected in inverted measuring cylinder by downward displacement of water. Temperature in each experiment is maintained constant with the variation of ± 0.2°C. Studies are carried out with and without addition catalyst in $NaBH_4/H_2O$ system. Experimental readings are taken thrice and average

readings have been shown in all the figures. For each data point, error bar is added to display the spread within one standard deviation from the mean of data point.

3.5. Quantitative analysis of hydrogen gas

Gas collected were analysed for the hydrogen content by gas chromatograph (using Nucon series 5900 (CPRI) Gas Chromatograph). A molecular sieve column of 6 feet length & 1/8 inch outer diameter and thermal conductivity detector (TCD) with nitrogen as carrier gas were used the same.

3.6. Characterization of residual material

Analysis of the residual material after hydrogen generation was performed using various characterization techniques. Black colored residue left after the reaction was completely dried and kept overnight in incubator at 50 to 70^{o}C. The dried residue was crushed and prepared for characterization. Morphology of the residue was observed by SEM (Scanning Electron Microscopy). To identify the elemental composition of the residue, it is characterized by EDS (Energy dispersive electron spectroscopy). FTIR (Fourier Transform Infrared Spectroscopy) could give the functional groups present in the residue and XRD (X-Ray Diffraction) indicated the final products formed in the residue.

3.6.1. Scanning electron spectroscopy

The morphology of the residue was observed on a scanning electron microscope (JEOL JSM-6510 LV). The specimens were coated with 50 μm of thick gold film in an automatic sputter coater (Polaron) to avoid charging under an electron beam prior to SEM.

3.6.2. Energy dispersive electron microscopy

Elemental percentages of byproducts of $NaBH_4$ hydrolysis is observed by energy dispersive electron microscopy (EDS). Scanning electron microscope (JEOL JSM-6510 LV) is equipped with integrated silicon drift detector (SDD) technology to carry EDS analysis.

3.6.3. Fourier transform infrared spectroscopy

To observe chemical bonds between the molecules of the residue, Fourier transform infrared (FTIR) spectra are used. Fourier transform infrared (FTIR) spectra of residue was recorded on a Agilent Cary 6610 FTIR spectrometer fitted with universal ATR sampling accessories. The spectra were recorded in the range of 4000-500 cm^{-1} with a resolution of 4 cm^{-1}.

3.6.4. X- ray Diffraction

Structural characterization of the residue was carried out by recording its X-ray diffraction patterns using PANalytical X'Pert Pro Diffractometer, operated at 45 kV and 40 mA with monochromatic Cu-Kα radiation (λ=1.5406 Å), in the 2θ range of 20-80°.

Therefore, the above experimental setup and procedure is used to conduct all the experimental runs to carry out kinetic studies. As described, above characterization techniques are applied to carry residual analysis.

CHAPTER 4

Studies on $NaBH_4/H_2O$ hydrogen storage system and selection of catalyst

4.1. Introduction

Hydrogen energy is a resolution considered at worldwide scale as a substitute to replace fossil fuels and to establish clean and secure energy future. Hydride based hydrogen storage, for instance sodium borohydride ($NaBH_4$) is recognized as a considerable concern and a potential hydrogen source for portable fuel cell applications. In this chapter, hydrogen generation is monitored by varying various factors effecting hydrogen generation (HG) and hydrogen generation rate (HGR). $NaBH_4$ is the prime material in the present study due to its limited equipment investment cost as compared with other hydrogen storage methods. It is stable compound, safe to use, handle and store.

$NaBH_4$ is sensitive towards moisture and undergoes self-hydrolysis at low pH conditions. This instability can be evaded by maintaining the solution at pH above 9. Sodium hydroxide (NaOH) is used as a stabilizer to raise the pH of solution and avoid $NaBH_4$ self-hydrolysis.

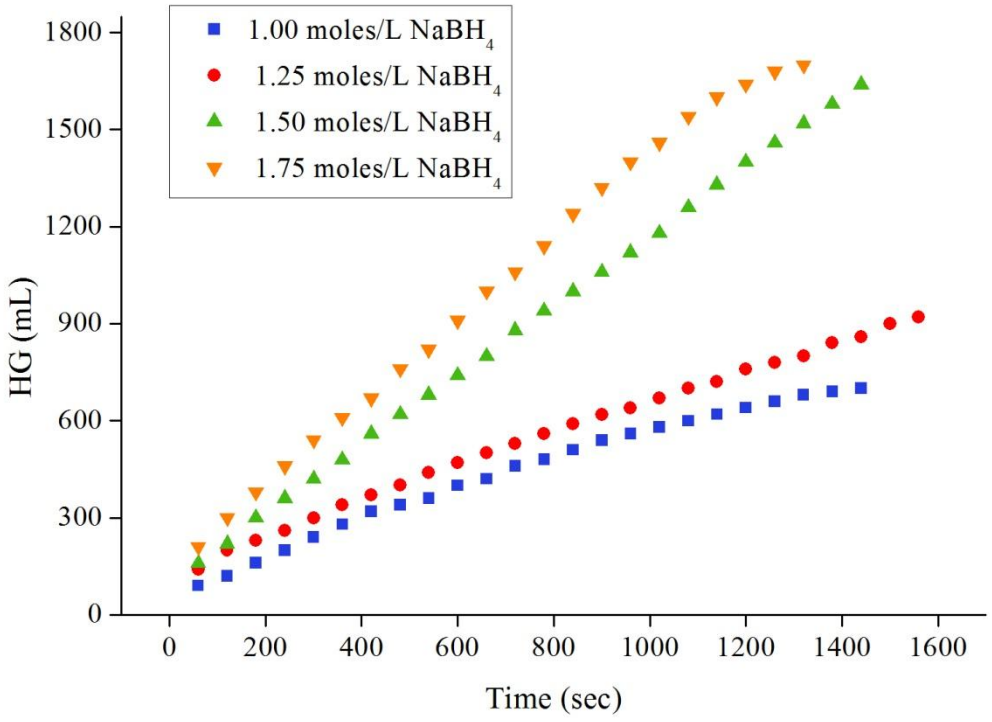

Figure 4.1: Hydrogen generation as a function of time

Preliminary studies were carried out without catalyst in $NaBH_4/H_2O$ system and it was noticed that the H_2 generation has been quite low without a catalyst (Fig. 4.1). It has also been reported in the literature that a suitable catalyst is needed to accelerate the reaction (Retanamma et al., 2011)

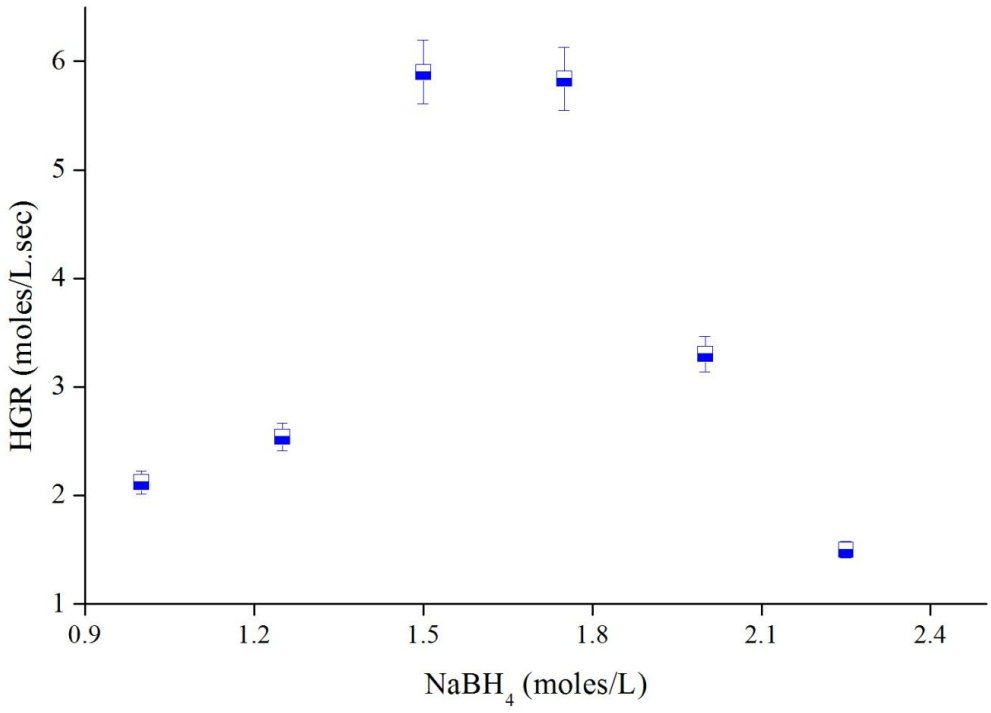

Figure 4.2: Variation of HGR with $NaBH_4$ without addition of catalyst

It is predicted from experiments that hydrogen generation is slow with time as shown in Figure 4.1. Lower values of HGR are reported in Figure 4.2 that is 2.12, 2.54, 5.90 and 5.84 moles/L.sec at 1.00, 1.25, 1.50 and 1.75 moles/L of $NaBH_4$ respectively. At higher concentrations of $NaBH_4$ hydrogen generation rate drops.

After observing these results, a detailed study is carried out to find the most potential catalyst for $NaBH_4/H_2O$ system. After the selection of catalyst, parameters that affect the rate of reaction like $NaBH_4$ concentration, NaOH concentration, catalyst concentration and temperature are studied and kinetic parameters are determined for this system.

4.2. Selection of catalyst for $NaBH_4/H_2O$ system

The major objective is to study hydrogen generation with and without catalyst and to find the most effective catalyst in terms of reactivity and low cost for $NaBH_4/H_2O$ system. As discussed in literature cobalt (Co) based catalysts are considered most reactive among other catalysts.

$NaBH_4$ is highly reactive with metal chlorides like iron(II) chloride, nickel(II) chloride, manganese(II) chloride, copper(II) chloride and cobalt(II) chloride and the end product formed is metal boride (Schlesinger et al., 1953). It is also observed that Co(II) chloride is most reactive among all above chlorides. On similar grounds based on HGR, high reactivity of $CoCl_2$ is also reported by Schlesinger et al. (1953); Levy et al. (1960) and Komova et al. (2008). Further, Akdim et al. (2011) investigated various cobalt based salts like $Co(CH_3COO)_2$, $CoSO_4$, CoF_2 and $Co(NO_3)_2$ in catalyzing $NaBH_4$ hydrolysis reaction. The most reactive catalyst with respect to gravimetric hydrogen storage capacity is $CoCl_2$.

The reactivity is explained by strong cationic charge and electrophilic nature of Co^{+2} ions. These Co^{+2} ions are highly reactive towards BH_4^- ions. On the other hand, Cl^- anion is compared among all the other anions CH_3COO^-, SO_4^{2-}, NO_3^-, F^- of Co based salts and it is found that diffusion coefficient of Cl^- is highest in aqueous solution shown in Table 4.1. This increases the solubility of Cl^- ions in the solution. Therefore, strong cationic charge on cobalt and high solubility of chlorine are the reasons behind high reactivity of $CoCl_2$ compared to other Co based salts.

Table 4.1: Diffusion coefficients (D) of various anions (Lide, 2004 and Apelblat and Manzurola, 1999)

S. No.	Material	Anion	Diffusion coefficient (D)($10^{-5}cm^2\ sec^{-1}$)
1.	$CoCl_2$	Cl^-	2.032
2.	$Co(CH_3COO)_2$	CH_3COO^-	1.089
3.	$CoSO_4$	SO_4^{2-}	1.065
4.	CoF_2	F^-	1.475
5.	$Co(NO_3)_2$	NO_3^-	1.902

The major byproduct formed after hydrolysis reaction of $NaBH_4$ with $CoCl_2$ as catalyst is cobalt boride (Co_2B), which is the most reactive species in $NaBH_4$ hydrolysis reaction. Below is the detailed reaction mechanism discussed by Glavee et al. (1993) that explains how protons or hydrogen is released through $CoCl_2$ as catalyst and due to the formation of active species cobalt boride.

$$CoCl_2 + 2NaBH_4 + 3H_2O \rightarrow 0.5Co_2B \downarrow + 2NaCl + 1.5HBO_2 + 6.25H_2 \uparrow \quad (4.1)$$

Without Co^{+2} ions from $CoCl_2$, the hydrolysis reaction of $NaBH_4$ is slow (equation 4.2) and pH increases with the formation of byproduct sodium metaborate ($NaBO_2$). The formation of $NaBO_2$ leads to the reversible reaction 4.3.

$$NaBH_4 + 2H_2O \rightarrow NaBO_2 + 4H_2 \quad (4.2)$$

$$NaBO_2 + H_2O \rightleftharpoons BO_2H + NaOH \quad (4.3)$$

In the presence of Co^{+2} ions the reaction kinetics is faster. As soon as $CoCl_2$ comes in contact with water, $Co(H_2O)_6^{2+}$ species is formed and series of reactions occur as below:

$$Co(H_2O)_6^{2+} \rightleftharpoons [(H_2O)_5CoOH]^+ + H^+ \quad (4.4)$$

$$[(H_2O)_5CoOH]^+ + H^+ + BH_4 \rightarrow H_2 + [(H_2O)_5\text{–}Co \quad OH\text{–}BH_3]^+ \quad (4.5)$$

$$[(H_2O)_5Co\text{–}OH\text{–}BH_3]^+ + Co(H_2O)_6^{+2} \rightarrow H_2 + [(H_2O)_5CoOH\text{–}BH_2\text{–}OH\text{–}Co(H_2O)_5]^{3+} \quad (4.6)$$

$$[(H_2O)_5CoOH\text{–}BH_2\text{–}OH\text{–}Co(H_2O)_5]^{3+} + 3BH_4^- \rightarrow (H_2O)_5Co\text{–}OH\text{–}BH_2\text{–}OH\text{–}Co(H_2O)_5 + 3[BH_3] + 1.5H_2 \quad (4.7)$$

$$3[BH_3] + 9H_2O \rightarrow 3B(OH)_3 + 9H_2 \quad (4.8)$$

$$(H_2O)_5Co\text{–}OH\text{–}BH_2\text{–}OH\text{–}Co(H_2O)_5 \rightarrow Co_2B + 12H_2O \quad (4.9)$$

The final reaction that is formed is

$$2Co(H_2O)_6^{2+} + 4\,BH_4^- + 9H_2O \xrightarrow{H_2O} Co_2B + 12.5H_2 + 3B(OH)_3 \quad (4.10)$$

It is also observed that some additional hydrogen is generated by reduction of borohydride ions given in equations 4.11 and 4.12.

$$BH_4^- + 2H_2O \xrightarrow{\text{catalyst}} BO_2^- + 4H_2 \quad (4.11)$$

$$BO_2^- + H_2O \rightleftharpoons OH^- + BO_2H \quad (4.12)$$

Equation 4.11 is responsible for rise in the pH of the solution. As pH rises reaction 4.12 slows down and another 1-2 moles of hydrogen is also generated. The above two reactions are responsible for generation of hydrogen in the absence of Co_2B species or when Co^{2+} ions are reduced to Co_2B.

Therefore, the final reactions are:

$$2Co^{2+} + 4BH_4^- + 9H_2O \rightarrow Co_2B + 12.5H_2 + 3B(OH)_3 \quad (4.13)$$

$$\frac{1}{2}BH_4^- + H_2O \xrightarrow{\text{catalyst}} \frac{1}{2}BO_2^- + 2H_2 \quad (4.14)$$

Above mechanism proves how the presence of $CoCl_2$ helps in release of protons in $NaBH_4/H_2O$ solution. On the basis of the above discussion, $CoCl_2$ is chosen as a catalyst for $NaBH_4/H_2O$ system.

4.3. Kinetic measurements for $NaBH_4/H_2O$ system

4.3.1. Materials

The chemicals used in this investigation are $NaBH_4$ as prime component for hydrogen generation, $CoCl_2$ as catalyst and NaOH as stabilizer in 10 mL of water. Considering the constraints in the experimental facility and practical operating conditions, experiments are carried out at specific concentrations of $NaBH_4$, $CoCl_2$ and NaOH. Four concentrations of $NaBH_4$ are taken for kinetic data that are 1.00, 1.25, 1.30, 1.75 moles/L with $CoCl_2$ 0.020, 0.024, 0.028, 0.032 moles/L and NaOH 1.16, 1.6, 2.06, 2.6 moles/L. Readings are taken according to the method discussed in experimental section.

4.3.2. Factors affecting HGR

Catalytic hydrogen generation process with $NaBH_4$ undergoes through three stages: induction, linear and non-linear. During induction period no HG is observed or HG is very slow. This step is considered as catalyst activation step. Type of catalyst and reaction temperature determines the duration and rate of this step. The linear process is catalytic hydrolysis reaction step and is dependent on the nature catalyst and reaction temperature. Decrease in H_2 generation defines non-linear process due to depletion of reactant concentration and formation of byproduct (sodium metaborate) (Retnamma et al., 2011). Thus, these three processes define the hydrolysis of $NaBH_4$. According to these three stages, all the factors that affect HGR are observed thoroughly.

The reaction rate of $NaBH_4$ hydrolysis is affected by NaOH, $NaBH_4$, catalyst concentration and reaction temperature. All these factors are explained as under:

Effect of NaOH concentration on HGR

Sodium borohydride is sensitive to moisture and hydrolysis reaction starts once it is in contact with moist air. Therefore, to suppress this self-hydrolysis and to further increase its shelf life, it is kept in aqueous solution. NaOH is commonly used to maintain $NaBH_4$ in alkaline conditions and to restrain its self-hydrolysis. As shown in Figure 4.3, increase in concentration of NaOH increases HGR. At very high concentration of NaOH, HGR decreases due to rise in alkalinity of the solution. The concentration of NaOH for further studies is selected as 1.61 moles/L as between 1.6 to 3.5 moles/L NaOH hydrogen generation rate is almost constant.

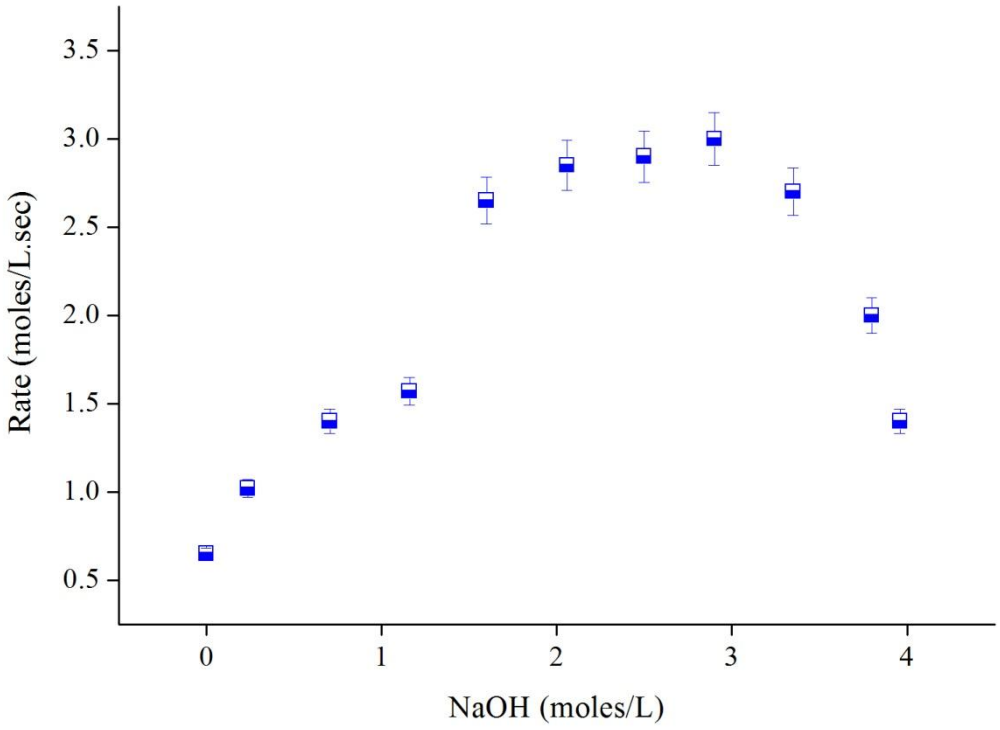

Figure 4.3: Variation of HGR with NaOH concentration

This result is supported by mechanism developed by Holbrook and Twist (2008) for basic medium with cobalt and nickel boride catalysts for $NaBH_4$ hydrolysis. They stated that presence of NaOH leads to formation of BH_3OH^- ions in the solution. They assumed that it has similar reactivity as of BH_4^- ions and release protons in similar way as BH_4^- ion releases. Non noble catalysts (Co and Ni) do not bind itself strongly with hydrogen therefore, with increase in NaOH concentration formation of BH_3OH^- ions increases and protons are released in the solution at higher rate. Thus, increase the rate of reaction with increase in NaOH concentration. Noble catalysts (ruthenium) have strong affinity for hydrogen ions and

prevent the reduction of BH_3OH^- ions in the solution and therefore, rate decreases with increase in NaOH concentration.

In present system $CoCl_2$ being non noble catalyst does not bind itself with hydrogen and BH_3OH^- ions reduce itself with release of protons in the solution. Thus, HGR increases with increase in NaOH concentration.

Effect of $CoCl_2$ concentration on HGR

Increase in concentration of $CoCl_2$ results is increase in HGR as shown in Figure 4.4. Hydrogen generation is also observed at higher concentrations (0.036 and 0.040 moles/L) of $CoCl_2$. It is depicted that hydrogen generation rate increases with increase in catalyst concentration. The reason behind this is increase in catalytic sites for BH_4^- ions to react and release hydrogen. Moreover, contact time between $NaBH_4$ and catalyst is also increased that eventually promotes hydrogen generation rate (Wang et al.,2016). As discussed earlier, higher reactivity of specifically $CoCl_2$ as catalyst is also due to its high diffusion coefficient and higher solubility as compared to other cobalt based salts.

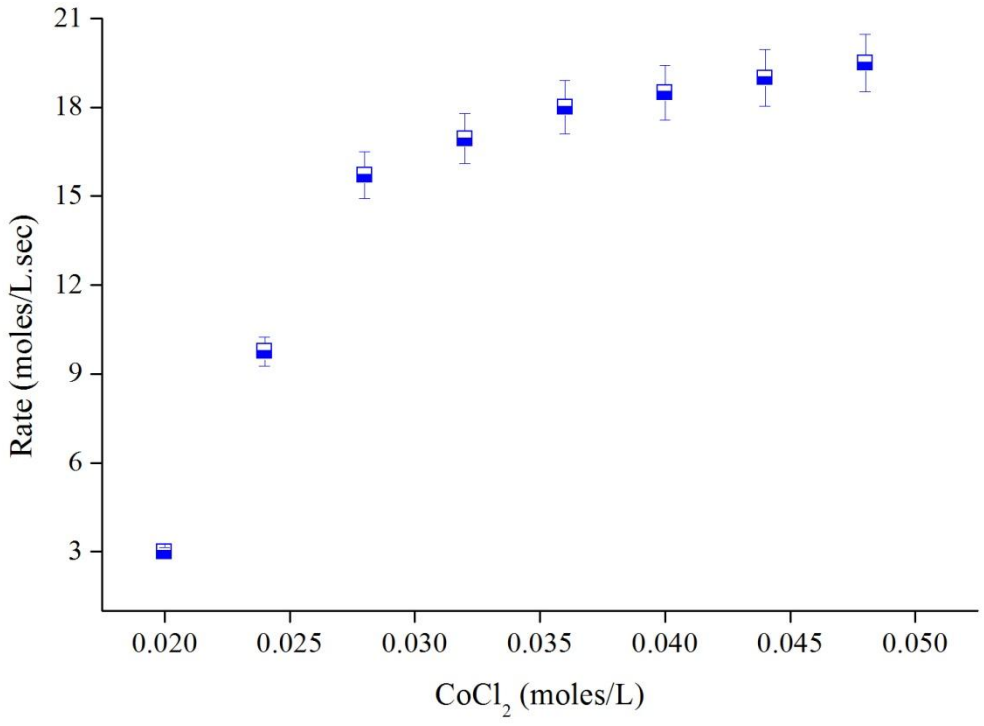

Figure 4.4: Variation of HGR with $CoCl_2$

At very high concentrations reaction becomes highly vigorous (greater than 0.040 moles/L) therefore, no further observations were observed with increase in catalyst concentration in the solution due to safety concerns.

Additionally, concentration of $CoCl_2$ for further study is selected on the basis of fast and vigorous nature of reaction and to obtain the substantial data for kinetic study that is effect of $NaBH_4$ concentration on hydrogen generation, catalyst concentration is selected as 0.02 moles/L.

Effect of $NaBH_4$ concentration on HGR

Reaction rate is highly dependent on $NaBH_4$ concentration. Effect of $NaBH_4$ on HGR is determined by performing series of experiments and varying the initial concentration of $NaBH_4$ and keeping the NaOH (1.6 moles/L) and $CoCl_2$ (0.02 moles/L) constant. On increasing the concentration of $NaBH_4$, reactant concentration increases and number of collisions between molecules increases, consequently increasing rate of reaction.

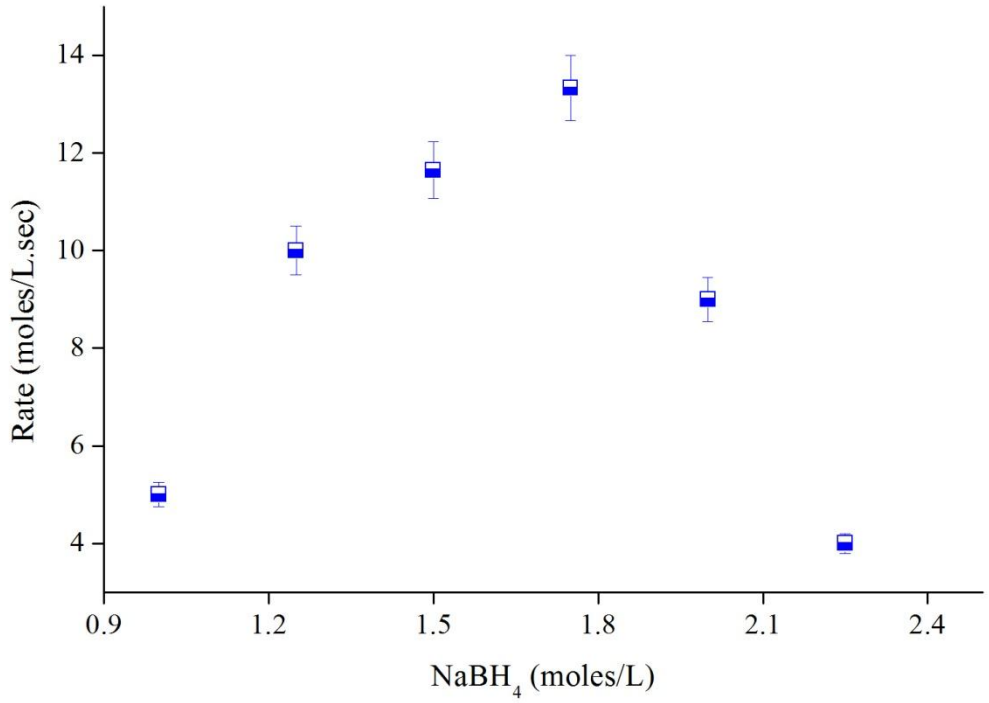

Figure 4.5: Variation of HGR with $NaBH_4$

As shown in Figure 4.5, HGR increases with increase in $NaBH_4$ concentration at constant NaOH and $CoCl_2$ concentrations. But at larger concentrations of $NaBH_4$ (2.00 and 2.25 moles/L) hydrogen generation rate decreases. The reason behind this is initially at lower concentrations of $NaBH_4$ the contact time between BH_4^- ions and catalyst is higher, as concentration of $NaBH_4$ increases formation of sodium metaborate byproduct is high and it probably blocks the reactive sites of catalyst thus, lowering hydrogen generation rate (Ding et al., 2010).

The results of hydrogen generation rate with addition of catalyst are 5, 10, 11.65, 13.39 moles/L.sec at 1.00, 1.25, 1.50 and 1.75 moles/L of $NaBH_4$. The values of HGR are higher than predicted without catalyst.

4.3.3. Kinetics

Various models are studied with respect to $NaBH_4$ based hydrolysis system like zero order, first order, second order, power law model, Langmuir-Hinshelwood model and Michaelis and Menton models (Retnamma et al., 2011). Zero order kinetic model is based on linear behavior of hydrogen generation volume with fixed concentrations of $NaBH_4$, NaOH and catalyst. Zero order kinetic model could not be implemented for practical H_2 generation systems because usually zero order kinetics shifts from zero order to non-zero order with respect to $NaBH_4$ concentrations due to byproduct formation and increase in water consumption (Amendola et al., 2000 a; Amendola et al., 2000 b; Ingersoll et al., 2007; Liu et al., 2006; Xu et al., 2008). First order and second order kinetic models give the dependence on catalyst and $NaBH_4$ concentrations and could not relate HGR with NaOH. This limits its practical considerations.

Langmuir-Hinshelwood model is based on assumption of constant $NaBH_4$ and NaOH concentrations and Michaelis and Menton model is based on constant NaOH and temperature consideration thus limiting its practical use. On the other hand, power law kinetic model is based on concentration of catalyst, $NaBH_4$ and NaOH. This model could predict order with respect to each factor independently. It does not require any assumption hence, making it useful for practical applications (Retnamma et al., 2011).

Considering the drawbacks of various above discussed kinetic models, present kinetic studies are based on power law kinetic model. HGR is observed with the variation of $NaBH_4$ concentration, catalyst concentration, NaOH concentration. The order for each reactant is calculated with individual rate constants. The power law kinetic model fits very well in concern to the practical application for present hydrogen generation system. This is first model to our best knowledge reported so far that deals with kinetics of NaOH in the $NaBH_4/H_2O$ based HG system with $CoCl_2$ as catalyst.

Kinetic analysis is performed according to power law kinetic model using equation 2.11. The rate depends on temperature and concentrations of $NaBH_4$, catalyst and NaOH according to the following expression:

$$-4\frac{d[NaBH_4]}{dt} = d\frac{[H_2]}{dt} = k_{overall}[NaBH_4]^a[CoCl_2]^b[NaOH]^c \quad (4.15)$$

Effects of concentrations of sodium borohydride, sodium hydroxide and cobalt chloride on hydrogen generation rate are monitored and overall hydrogen generation rate can be expressed as,

$$r_{H_2} \propto [NaBH_4]^a[CoCl_2]^b[NaOH]^c \quad (4.16)$$

Where, r_{H_2} is hydrogen generation rate in moles/L.sec, [$NaBH_4$] is the concentration of $NaBH_4$, [$CoCl_2$] is concentration of cobalt chloride, [NaOH] is concentration of NaOH in moles/L and a, b, c are the apparent order with respect to $NaBH_4$, $CoCl_2$, NaOH concentrations. On the basis of kinetic studies, the overall order of reaction and activation energy is calculated.

4.4. Rate equations

4.4.1. Rate with respect to $NaBH_4$

Hydrogen generation rate is increases with increase in the concentration of $NaBH_4$ (Figure 4.2); therefore, rate of hydrogen generation could be expressed as equation 4.17.

$$r_{H_2[NaBH_4]} = k_1[NaBH_4]^a \quad (4.17)$$

Here $r_{H_2[NaBH_4]}$ is rate of hydrogen generation and k_1 is rate constant with respect to $NaBH_4$ with concentrations of other components constant. Hydrogen generation (HG) versus time graph is plotted as shown in Figure 4.6(a). Plotting the HGR versus $NaBH_4$ on logarithmic scale (Figure 4.6 b), the order of reaction is calculated as 1.5 and k_1 is calculated as 6 $(sec)^{-1}$(L/moles). The results are observed at pH of solution between 8 to10.

These results are in agreement with the results obtained by Patel et al. (2008). They reported first order kinetics with respect to $NaBH_4$ for basic $NaBH_4$ solution (pH = 13) with Pd/C catalyst. Dai et al. (2008) observed kinetics of $NaBH_4$ hydrolysis reaction with Co-B catalyst supported on Ni foam. They observed that initially HG increases linearly with time but as the reaction proceeds, HG curve deviates from linear relationship.

On similar terms, it is observed that as the reaction proceeds and concentration of reactants decreases in the solution and eventually hydrogen gas evolution become less. This can be explained by the mechanism proposed by Zahmakiran and Ozkar (2006) as they stated that

borohydride anion initiates hydrolysis reaction by attacking hydronium ion that results in release of proton in the solution. With time, concentration of reactants decreases thus decreasing proton concentration in the solution that decreases HGR. Thus kinetics of the system is dependent on $NaBH_4$ concentration.

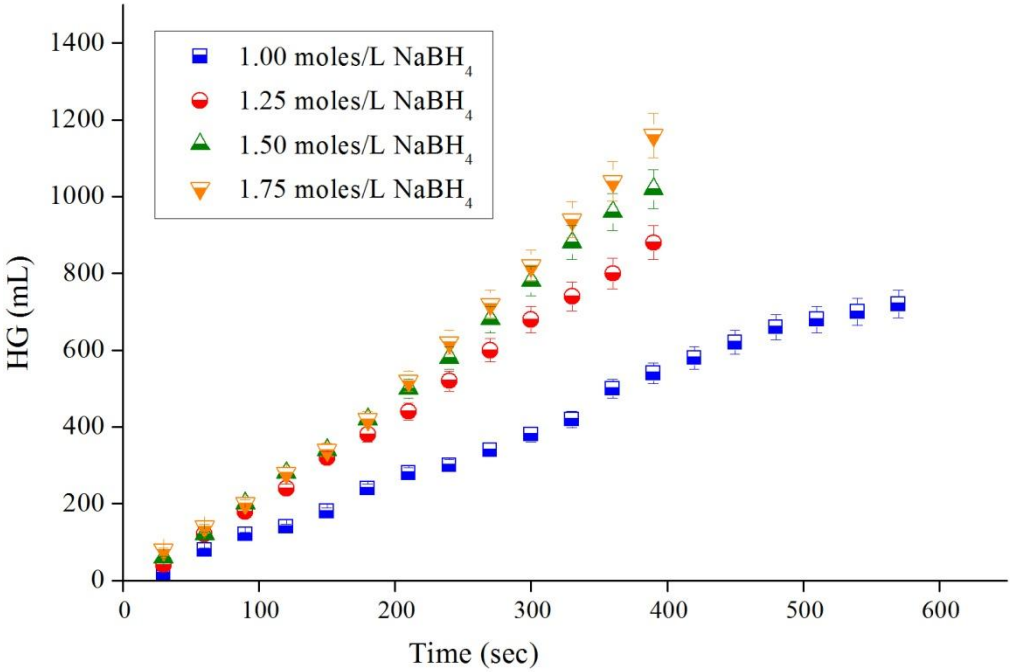

Figure 4.6 (a): Hydrogen generation as a function of time with different $NaBH_4$ concentrations

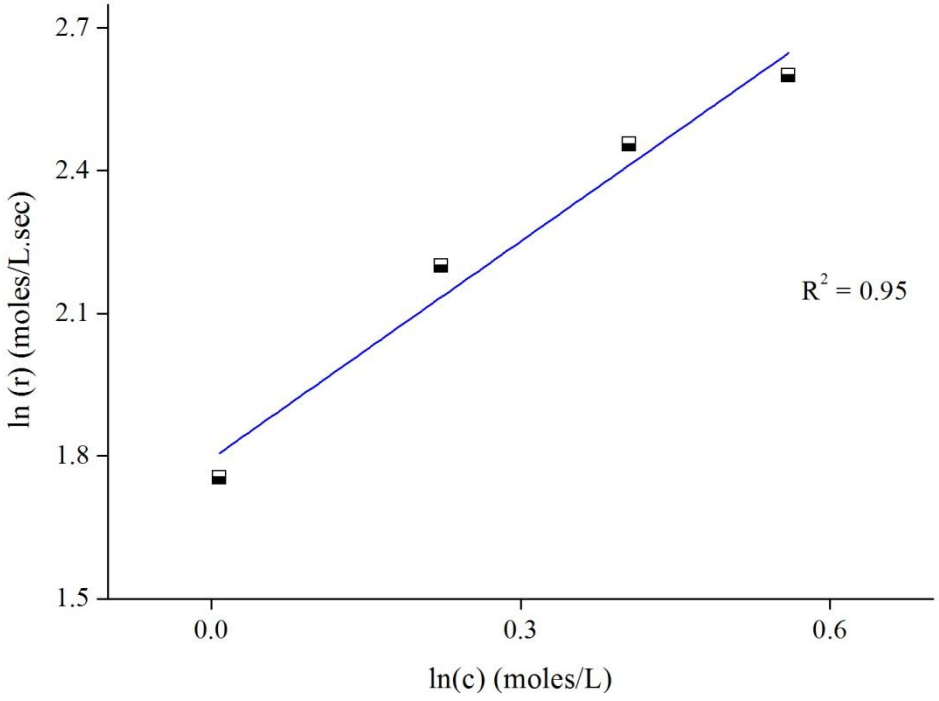

Figure 4.6 (b): Hydrogen generation rate as a function of $NaBH_4$ concentration

Results in the present study are also supported by the orders reported by different researchers for $NaBH_4$ using power law kinetic model. For example, Levy et al. (1960) investigated kinetics of dilute $NaBH_4$ solutions at temperature range from 20 to 35°C with $CoCl_2$ as catalyst. They reported order of 0.34 for $NaBH_4$. Shang and Chen (2006) reported first order kinetics for $NaBH_4$ with ruthenium supported on carbon as catalyst. Patel et al. (2009) investigated kinetics with $NaBH_4$ solutions at temperature range between 25-40°C with Co-P-B catalyst and reported order of 0.07 for $NaBH_4$.

On contrary, zero order kinetics is also reported by various researchers with ruthenium based catalyst, for example Ru metal, Ru(0) nanoclustures and acetate stabilized ruthenium(0) nanoclusters (Amendola et al., 2000b; Ozkar and Zahmakiran, 2005 and Zahmakiran and Ozkar, 2006). They predicted that hydrogen generation volume increased linearly with time at fixed concentration of $NaBH_4$, catalyst and NaOH. These results are reported at high $NaBH_4$/catalyst concentrations (Retnamma et al., 2011).

As a result, it can be concluded that kinetics with respect to $NaBH_4$ could be zero order or non-zero order and is dependent on $NaBH_4$/catalyst concentrations. At low $NaBH_4$/catalyst concentrations, reactants are consumed with time and converted to products thus resulting in non-zero order reaction kinetics, whereas at high $NaBH_4$/catalyst concentrations catalyst provides enough number of reacting sites to $NaBH_4$ and HG increases linearly with duration of time thus forming zero order kinetics with respect to $NaBH_4$.

4.4.2. Rate with respect to $CoCl_2$

Rate kinetics as a function $CoCl_2$ concentration is calculated according to the rate equation (4.18),

$$r_{H_2[CoCl_2]} = k_2[CoCl_2]^b \qquad (4.18)$$

Here $r_{H_2[CoCl_2]}$ is rate of hydrogen generation and k_2 is rate constant with respect to $CoCl_2$ concentration. Hydrogen generation versus time plot for different $CoCl_2$ concentrations and at constant $NaBH_4$ (1.25 moles/L) and NaOH (1.6 moles/L) concentrations is shown in Figure 4.7(a). Plotting the HGR versus $CoCl_2$ on logarithmic scale in Figure 4.7(b), slope calculated is 2. The order of reaction with respect to $CoCl_2$ is 1.7 with rate constant 4.9×10^3 $(sec)^{-1}$ $(L/mole)^{0.7}$.

Order with respect to the catalyst ($CoCl_2$) concentration is 1.7 shows that this system is highly dependent on catalyst concentration and the order calculated is in similar terms as given in literature discussed below. It gives an idea that increase in catalyst concentration increases active sites of the catalyst, thus increasing HGR and making the system dependent on catalyst concentration. It is also observed that at very high catalyst concentration, reactants are consumed rapidly and reaction ceases after short duration.

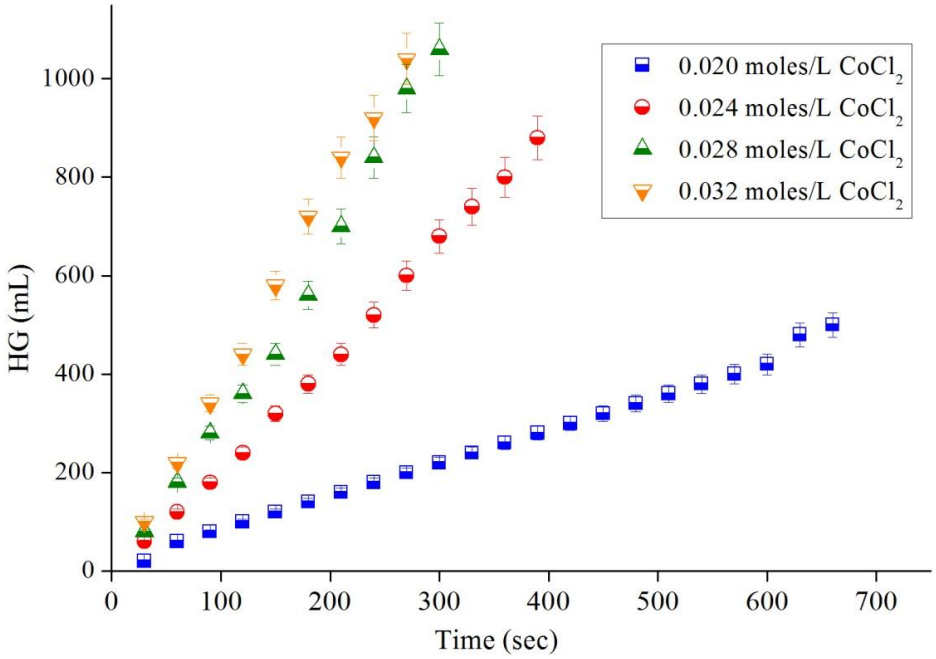

Figure 4.7 (a): Hydrogen generation as a function of time with different $CoCl_2$ concentrations

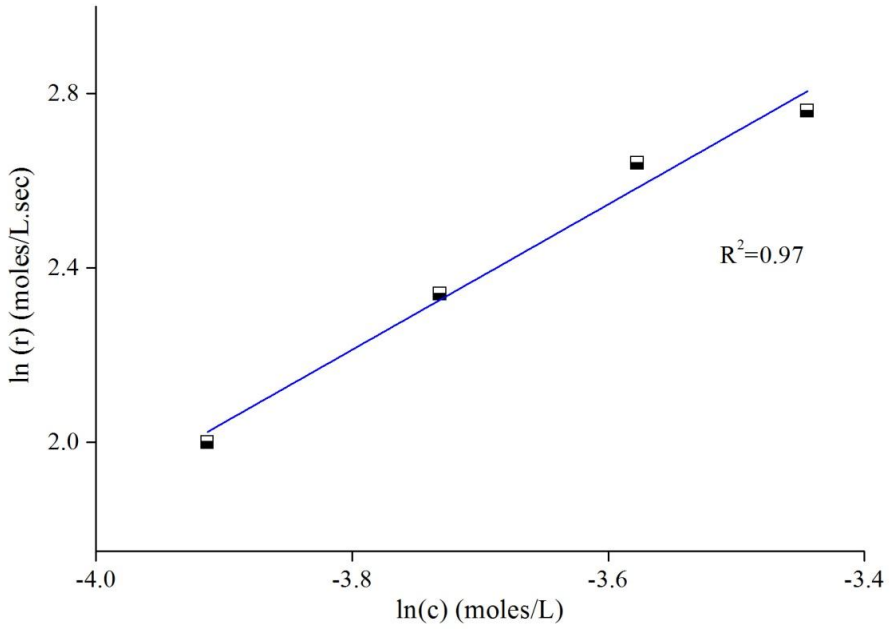

Figure 4.7 (b): Hydrogen generation rate as a function of $CoCl_2$ concentration

These results are supported with results of Guella et al. (2006), Levy et al. (1960), Metin and Ozkar (2009), Ozkar and Zahmakiran (2005), Zahmakiran and Ozkar (2006). They found first order kinetic dependence on catalyst with $CoCl_2$, Ru, Pd-C catalyst, Ni catalyst and PVP-stabilized cobalt(0) nanoclusters. Similarly, Demici and Garin (2008) confirmed that HG increases with increase in catalyst concentration with Ru-promoted sulphated zirconia catalyst and reported the order of 1.27. Similar observations are made by Fernandes et al. (2009) with (Co-P-B) based catalyst with order of 1.05.

4.4.3. Rate with respect to NaOH

Rate is represented by the following rate equation (4.19),

$$r_{H_2[NaOH]} = k_3[NaOH]^c \qquad (4.19)$$

Here $r_{H_2[NaOH]}$ is rate of hydrogen generation and k_3 is rate constant with respect to NaOH concentration. Hydrogen generation versus time for different NaOH concentrations and at constant $NaBH_4$ (1.25 moles/L) and $CoCl_2$ (0.02 moles/L) concentrations is demonstrated in Figure 4.8(a).

Plotting the HGR versus NaOH concentration graph on logarithmic scale is shown in Figure 4.8(b), the slope calculated is 0.84. Thus, the order of reaction with respect to NaOH is 0.84 with rate constant 5.9 $(sec)^{-1}$ $(mole/L)^{0.16}$. It is observed from literature that HGR varies with NaOH according to the nature of catalysts (noble and non-noble) (Walter et al., 2008). For example, zero order kinetics is reported in basic medium for noble zeolite-confined ruthenium(0) nanoclusters catalyst (Zahmakiran and Ozkar, 2009).

The order changes from first order in aqueous medium to zero order in basic medium with water-soluble polymer-stabilized cobalt nanoclusters(0) catalyst (Metin and Ozkar, 2009).

Furthermore, both positive and negative orders are monitored with NaOH depending on the catalyst used in hydrogen generation system. Demirci and Garin (2008) investigated negative order (−0.35) for NaOH with Ru-promoted sulphated zirconia catalyst and Fernandes et al. (2009) stated that the order is 0.12 with (Co-P-B) based catalyst. Additionally, it is also observed that HGR increases with increase in NaOH till solution becomes highly alkaline.

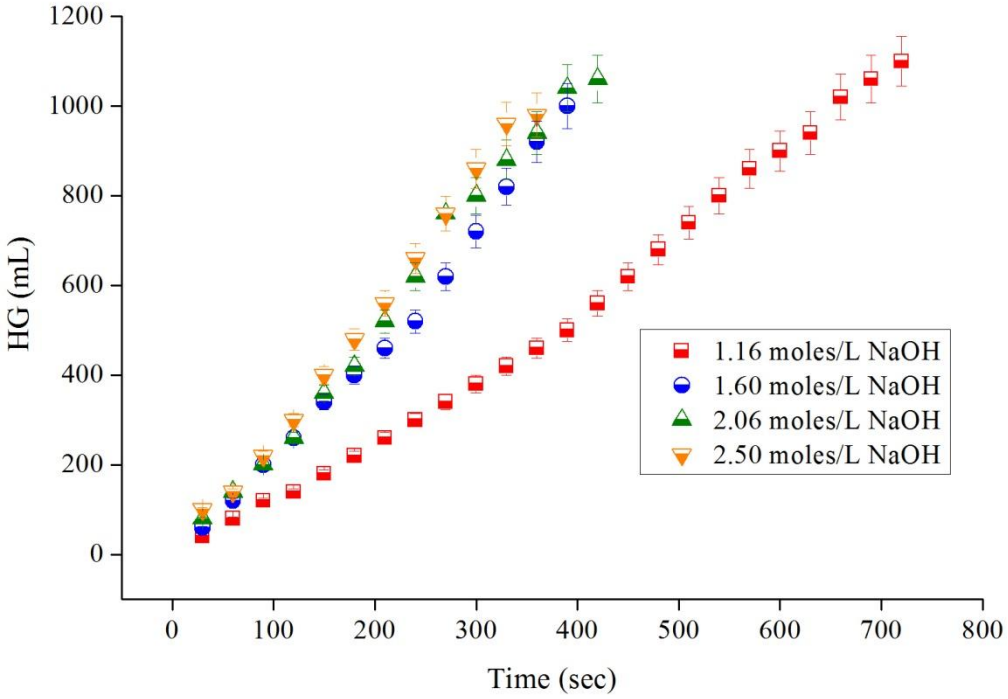

Figure 4.8 (a): Hydrogen generation as a function of time with different NaOH concentrations

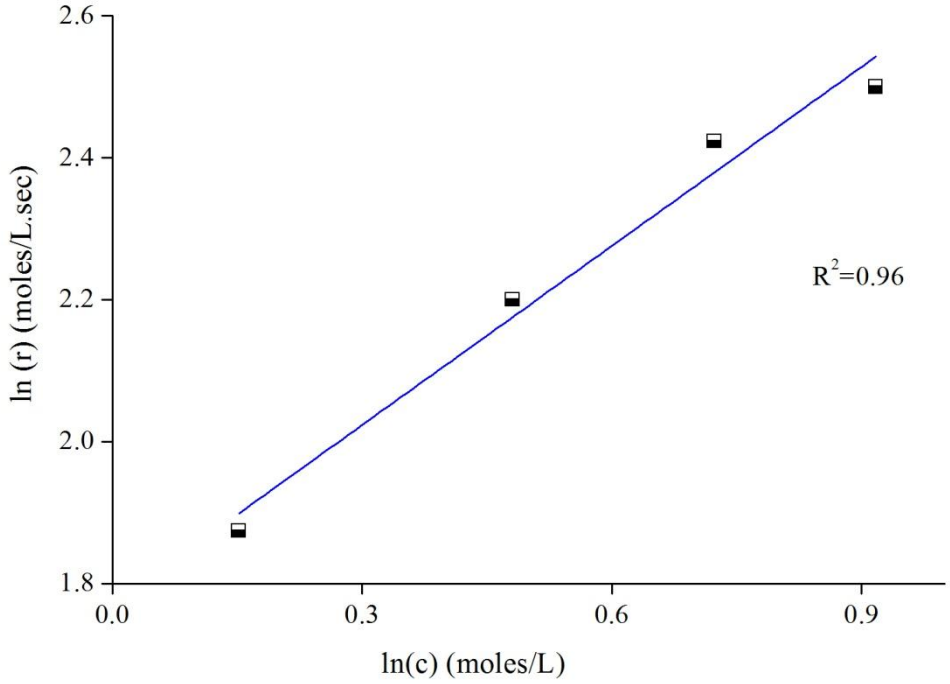

Figure 4.8 (b): Hydrogen generation rate as a function of NaOH concentration

It could be concluded from the results that order of reaction is highly based on nature of catalyst and in the present system non noble catalyst ($CoCl_2$) is used that does not bind itself with hydrogen and promotes the release of protons in the solution with increase in NaOH

concentration, thus increasing HGR and hence overall kinetics of the system is dependent on NaOH.

The overall rate of the system could be expressed as equation 4.20.

$$r_{H_2} = k_{overall}[NaBH_4]^{1.5}[CoCl_2]^{1.7}[NaOH]^{0.84} \quad (4.20)$$

4.4.4. Effect of temperature on HGR

Temperature indicates the kinetic energy of a system. Higher temperature implies higher average kinetic energy of molecules and more collisions occurring per unit time. Acceleration of H^+, OH^-, BH^{4-} and Cl^- ions is directly related to temperature of hydrolysis reaction (Walter et al., 2008). The reaction rate is expected to increase with increase in temperature as indicated by slope of the line shown in Figure 4.9 (Arrhenius plot).

HGR is investigated at different temperatures and at constant $NaBH_4$ (1.25 moles/L), NaOH (1.6 moles/L) and $CoCl_2$ (0.02 moles/L) concentrations. Slope of volume of HG versus time

graph gives the rate at each temperature (293, 303, 313 and 323 K) therefore, $k_{overall}$ is calculated at different temperatures. Different k values against temperature are shown in Table 4.2.

Table 4.2: Values of $k_{overall}$ at different temperatures

S. No.	T (K)	$k_{overall}$	(1/T)	ln ($k_{overall}$)
1.	293	210×10^4	0.0034	14.56
2.	303	323×10^4	0.0033	15.02
3.	313	754×10^4	0.0032	15.84
4.	323	998×10^4	0.0031	16.12

ln ($k_{overall}$) versus (1/T) is plotted as shown in Figure 4.9, to calculate the activation energy for the present system. The activation energy is calculated according to equation (4.22).

$$\ln(k_{overall}) = \ln(A) - \frac{E}{RT} \quad (4.22)$$

Here A is pre exponential factor (units of $k_{overall}$), E is apparent activation energy (kJ/mole), R is 8.314 J/mole.K, T is absolute temperature (in Kelvin) and $k_{overall}$ is over all rate constant at each temperature with units $(sec)^{-1}(L/mole)^{4.84}$. The apparent activation energy calculated for the present system is 46 kJ/mole and A is 2.78×10^{14} $(sec)^{-1}(L/mole)^{3.04}$.

The results are compared with the results of other non-noble metal catalysts. The activation energy of bulk metal catalysts like Co is reported to be 75 kJ/mole, for nickel activation energy is 71 kJ/mole and for Raney nickel, it is 63 kJ/mole (Zahmakiran and Ozkar, 2006). The results are also compared with results of Demirci et al. (2008) using Ru-promoted sulphated zirconia catalyst. The activation energy of this system was 76 kJ/mole. Zang et al. (2007) reported activation energy of 52 kJ/mole by using Ni-supported bimetallic catalyst for hydrolysis of $NaBH_4$. Thus the activation energy of this system is lower than all the above stated systems.

Low activation energy for this system is due to strong catalytic activity of hydrated Co salt. Co based salts induce a violent reaction and comparatively fast hydrogen generation kinetics at lower temperatures compared to Ni and Ru based catalyst (Liu et al., 2006). Thus the value of the activation energy of this system varies favorably as compared with other systems.

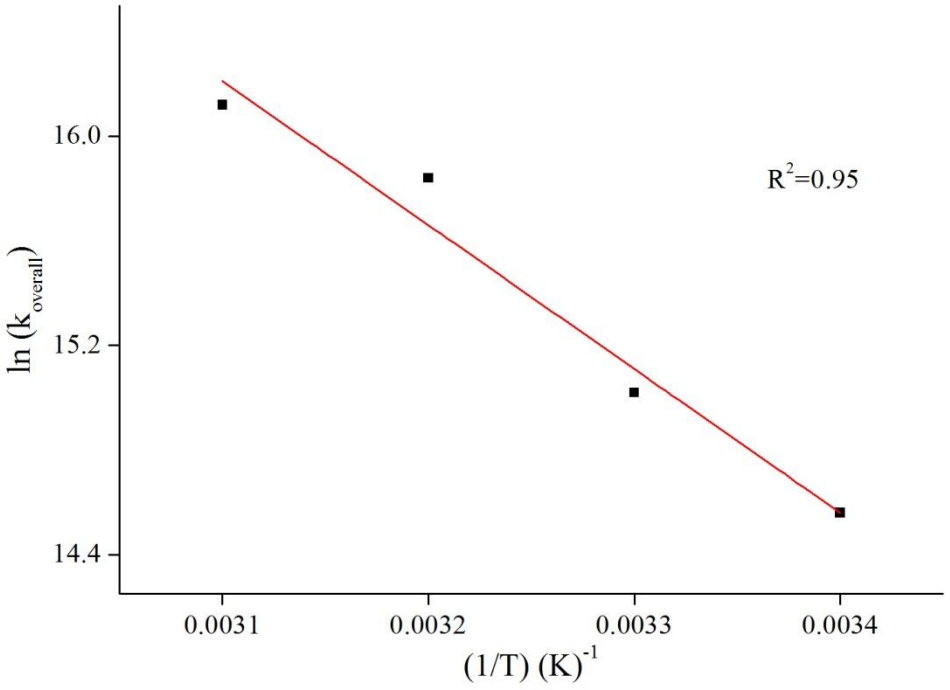

Figure 4.9: Arrhenius plot of $\ln(k_{overall})$ versus (1/T)

4.5. Characterization of the residue from $NaBH_4/H_2O$ system with $CoCl_2$ as catalyst

The morphology of black colored solid residue formed after hydrolysis reaction of $NaBH_4$ in presence of $CoCl_2$ catalyst is conducted by SEM and the images are shown in Fig. 4.10(a, b, c and d). The particles are observed to agglomerate together and the rough surface indicates the presence of cobalt (Demirci et al., 2010).

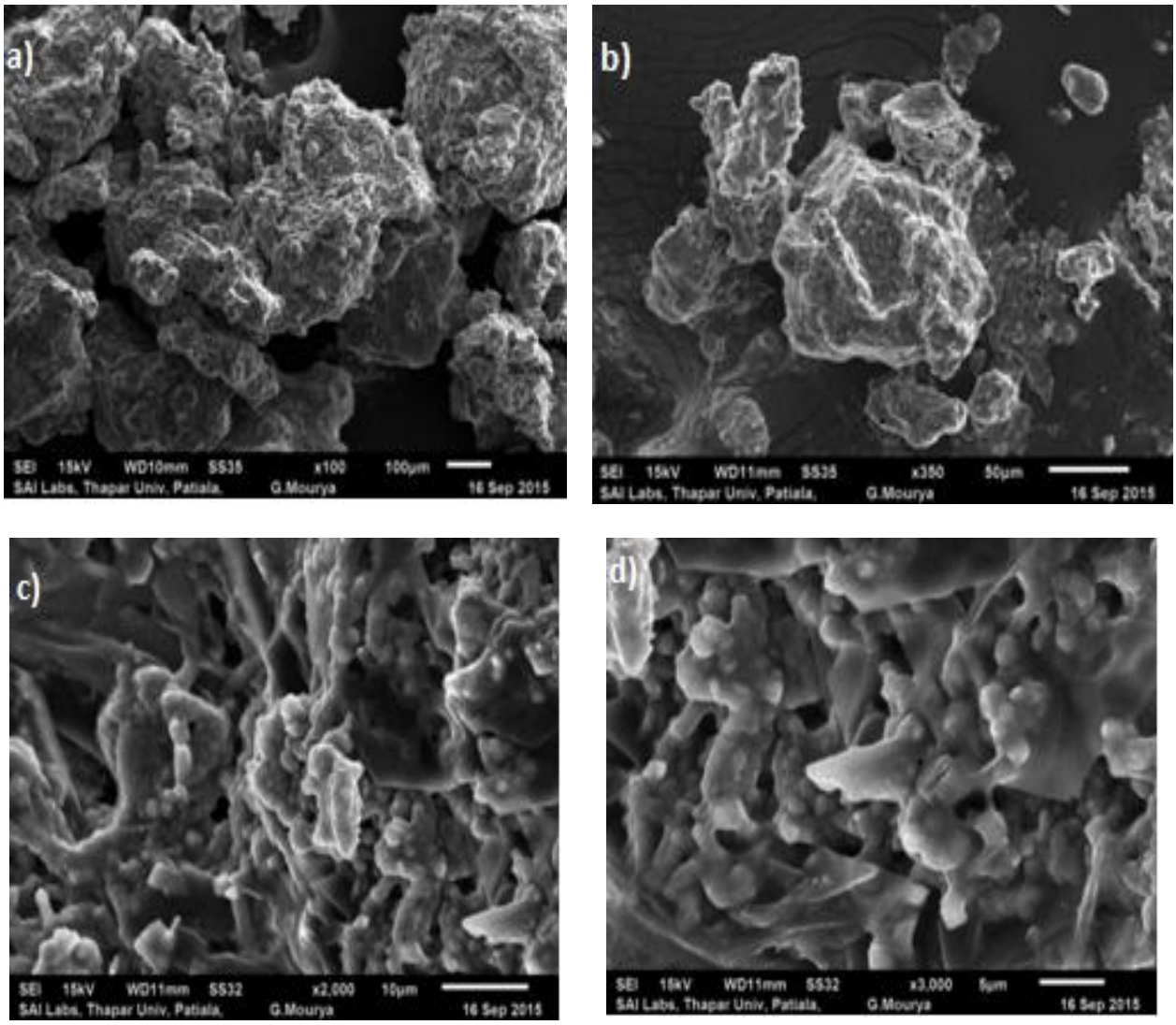

Figure 4.10 (a, b, c and d): SEM images of the residual material

EDS analysis of residual material's surface (Figure 4.11) provides the quantitative information about its elemental composition. Elemental percentages of byproducts of $NaBH_4$ hydrolysis is given in Table 4.3.

It is observed that boron (78.46 wt%) is present in maximum percentage in the residue followed by oxygen (18.01 wt%), sodium (3.41 wt%), chlorine (0.07 wt%) and cobalt (0.05 wt%). It is predicted from results of EDS analysis that boron is present in maximum percentage, this is further verified by XRD analysis. As observed in XRD analysis, boron based compounds are formed in the residue with maximum percentage that justifies EDS results.

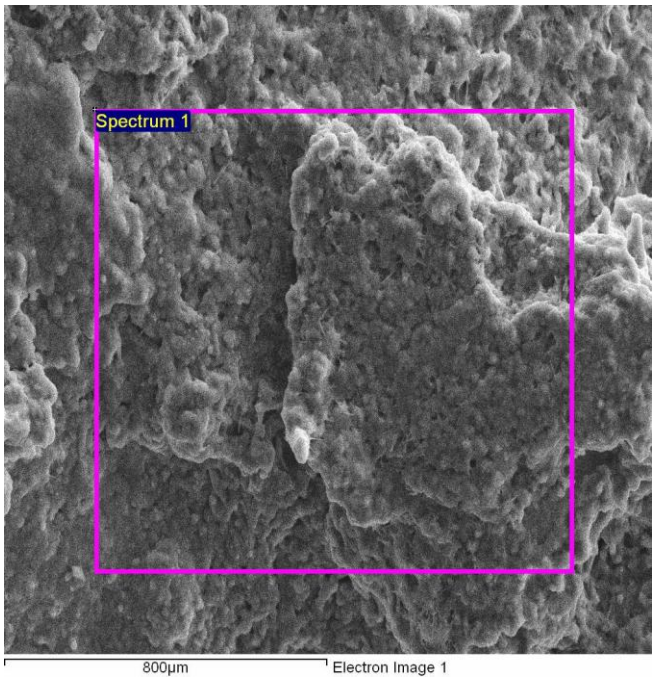

Figure 4.11: Sectioned area of residual material for EDS analysis

Table 4.3 Elemental analysis of residual material

S. No.	Element	Weight (%)	Atomic (%)
1.	B	78.46	85.04
2.	O	18.01	13.19
3.	Na	3.41	1.74
4.	Cl	0.07	0.02
5.	Co	0.05	0.01

According to literature, cobalt boride (Co_2B, Co_3B) and other Co-B compounds with different degrees of oxidation are expected to be present in residue obtained after hydrolysis of $NaBH_4$ in presence of $CoCl_2$ catalyst (Glavee et al., 1993). The presence of cobalt boride confirms the presence of active catalytic site for $NaBH_4$ hydrolysis.

These compounds are reported to be amorphous mixture of Co-B based catalysts having varying cobalt, boron and oxygen contents (Arzac et al., 2011). The amorphous state of cobalt based catalyst is highly crucial for its reactivity. The X-ray diffraction peaks around 2θ range between 40^o and 50^o are assigned to cobalt borides (Co_xB) or metallic Co^o phases (Boss et al., 2015).

Similar results are observed from XRD analysis (Figure 4.12) of residual material. Diffraction peaks around $2\theta = 45^o$ confirms the presence of Co_2B (ICDD No. 01-089-1994)

(Demirci and Miele, 2014). Other Co-B based compound like cobalt borate $Co_2B_2O_5$ (ICDD No. 01-073-1772) and Na based byproducts like sodium borate hydrate oxide $Na_2B_4O_7.10H_2O$ (ICDD No. 01-088-1411) and sodium boride Na_3B_2O (ICDD No. 00-012-0) are also present in residue.

The boron based compounds are formed with maximum percentage that justifies EDS analysis results. Reduction activity by cobalt is observed with the formation of cobalt borate, sodium borate hydrate oxide and sodium boride. Therefore, it could be concluded that highly active species Co_xB reduce $NaBH_4$ efficiently and help in release of hydrogen from the solution.

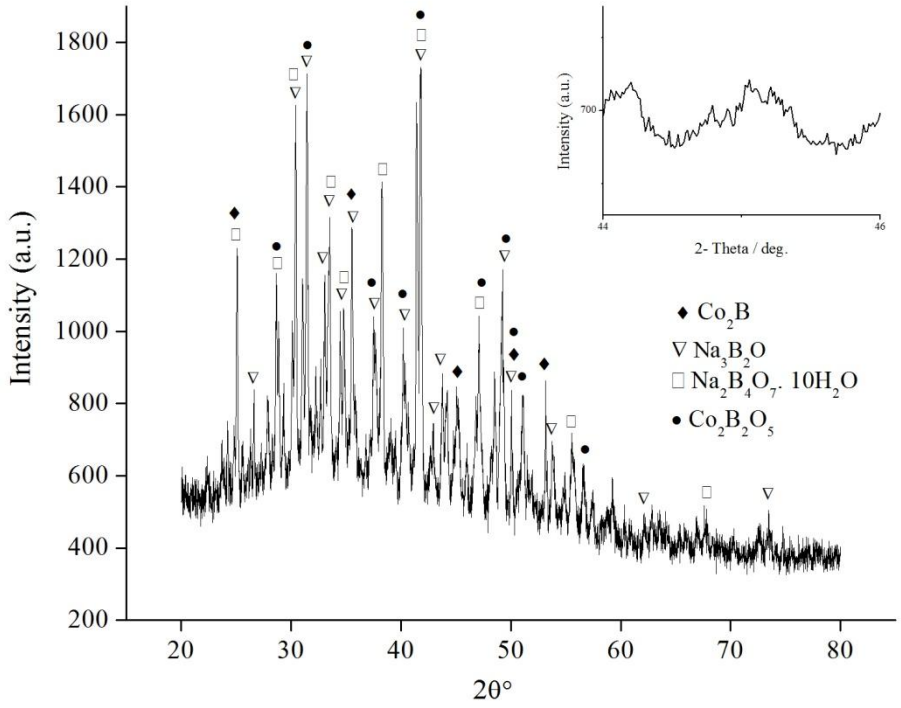

Figure 4.12: XRD analysis of residual material

4.6. Theoretical and experimental hydrogen capacities

To optimize present system for maximum HG, efficiencies are calculated at different concentrations of $NaBH_4$. Theoretical and experimental hydrogen densities are calculated on the basis of moles of hydrogen released from sodium borohydride hydrolysis reaction. As in equation 2.11, 4 moles of H_2 is generated from 1 mole of $NaBH_4$ and 2 moles of H_2O. Molecular weight of $NaBH_4$ is 37.87 g/mole, H_2 is 2 g/mole, H_2O is 18.02 g/mole. Therefore, gravimetric theoretical H_2 capacity of $NaBH_4$ can be calculated is 10.8 wt% (Murooka et al., 2012).

Experimental hydrogen amount is calculated on gram basis with modified form of Equation 2.11, which is equation 4.23 given below (Dai et al., 2011).

$$1g\ NaBH_4 + 0.95\ g\ H_2O \rightarrow 0.21g\ H_2 \quad (4.23)$$

The calculations are performed at constant $CoCl_2$ and NaOH concentrations. The theoretical and experimental hydrogen capacities and efficiencies of $NaBH_4/H_2O$ system at different concentrations of $NaBH_4$ are summarized in Table 4.4.

Table 4.4: Theoretical and experimental H_2 capacities

S. No.	$NaBH_4$(g)	H_2 Density (wt %)		Efficiency (%)
		Theoretical	Experimental	
1.	0.4	10.76	6.6	61
2.	0.5	10.76	7.3	67
3.	0.6	10.76	7.5	69
4.	0.7	10.76	7.9	73

Hydrogen generation capacities of this system at different $NaBH_4$ ratios are compared and it is observed that experimental hydrogen capacity is less than theoretical hydrogen capacity. Thus, this system requires perfection in terms of overall efficiency and in this regard further studies are required to make the system more competent and proficient.

According to kinetic studies carried out in this chapter, it is concluded that $NaBH_4/H_2O$ system with cobalt chloride as catalyst is an efficient HG system. $CoCl_2$ is most probable catalyst as compared with platinum and ruthenium based catalysts that are not suitable for long term use due to the cost issues. Difference in the theoretical and experimental hydrogen capacities creates a necessity to study this system for high overall efficiency. Kinetics of this system could be enhanced by addition of a catalyst promoter. Studies with different catalyst promoters are discussed in the next chapter.

CHAPTER 5

Hydrogen generation from $NaBH_4/H_2O$ system: effects of catalyst and promoters

5.1. Introduction

Effectiveness of the catalyst promoter is directly related to its surface area and particle size. Smaller particle size of promoter provides more reactive sites to the catalyst to bind. Thus, contact time of reactant increases with the catalyst leading to better dispersion and reactivity. Therefore, use of promoter with high surface area gives substantial route to achieve better reactivity of reactant with catalyst. Moreover, promoter added to the system also helps to reduce the cost of the catalyst. $NaBH_4$ could easily reach the reactive sites of the catalyst and byproducts could leave active sites smoothly. Consequently, the concept of adding a support or promoter to the catalyst enhances the overall hydrogen generation of the system.

Various catalyst promoters such as γ-Al_2O_3 nanoparticles, γ-Al_2O_3 particles, CNT, MMT clay, SiO_2, zeolite and zirconia sand are compared with respect to hydrogen generation (HG) and hydrogen generation rate (HGR). After selection of most efficient promoter comparative studies are performed on various other catalysts based on salts like $CoSO_4.7H_2O$, $(CH_3COO)_2Co.4H_2O$, $Co(NO_3)_2.H_2O$, $CdSO_4$, $CuSO_4.5H_2O$.

5.2. Methods

The equipment used in H_2 generation experiment is described in experimental section. Reagents are added to 250 mL three neck glass reactor in predetermined amounts in powdered form. The concentration of $NaBH_4$ and NaOH added is fixed as 1.26 moles/L and 0.93 moles/L, respectively.

Table 5.1: Properties of promoters (Marek, 2009 and Vyas et al., 2004).

S. No.	Promoter	Surface area (m^2/g)	Point of zero charge
1.	γ- Al_2O_3 (nanoparticles)	180	9
2.	γ- Al_2O_3 particles	100	9
3.	CNT	40-600	11.9
4.	MMT clay	250	2.7
5.	Silica	175-225	2
6.	Zeolite (13X)	571	6.5-7.5
7.	Zirconia sand	1	7

While performing comparative studies the concentration of chemicals selected as catalysts and promoters is fixed as 0.02 moles/L and 0.12 moles/L, respectively. Ten mL solution of NaOH is added by pressure equalizing funnel connected to the middle port of reactor. H_2 generated is collected in inverted cylinder through a plastic tube attached to the right hand port of reactor as described in Figure 2.1 in experimental section.

5.3. Comparison among different promoters

Different promoters namely γ-Al_2O_3 nanoparticles, γ-Al_2O_3 particles, CNT, MMT clay, SiO_2, zeolite and zirconia sand are evaluated for HG as shown in Figure 5.1. It is observed that γ-Al_2O_3 nanoparticles give higher HG than other promoters.

It could be due to better reactivity of reactants with γ-Al_2O_3 nanoparticles which in turn is caused by high surface area, hydrophilic and amorphous nature of γ-Al_2O_3 nanoparticles. Comparison among different promoters with respect to maximum HGR is shown in Table 5.1. With respect to maximum HGR following order is observed for promoters: γ-Al_2O_3 nanoparticles > zeolite > MMT clay > CNT > zirconia sand > γ-Al_2O_3 particles > silica.

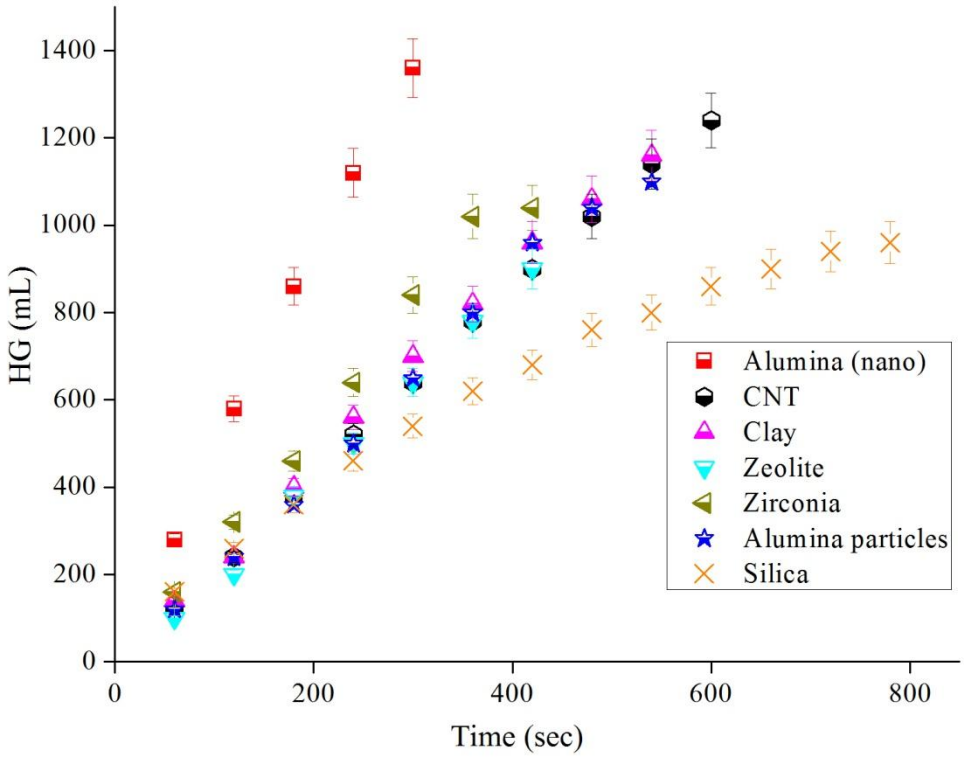

Figure 5.1: Hydrogen generation (HG) using different promoters with $CoCl_2.6H_2O$ as catalyst

Table 5.2: HGR using different promoters (with $CoCl_2$ as catalyst)

S. No.	Promoter	Maximum HGR (moles/L.sec)
1.	γ- Al_2O_3 (nanoparticles)	19.47
2.	γ- Al_2O_3 particles	8.46
3.	CNT	9.97
4.	MMT clay	11.24
5.	Silica	7.01
6.	Zeolite (13X)	12.57
7.	Zirconia sand	9.81

These results are supported by studies carried out by Demirci et al. (2010) between γ-Al_2O_3 and active carbon. They reported that though γ-Al_2O_3 and active carbon have high surface area, γ-Al_2O_3 exhibits higher HGR than active carbon on account of its hydrophilic character as compared to hydrophobic nature of carbon. This is an explanation to why Al_2O_3 nanoparticles show high reactivity than CNT (Rajoria et al., 2007)

Chemical behavior of γ-Al_2O_3 is highly dependent on its surface structure. It is known that at least a monolayer of water is chemisorbed by alumina when exposed to moisture at room temperature. When the surface is hydrated, water molecules are chemisorbed at top oxide layer of γ-Al_2O_3 as shown in reaction 5.1(Soler et al., 2009),

$$Al_2O_3 + 3H_2O \rightarrow 2Al(OH)_3 \qquad (5.1)$$

These hydroxyl ions are coordinated in various ways to aluminium cations that represent the reactive functional groups on alumina surface. The formation of two oxide forms (α-Al_2O_3 and γ-Al_2O_3) of alumina is decided by distribution of these hydroxide groups i.e. which OH is exposed to the surface and how aluminium ions are arranged. Additionally, γ-Al_2O_3 is extensively used because of its high catalytic activity.

There are two ways according to which surface hydroxyl groups are coordinated; hydroxyl group with one aluminium ion and hydroxyl groups with two aluminium ions. Singly coordinated hydroxyl group is more basic in nature and the hydroxyl group coordinated with two aluminum ions is highly acidic in nature. This is the reason behind the amphoteric nature

of hydrated alumina i.e. it can adsorb and release protons. Further ionization reactions of hydroxyl groups are described as (Sposito, 1996),

$$AlOH + H^+ = AlOH_2^+,\ AlOH = AlO^- + H^+ \quad (5.2)$$

Therefore, according to the above theory, surface hydroxyl groups in the solution enhance the reactivity or catalytic activity of γ-Al_2O_3 nanoparticles in the present system. The hydroxyl groups are expected to be singly co-ordinated with aluminium ions that could develop the basic nature. The assumption of basic nature of γ-Al_2O_3 is further discussed in the following section.

The solution pH decides the charge and nature of the aluminium oxide (acidic or basic due to amphoteric nature of Al_2O_3). For example according to principle of electroneutrality, in acidic medium the oxide particle will be positively charged and to compensate this charge layer of particles with opposite charge (negative charge) will be present in the solution that will surround the oxide particles.

Similarly, in basic medium, oxide particles will be negatively charged and layer of positively charged particles will be present in the solution that surrounds the oxide particle.

Isoelectric point of oxide further defines the nature of oxide, as γ-Al_2O_3 is amphoteric in nature. Isoelectric point is that value of solution pH when the net oxide particle charge is zero. The isoelectric point of alumina is at pH = 8, this implies alumina will adsorb anions at solution pH less than 8 and adsorb cations at solution pH greater than 8 (Sposito, 1996 and Brunelle, 1978).

The above prediction could be related to the present system as the pH of the solution is greater than 9 and rise in solution pH could cause the adsorption of metal ions on the alumina surface. Therefore, cationic adsorption of Co^{+2} or Na^+ could occur on hydroxide layer of alumina surface that leads to the formation of aluminates in the solution as shown in reaction 5.3 (Fan et al., 2013 and Grenman et al., 2010),

$$Al(OH)_3 + NaOH \rightleftharpoons NaAl(OH)_4 \quad (5.3)$$

Increase in HGR is observed by the formation of aluminates in the system. Na and Co aluminates are formed as predicted by XRD results of residue (given in chapter 6). The polymeric form of aluminate ions like $Na_2Al_{22}O_{34}$ and $CoAl_2O_4$ prevent surface passivation

of aluminum surface. Surface passivation traps H_2O molecules that usually react with metal (Al) and help in release of H_2 in the form of protons (Fan et al., 2013). It could be concluded that if aluminates are present in the solution, surface passivation on aluminium does not occur and the release of hydrogen is at faster rate. This process promotes reaction 5.4 and affects overall HGR of the system (Li et al., 2005, Buchner et al., 1999 and Kanturk et al., 2008).

$$2Al + 6H_2O \rightarrow 2Al(OH)_3 + 3H_2 \quad (5.4)$$

Furthermore, aluminate concentration boosts the deposition process of $Al(OH)_3$ on Co particles and speeds up the formation of highly activated Co/Al complex. This complex enhances HGR by promoting reaction 5.5. Hence, $Al(OH)_3$ acts as a catalyst carrier and promotes the catalytic activity of Co_xB species formed during $NaBH_4$ hydrolysis reaction with $CoCl_2$ as catalyst.

There exists a synergistic catalytic effect between Co and Al for $NaBH_4$ hydrolysis that improves overall HGR (Fan et al., 2013 and Soler et al., 2007),

$$NaBH_4 + 4H_2O \xrightarrow{\text{Catalyst}} NaBO_2.2H_2O + 4H_2 \quad (5.5)$$

Formation of byproduct ($NaBO_2.H_2O$) by the reaction 5.6 significantly affects Al hydrolysis due to its alkaline nature, as increase in alkalinity increases NaOH based reactions (reaction 5.6 and 5.7). This leads to the promotion activity of reaction 5.3 and eventually reaction 5.4 (Liu et al., 2006 and Soler et al., 2009).

$$NaBO_2.2H_2O \rightleftharpoons NaB(OH)_4 \quad (5.6)$$

$$NaB(OH)_4 \rightleftharpoons H_3BO_3 + NaOH \quad (5.7)$$

The above chemical reactions describe that Al_2O_3 (nanoparticles) enhance kinetics of $NaBH_4$ hydrolysis reaction. Presence of Al_2O_3 nanoparticles in the solution improves the catalytic activity of $CoCl_2$ as a catalyst and it significantly promotes overall HGR of the system.

5.4. Comparison among different catalysts

To our best knowledge no study has been reported so far that deals with the comparison among most appropriate catalyst with addition of Al_2O_3. Therefore, after the selection of catalyst promoter, different catalyst namely $CoCl_2.6H_2O$, $CoSO_4.7H_2O$, $(CH_3COO)_2Co.4H_2O$, $Co(NO_3)_2.H_2O$, $CdSO_4$, $CuSO_4.5H_2O$ are evaluated. The results are shown in Figure 5.2.

Not much hydrogen is evolved with $CdSO_4$ and $CuSO_4.5H_2O$. $CoCl_2.6H_2O$ gives maximum HG. Comparison of HGR using different cobalt based salts as catalyst with alumina nanoparticles as promoter is given in Table 5.2. Following order for maximum and overall HGR is observed: $CoCl_2.6H_2O > CoSO_4.7H_2O > (CH_3COO)_2Co.4H_2O > Co(NO_3)_2.H_2O$

Table 5.3: HGR using different cobalt based salts as catalyst (with alumina nanoparticles as promoter)

S. No.	Catalyst	Maximum HGR (moles/L.sec)	Overall HGR (moles/L.sec)
1.	$(CH_3COO)_2Co.4H_2O$	15.49	14.54
2.	$CoCl_2.6H_2O$	19.47	17.89
3.	$Co(NO_3)_2.6H_2O$	11.27	9.66
4.	$CoSO_4.7H_2O$	16.93	16.06

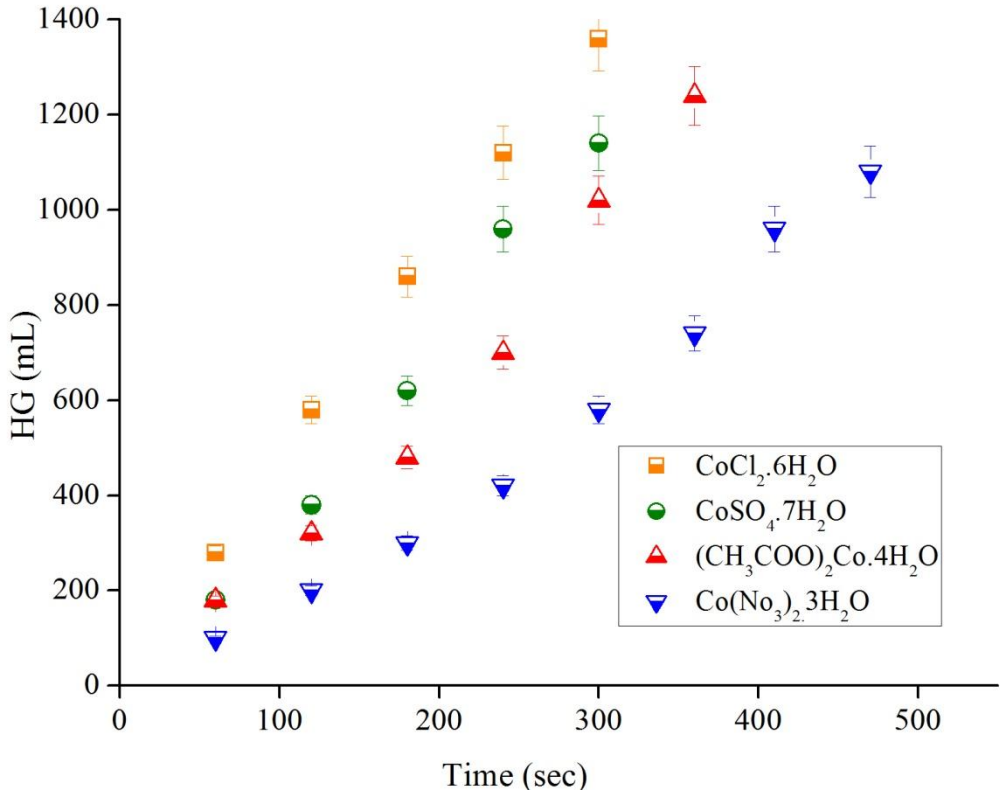

Figure 5.2: Hydrogen generation (HG) using different cobalt based salts as catalysts

Literature reports that the catalytic activity of Co based metal salts are dependent on Co^{+2} cation due to its electrophilic nature that is strongly attracted towards BH_4^- ions from $NaBH_4$, thus enhancing the hydrolysis of $NaBH_4$ (Demirci et al., 2010).

As the cation Co^{+2} is similar among all salts studied in the present work and $CoCl_2$ exhibits high HGR, the anions CH_3COO^-, Cl^-, SO_4^{2-}, NO_3^- could be another factor affecting the catalytic activity of metal catalysts. This is explained by Akdim et al. (2009 a) that maximum solubility of anions in solution, defined by coefficient of diffusivity, is higher for Cl^- ions when compared with anions of other salts. This could be the reason behind high HGR with $CoCl_2$ as compared with other salts. Similar results are observed by Akdim et al. (2009 b) where Co is tested among different cobalt based salts, it is reported that $CoCl_2$ is 4 times more reactive than $Co(CH_3COO)_2$, $CoSO_4$, CoF_2 and $Co(NO_3)_2$ in catalyzing $NaBH_4$ hydrolysis reaction. Additionally, $CoCl_2$ is also compared with $CdSO_4$ and $CuSO_4$ salts and it is observed that no hydrogen is released with $CdSO_4$ while the reaction got terminated with $CuSO_4$ after 10 seconds only. The reason could be the less affinity of Cu^{+2}, Cd^{+3} towards BH_4^-.

5.5. Effect on HG and HGR with varying particle size of γ-Al_2O_3

Comparative studies are performed between γ-Al_2O_3 (100-200 μm), γ-Al_2O_3 (40 nm) and γ-Al_2O_3 (20 nm) to observe the difference in hydrogen generation (HG). Higher HG is observed with γ-Al_2O_3 having particle size of 20 nm than γ-Al_2O_3 having particle size of 40 nm and 100-200 μm as shown in Figure 5.3. Thus, surface area of γ-Al_2O_3 nanoparticles is an important factor that affects HG.

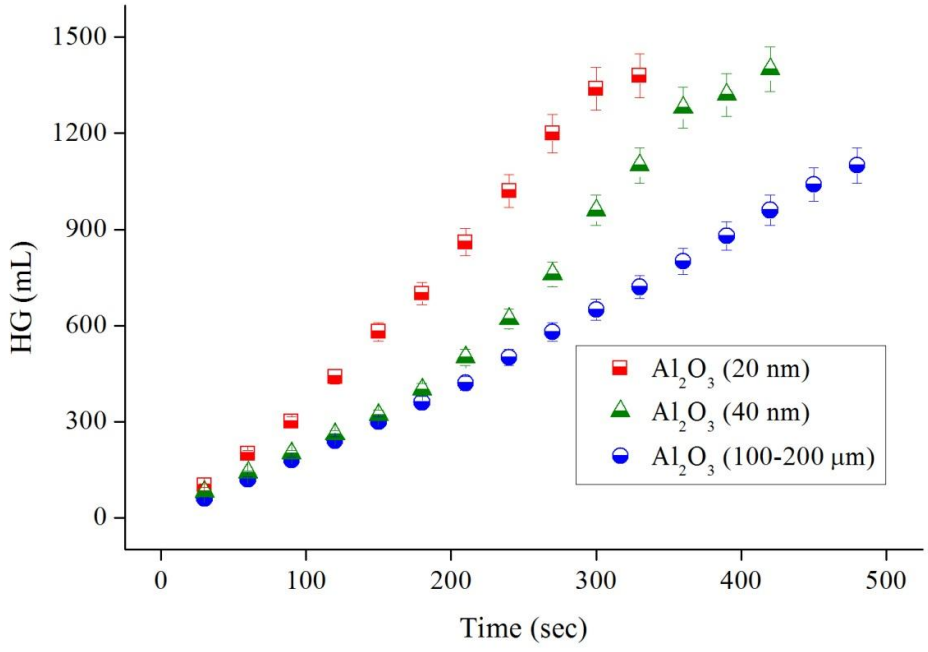

Figure 5.3: Comparison of HG using γ-Al_2O_3 (100-200 μm), γ-Al_2O_3 (40 nm) and γ-Al_2O_3 (20 nm)

All the above experiments were carried out at 1.01 moles/L $NaBH_4$, 0.02 moles/L $CoCl_2$, 0.09 moles/L Al_2O_3 and 1.40 moles/L NaOH concentration. Due to lower particle size of alumina, its reactivity towards the reactants increases thus promoting HG and HGR**.** Therefore, it is concluded from the above experiments, that higher HG is observed with γ-Al_2O_3 having particle size of 20 nm, therefore, it is selected as promoter for the present $NaBH_4/H_2O$ system with $CoCl_2$ as catalyst.

5.6. Closure

Various catalyst promoting materials like γ-Al_2O_3 nanoparticles, γ-Al_2O_3 particles, CNT, MMT clay, SiO_2, zeolite and zirconia sand are compared with respect to hydrogen generation rate and maximum HGR of 17.9 moles/L.sec is obtained with Al_2O_3 nanoparticles in $NaBH_4/H_2O$ system with $CoCl_2$ as catalyst. After selection of promoter different catalyst namely $CoCl_2.6H_2O$, $CoSO_4.7H_2O$, $(CH_3COO)_2Co.4H_2O$, $Co(NO_3)_2.H_2O$, $CdSO_4$, $CuSO_4.5H_2O$ are evaluated for maximum HGR. Following order for maximum and overall HGR is observed: $CoCl_2.6H_2O$ > $CoSO_4.7H_2O$ > $(CH_3COO)_2Co.4H_2O$ > $Co(NO_3)_2.H_2O$. Thus Al_2O_3 nanoparticles are selected as promoter and $CoCl_2.6H_2O$ is selected as catalyst for present $NaBH_4/H_2O$ system.

CHAPTER 6

Hydrogen generation from $NaBH_4/\gamma\text{-}Al_2O_3$ nanoparticles/H_2O with $CoCl_2$ as catalyst

6.1. Introduction

In this chapter we report a chemical hydride based hydrogen storage system composed of $NaBH_4$/ γ-Al_2O_3 nanoparticles (20nm)/H_2O with $CoCl_2$ as catalyst. Previous chapter presents detail depiction of γ-Al_2O_3 nanoparticles (20nm) showing highest HGR among other promoters. Concept of dual-solid-fuel system is introduced in this chapter by $NaBH_4$ being the representative chemical hydride in this study combined with γ-Al_2O_3 nanoparticles which itself is a supporting component for increasing HG of the system. Comparing conventional $NaBH_4/H_2O$ system, this dual-solid-fuel system exhibits advantages in hydrogen generation rate and hydrogen storage densities. Previous studies also suggest that cobalt chloride is a promising catalyst that accelerates $NaBH_4$ hydrolysis and γ-Al_2O_3 nanoparticles forms activated complex with $CoCl_2$ that increases its catalytic activity. Consequently, $CoCl_2$ is selected as a catalyst for this HG system. All the factors that influence the kinetics of this system are observed. Power law kinetic model is extensively used to study the kinetics due to its distinct advantages over other kinetic models. Residue of this system is characterized by EDS, XRD and FTIR to observe the components that could form in the solution and that could affect overall HGR of the system.

6.2. Kinetic measurements for $NaBH_4/Al_2O_3/H_2O$ system

6.2.1. Materials

The chemicals used in this investigation are $NaBH_4$ as prime component for hydrogen generation, $CoCl_2.6H_2O$ as catalyst, γ-Al_2O_3 nanoparticles (20nm) as catalyst promoter and NaOH as stabilizer. Considering the constraints in the experimental facility and practical operating conditions, experiments were performed at specific concentrations of $NaBH_4$, $CoCl_2$, Al_2O_3 and NaOH. Four concentrations of $NaBH_4$ are taken for kinetic data that are 1.00, 1.25, 1.30, 1.75 moles/L, for $CoCl_2$ 0.020, 0.024, 0.028, 0.032 moles/L, for Al_2O_3 0.06, 0.07, 0.08, 0.09 moles/L and for NaOH 1.16, 1.6, 2.06, 2.6 moles/L.

6.2.2. Factors affecting HGR

The hydrolysis kinetics is affected by multiple factors like concentration of stabilizer (NaOH), promoter (γ-Al_2O_3 nanoparticles), $NaBH_4$ and catalyst ($CoCl_2.6H_2O$). All these factors are observed by varying their concentrations and observing the change in HGR and

keeping the concentration of other components constant. The change in concentration of each component will cause change in viscosity and density in the solution, this change will affect the HGR of the system as discussed below.

Effect of NaOH concentration on HGR

As discussed earlier, sodium borohydride undergoes self-hydrolysis therefore, NaOH is used as stabilizer. NaOH considerably hinder unprompted hydrolysis of $NaBH_4$. Additionally, the kinetics is dependent on solution pH. The solution pH is controlled by NaOH concentration and thus affects kinetics of the whole system. Therefore, role of stabilizer (NaOH) on hydrolysis reaction of $NaBH_4$ is determined first and its effect on hydrogen generation is observed in presence of $CoCl_2$ catalyst and γ-Al_2O_3 nanoparticles as promoter. Effect of NaOH on hydrogen generation rate is evaluated by performing number of experimental runs at different NaOH concentrations as shown in Figure 6.1. In these experiments the concentration of $NaBH_4$, Al_2O_3 and $CoCl_2$ were kept constant as 1.25 moles/L, 0.09 moles/L and 0.02 moles/L, respectively.

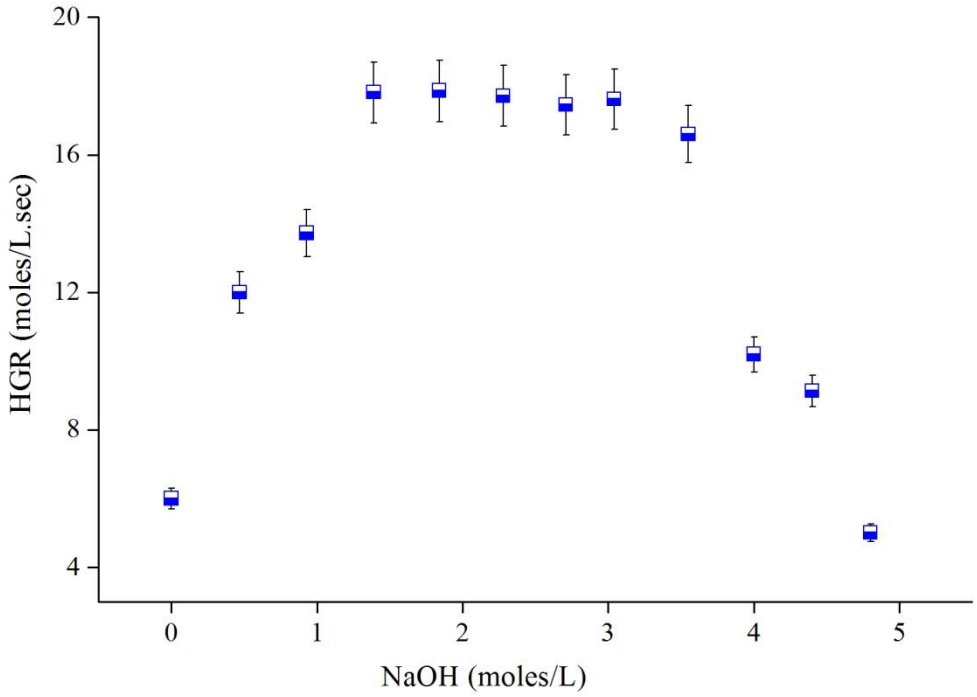

Figure 6.1: Variation of HGR with NaOH concentration

It is observed from the Figure 6.1, after 1.4 moles/L NaOH, HGR is almost constant till 3.5 moles/L NaOH. As the concentration of NaOH exceeds 3.5 moles/L, HGR decreases due to high level of alkalinity in the solution that suppresses hydrogen release.

Increasing the alkali concentration in the solution results in increase is HG kinetics till the solution becomes highly viscous. Therefore, 1.4 moles/L concentration of NaOH is selected to carry further kinetic studies. As discussed earlier, addition of NaOH increases alkalinity of the solution and increases NaOH based byproducts formation, which results in formation of sodium aluminates in the solution and increases Al hydrolysis (Kanturk et al., 2008 and Buchner et al., 1999). Additionally, presence of aluminates in the solution prevents the formation of passive layer on aluminium surface that prevents interaction of water molecules with Al atoms. Aluminate ions act as a barrier in the formation of hydroxide layer and speed up the interaction of Co ions with active sites of alumina. This process promotes the kinetics of $NaBH_4$ hydrolysis (Li et al., 2005, Buchner et al., 1999 and Kanturk et al., 2008). Thus, concentration of NaOH is an important parameter for improving hydrolysis of $NaBH_4$ and Al.

Effect of $CoCl_2$ concentration on HGR

Experiments were carried out at different concentrations of $CoCl_2$ (0.02, 0.024, 0.028, 0.032 moles/L) and keeping other chemical components constant, i.e. 0.09 moles/L Al_2O_3, 1.25 moles/L $NaBH_4$ and 1.0 moles/L NaOH. It is observed that kinetics of $NaBH_4/H_2O$ is highly affected by $CoCl_2$. Effect of $CoCl_2$ on HGR is presented in Figure 6.2 and it is depicted that HGR shoots to twice of its original value at 0.028 moles/L of $CoCl_2$. This means that reaction time decreases to half of its original time as $CoCl_2$ concentration increases in the solution.

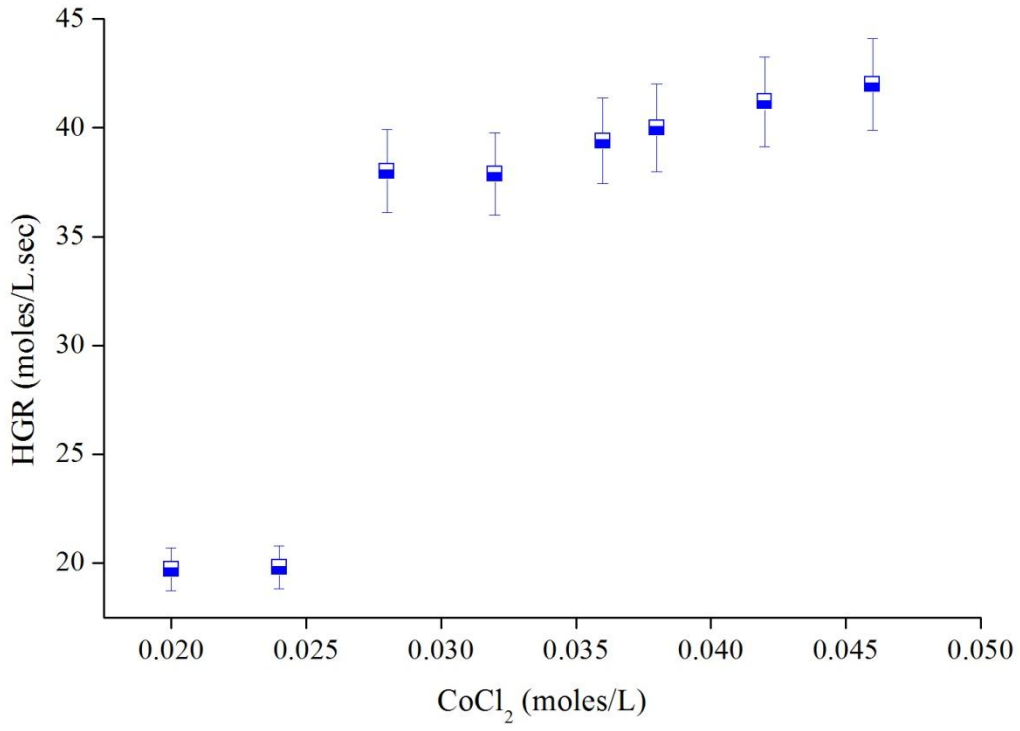

Figure 6.2: Effect of $CoCl_2$ concentration on HGR

Hydrogen generation is also observed at higher concentrations (0.036 and 0.046 moles/L) of $CoCl_2$. As observed earlier, hydrogen generation rate increases with increase in catalyst concentration. As discussed in chapter 4, increase in the concentration of $CoCl_2$ in solution results in reduction of BH_4^- ions at faster rate due to the formation of Co_2B active species in the solution due to electrophilic nature of Co^{2+} that leads to high reactivity towards BH_4^- ions. This affects the kinetics of $NaBH_4$ hydrolysis reaction and results in increase in HGR (Akdim et al., 2009). In presence of γ-Al_2O_3 nanoparticles in the solution cobalt forms active species with alumina (cobalt aluminate). Alumina promotes the catalytic activity of Co_xB active species in the solution. This improves the kinetics of the system by significantly affecting hydrolysis of $NaBH_4$. Thus, there exist a synergistic catalytic affect between Co/Al that enhances the hydrolysis of $NaBH_4$. Therefore, increase in $CoCl_2$ concentration increases the formation of Co/Al activated complex and appreciably increases HGR.

At higher concentrations, reaction becomes highly vigorous as $NaBH_4/H_2O$ system without addition of alumina. Therefore, likewise no further observations were observed with increase in catalyst concentration in the solution due to safety concerns. Reaction is highly vigorous and fast at higher concentrations of $CoCl_2$ (0.028 and 0.032 moles/L) and to obtain considerable kinetic data and to observe variation of HGR with $NaBH_4$ and alumina further kinetic studies are carried out at 0.02 moles/L of $CoCl_2$.

Effect of Al_2O_3 concentration on HGR

The system is monitored by increasing Al_2O_3 concentration and keeping other components constant as shown in Figure 6.2. Experiments were performed at four concentrations of $NaBH_4$ (1.00, 1.25, 1.50, 1.75 moles/L) with 0.02 moles/L $CoCl_2$ and 1.40 moles/L NaOH concentrations. As depicted from Figure 6.3, HGR increases with increase in Al_2O_3 nanoparticles till 0.09 moles/L and after 0.09 moles/L HGR is either constant (1.00 moles/L $NaBH_4$) or decreases (1.75 moles/L $NaBH_4$). Thus, 0.09 moles/L Al_2O_3 is selected for further studies.

This is due to consumption of reactants at faster rate that tends to increase the viscosity of the solution, thus affecting HGR of the system. Therefore, it could be concluded form the results that HGR increases with increase in concentration of Al_2O_3 nanoparticles till the solution becomes highly viscous and all the reactants are consumed.

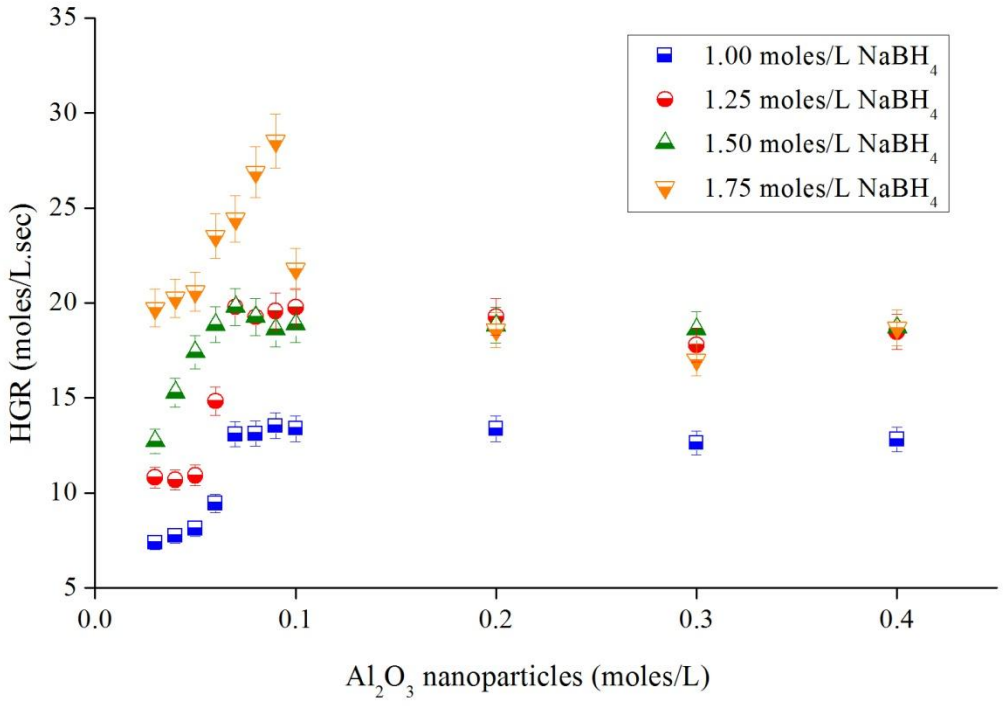

Figure 6.3: Effect of Al_2O_3 concentration on HGR

Alumina concentration in the solution is a significant factor that promotes kinetics of $NaBH_4$ hydrolysis reaction. As discussed earlier, hydrophilic nature of alumina and particle size of alumina nanoparticles increases its solubility in the solution following reaction 5.2. The coordination of surface hydroxyl groups formed after adsorbtion of water is responsible for its amphoteric nature given in reaction 5.1. Here the solution pH is greater than 9 and rise in solution pH results in formation of polymeric aluminates. These aluminates prevent surface passivation and increases hydrolysis of aluminium following reaction 5.4. Moreover, it forms active complex (Co/Al) with Co_xB species and promote the activity of catalyst following reaction 5.5 (Fan et al., 2013). Therefore, γ-Al_2O_3 nanoparticles promote and relevantly affect overall HGR of the system.

Effect of $NaBH_4$ concentration on HGR

$NaBH_4$ is prime component in the present hydrogen generation system. HGR is directly proportional to the concentration of $NaBH_4$. Experiments were carried out with four different Al_2O_3 concentrations (0.06, 0.07, 0.08, 0.09 moles/L) with 0.02 moles/L $CoCl_2$ and 1.40 moles/L NaOH while varying the $NaBH_4$ concentration. After 1.75 moles/L HGR decreases due to increase in viscosity in the solution.

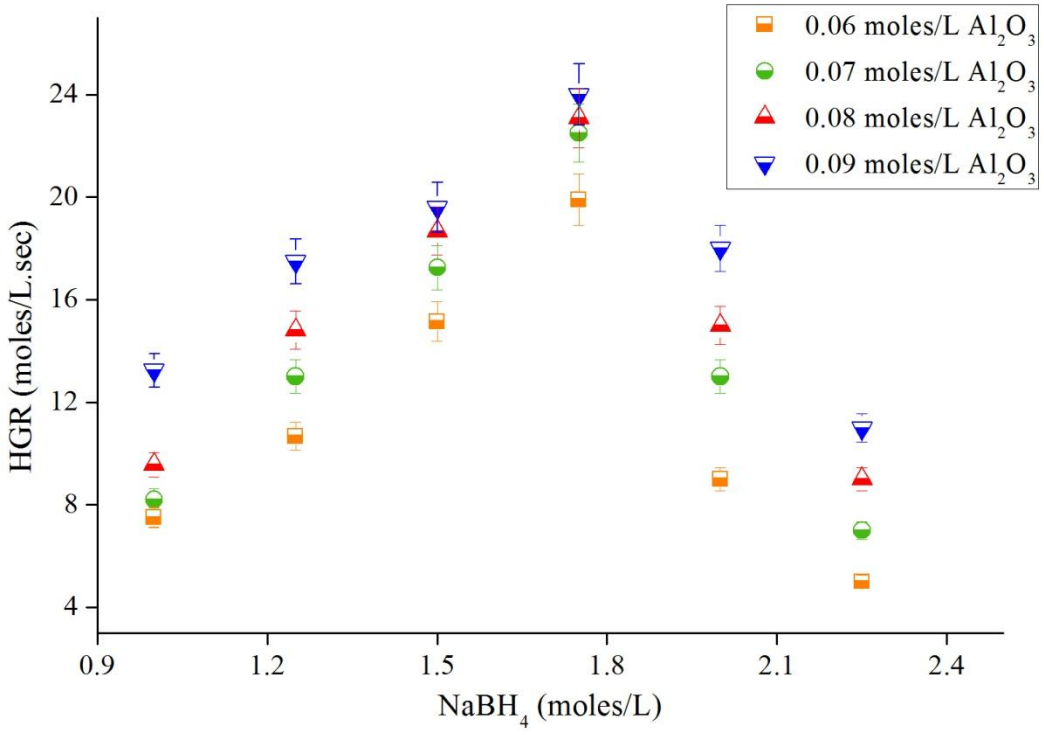

Figure 6.4: Effect of $NaBH_4$ concentration on HGR

The change in HGR with increasing $NaBH_4$ concentration is demonstrated in Figure 6.4 and it is observed that as the concentration of $NaBH_4$ increases HGR increases. Higher concentration of $NaBH_4$ in the system indicates high availability of hydrogen source in the solution or higher concentration of sodium and borohydride ions concentration in the solution. Borohydride ions are responsible in release of protons in the solution. Highly active $CoCl_2$ catalyst and Al_2O_3 nanoparticles efficiently help in release of protons from borohydride ions in the solution. On the other hand, Na^+ ions from $NaBH_4$ form aluminates in the solution that promotes Al hydrolysis reaction in the system. Therefore, it could be concluded that increase in $NaBH_4$ concentration increases HGR of the system.

6.2.3. Kinetics

It is concluded from above studies that hydrogen generation rate depends on NaOH, Al_2O_3, $NaBH_4$ and $CoCl_2$ concentrations. Theoretically, maximum HGR occurs at the beginning of the reaction as the concentrations of reactants are highest.

Considering the constraints in zero order, first order, Langmuir-Hinshelwood model, Michaelis and Menton kinetic models, discussed in chapter 4, that limit their practical use, kinetic studies for this system is performed according to power law kinetic model as per equation 6.1.

The rate depends on temperature and concentrations of $NaBH_4$, Al_2O_3 catalyst and NaOH according to the following expression (Fogler, 2000):

$$-4\frac{d[NaBH_4]}{dt} = d\frac{[H_2]}{dt} = k_{overall}[NaBH_4]^a[Al_2O_3]^{b_1}[CoCl_2]^c[NaOH]^d \qquad (6.1)$$

Effect of concentrations of sodium borohydride, alumina, sodium hydroxide and cobalt chloride on hydrogen generation rate is monitored and overall hydrogen generation rate can be expressed as,

$$r_{H_2} \propto [NaBH_4]^a[Al_2O_3]^{b_1}[CoCl_2]^c[NaOH]^d \qquad (6.2)$$

Where, r_{H_2} is hydrogen generation rate in (moles/L.sec), $[NaBH_4]$ is the concentration of $NaBH_4$, $[Al_2O_3]$is concentration of alumina, $[CoCl_2]$ is concentration of cobalt chloride, [NaOH] is concentration of NaOH in (moles/L) and a, b_1, c, d are the apparent order with respect to $NaBH_4$, Al_2O_3, $CoCl_2$, NaOH concentrations. On the basis of kinetic studies, the overall order of reaction and activation energy is calculated.

Rate kinetics with respect to $NaBH_4$

The hydrogen generation rate as a function of $NaBH_4$ is studied according to the rate equation 6.3,

$$r_{H_2[NaBH_4]} = k_1[NaBH_4]^a \qquad (6.3)$$

Here $r_{H_2[NaBH_4]}$is rate of hydrogen generation and k_1 is the rate constant with respect to $NaBH_4$ and concentrations of other components constant. Experiments are conducted at different concentrations of $NaBH_4$ (1.00, 1.25, 1.50 and 1.75 moles/L), at constant $CoCl_2$ (0.02 moles/L), NaOH (1.4 moles/L) and Al_2O_3 (0.09 moles/L) concentrations. Hydrogen generation (HG) versus time graph is plotted as shown in Figure 6.5(a). It is observed that HG increases with time. Hydrogen release is dependent on reactivity between BH_4^- ions and catalyst surface. The valance electrons of catalyst enter into the anti-bonding orbital of BH_4^- ions. This results in breaking of B-H bond and helps in release of hydrogen. It could be concluded that optimum electron density should be present on the d band center of catalyst for maximized catalytic activity.

It could be expected that activated complex formed between Co/Al is present with optimal electron density in the solution to weaken BH_4^- ions and helps in release of hydrogen (Holbrook and Twist, 1971 and Zhuang et al., 2013).

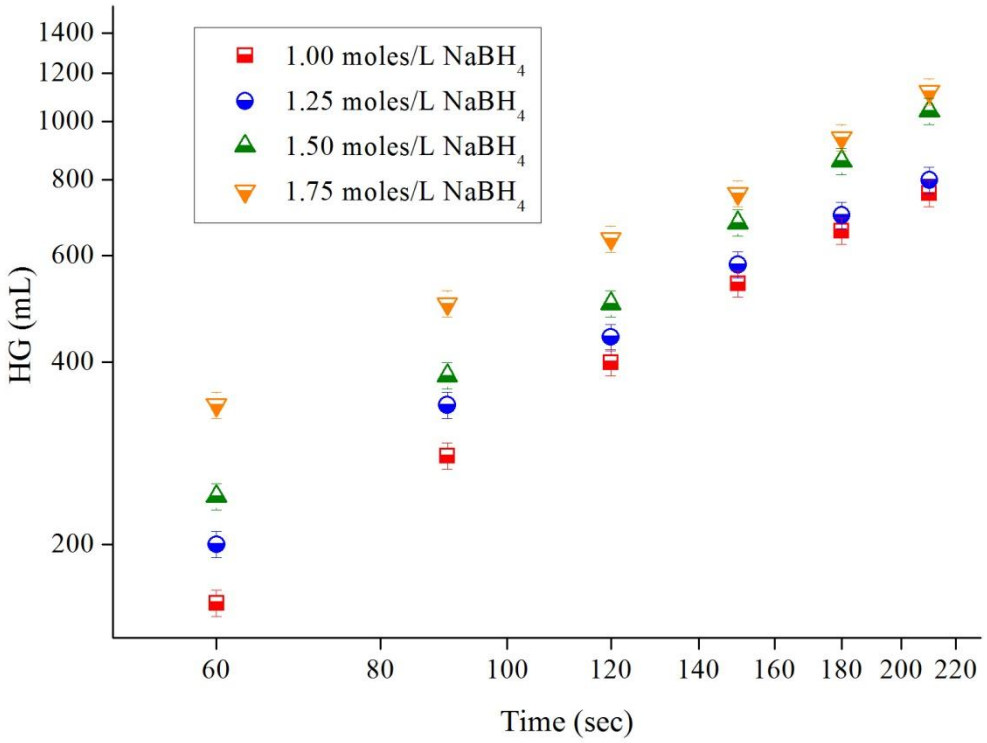

Figure 6.5 (a): Hydrogen generation as function of time at different $NaBH_4$ concentrations

Plotting the HGR versus $NaBH_4$ concentration on logarithmic scale as shown in Figure 6.5(b) gives the order of reaction 0.9 ~ 1, with k_1 = 14.58 $(sec)^{-1}$. Present result predicts first order kinetics with $NaBH_4$ making system dependent on $NaBH_4$ concentration with kinetic order calculated as 1.

Present results are in agreement with the results of Levy et al. (1960). They reported order 0.39 for $NaBH_4$ with $CoCl_2$ as catalyst without using stabilizer in solution. Demirci and Garin (2008) also worked on $NaBH_4$ based system with Ru-promoted sulphated zirconia (Ru-SZ) catalyst. They also used power law kinetic model and reported order of 0.23 for $NaBH_4$. On contrary, as stated by Metin et al. (2009) with cobalt(0) nanoclusters as catalyst, order changes from first order in aqueous medium and zero order in basic medium. Similar results were obtained by Shang and Chen (2006) with ruthenium supported on carbon as catalyst. They used semi-empirical hydrogen generation model for calculating orders of $NaBH_4$ hydrolysis reaction and predicted that without NaOH in solution HGR is proportional to

molality of $NaBH_4$ and with addition of NaOH, HGR decreases. Order calculated with respect to $NaBH_4$ is 1.

The result is also supported by observation of Patel et al. (2009). They reported first order kinetics with respect to $NaBH_4$ at low $NaBH_4$ concentrations and order of 0.07 at high $NaBH_4$ concentrations with Co-P-B catalyst.

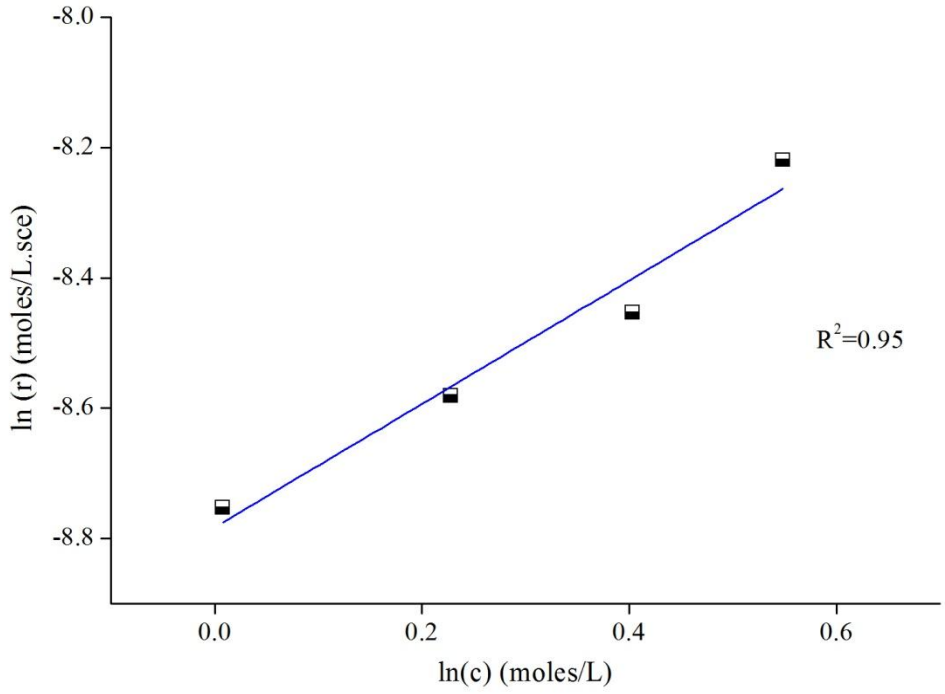

Figure 6.5 (b): Hydrogen generation rate as a function of $NaBH_4$ concentration

Rate kinetics with respect to Al_2O_3 nanoparticles

The hydrogen generation rate with change in alumina concentration is studied according to the rate equation 6.4,

$$r_{H_2[Al_2O_3]} = k_a [Al_2O_3]^{b_1} \qquad (6.4)$$

Here $r_{H_2[Al_2O_3]}$ is rate of hydrogen generation and k_a is rate constant with respect to alumina. Hydrogen generation versus time plot for different Al_2O_3 concentrations at constant $NaBH_4$ (1.25 moles/L), NaOH (1.4 moles/L) and $CoCl_2$ (0.02 moles/L) concentrations is shown in Figure 6.6(a). As the concentration of Al_2O_3 increases HG increases with time.

As discussed in chapter 5, γ-Al_2O_3 plays a vital role in HG for the present system. Hydrophilic and amphoteric nature of γ-Al_2O_3 defines its high catalytic activity in the solution.

.

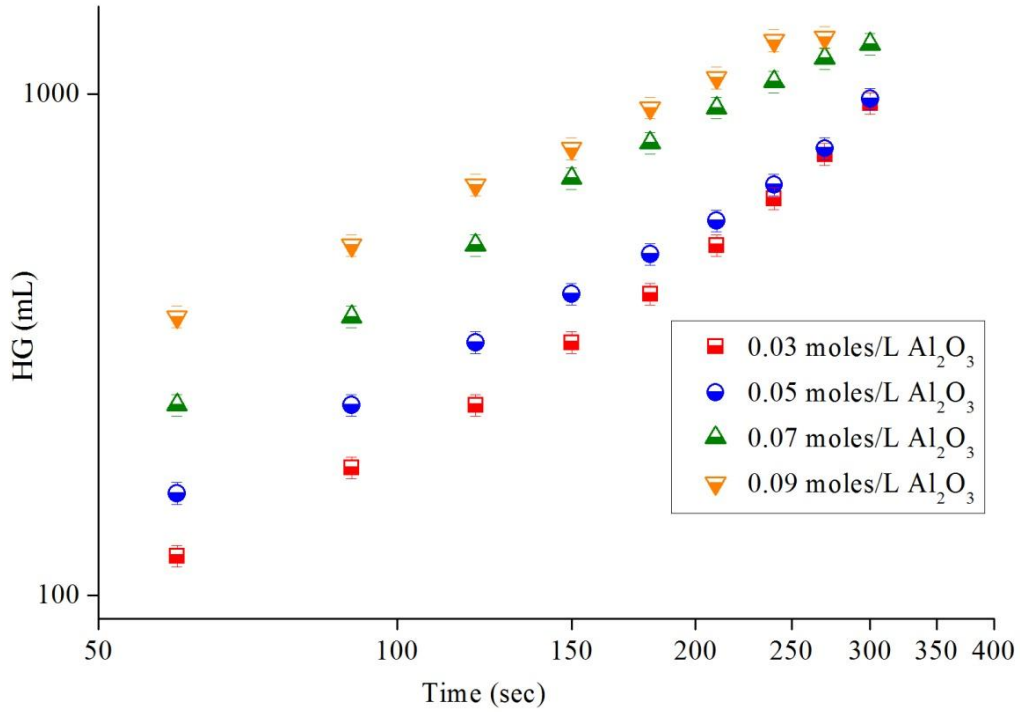

Figure 6.6 (a): Hydrogen generation as a function of time at different alumina concentrations

Plotting the HGR versus alumina concentration on logarithmic scale gives a slope 0.45 ~ 0.5. Thus, the order of reaction with respect to alumina nanoparticles is 0.5 with rate constant k_2 of 69.43 $(sec)^{-1}$ $(moles/L)^{0.5}$ as shown in Figure 6.6(b). This result confirms that HGR is dependent on Al_2O_3 concentration

It is predicted that addition of alumina in the solution affects the kinetics of the system by forming aluminates and Co/Al active complex. Alumina acts as a catalyst carrier for Co_xB species, thus increasing the activity of catalyst as discussed in previous chapter. Formation of Co/Al complex also suggests that reactive sites of catalyst increase for the reactants. Moreover, there exists synergistic catalytic effect between Co_xB and hydroxylates of alumina that promotes $NaBH_4$ hydrolysis. Order of 0.5 for alumina concentration suggests HGR is reliant of alumina concentration thus the kinetics of the overall system becomes dependent on alumina in terms of HGR.

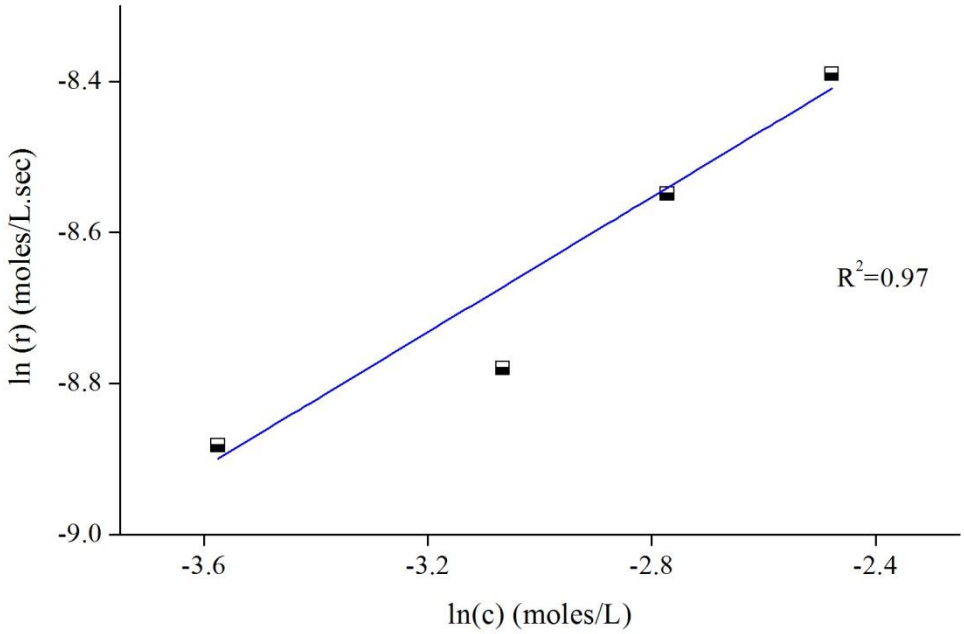

Figure 6.6 (b): Hydrogen generation rate as a function of alumina concentration

Rate kinetics with respect to $CoCl_2$

According to the rate equation 6.5,

$$r_{H_2[CoCl_2]} = k_3[CoCl_2]^c \qquad (6.5)$$

Here $r_{H_2[CoCl_2]}$ is rate of hydrogen generation and k_3 is rate constant with respect to $CoCl_2$ concentration. Hydrogen generation versus time plot for different $CoCl_2$ concentrations and at constant $NaBH_4$ (1.25 moles/L), NaOH (1.16 moles/L), and Al_2O_3 (0.084 moles/L) concentrations is presented in Figure 6.7(a). Increase in HG is observed with time, with increase in $CoCl_2$ concentration.

Plotting the HGR versus $CoCl_2$ on logarithmic scale in Figure 6.7(b), slope calculated is 1.5. The order of reaction with respect to $CoCl_2$ is 1.5 with rate constant 12.088×10^3 $(sec)^{-1}$ $(L/moles)^{0.5}$.

Therefore, it could be predicted from the results that HG is dependent on concentration of catalyst. Increases in catalyst concentration also increases number of catalytic sites available for the reactants that affect overall HGR of the system. It is also being predicted that Co/Al active complex could also form in the solution at higher rate that helps in increasing the kinetics of overall system.

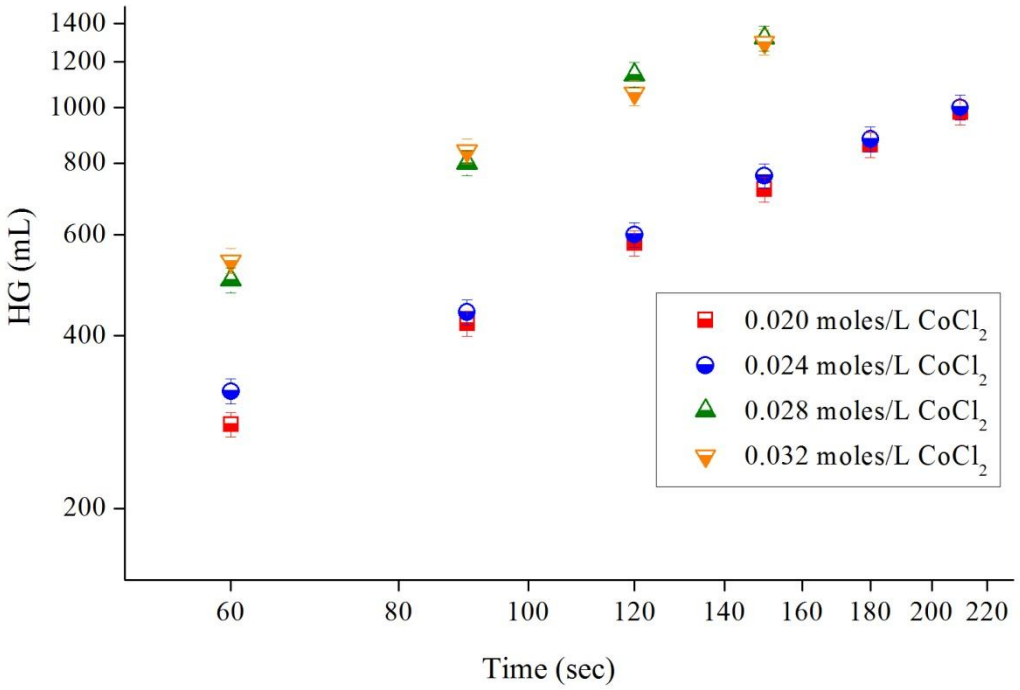

Figure 6.7 (a): Hydrogen generation with time at different $CoCl_2$ concentrations

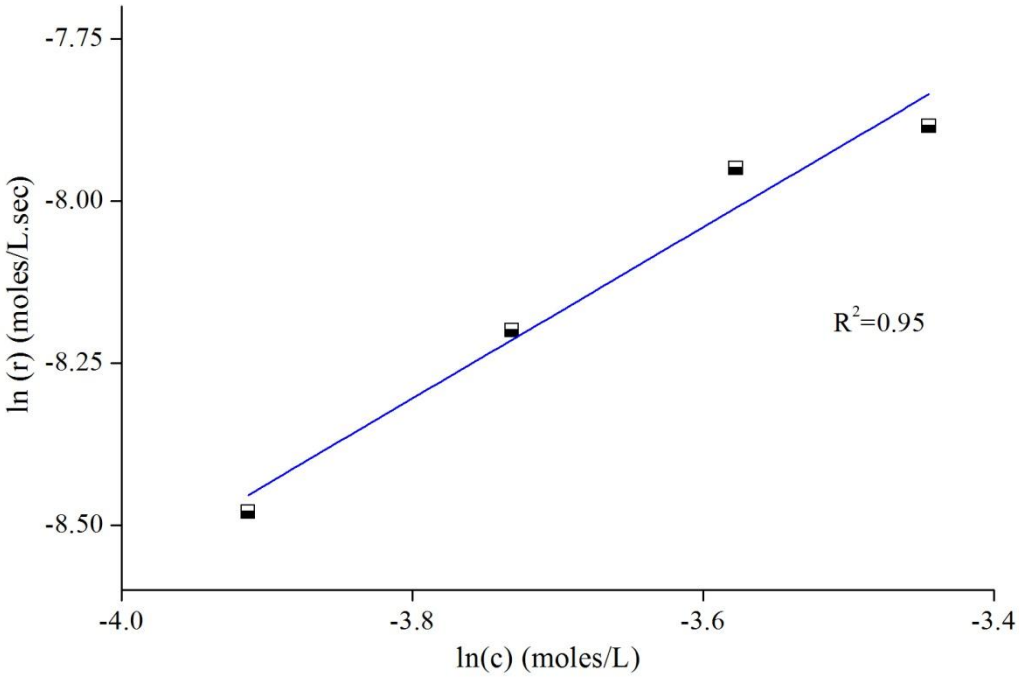

Figure 6.7 (b): Hydrogen generation rate as a function of $CoCl_2$ concentration

It is observed that order of hydrolysis reaction with respect to $CoCl_2$ by using power law kinetic model is different as per the nature of catalyst. Demirci and Garin (2008) reported order of 1.27 for Ru-promoted sulphated zirconia catalyst. The reaction is carried out at low temperature range (0 to 24°C). Patel et al. (2009) reported order to be 1.07 with respect to Co-P-B catalyst for low as well as high $NaBH_4$ concentration. Similar observations are made by Fernandes et al. (2009) with (Co-P-B) based catalyst with order of 1.05 and Levy et al. (1960) gives first order kinetics with $CoCl_2$ as catalyst without using stabilizer concentration in the solution.

Rate kinetics with respect to NaOH

From the present study, it is observed that HGR increases with increase in NaOH till solution becomes highly alkaline. Rate is represented by the following rate equation 6.6,

$$r_{H_2[NaOH]} = k_4[NaOH]^d \qquad (6.6)$$

Here $r_{H_2[NaOH]}$ is rate of hydrogen generation and k_4 is rate constant with respect to NaOH concentration. Hydrogen generation versus time for different NaOH concentrations and at constant $NaBH_4$ (1.25 moles/L), Al_2O_3 (0.09 moles/L), $CoCl_2$ (0.02 moles/L) concentrations is shown in Figure 6.8(a). It is observed that with increase in NaOH concentration HG increases with time. Hydrogen generation is dependent on the nature of catalyst used in alkaline solution. The reaction in which the catalyst does not bind strongly itself with hydrogen, results in higher HGR with increase in NaOH concentration (Walter et al., 2008).

Plotting the HGR versus NaOH concentration graph on logarithmic scale as shown in Figure 6.8(b), the calculated slope is 0.15. Thus, the order of reaction with respect to NaOH is 0.15 with rate constant 16.44 $(sec)^{-1}$ $(moles/L)^{0.85}$.

As discussed in chapter 4, with increase in NaOH concentration formation of BH_3OH^- ions increases and protons are released in the solution at higher rate. It is concluded that as NaOH concentration increases from 0.47-1.83 moles/L and due to the formation of sodium aluminates, pH of the solution becomes greater than 12 and HGR becomes less dependent on hydronium ion concentration and order decreases to very low value of 0.15 (Davis and Swain 1960; Davis et al., 1960 and Davis et al., 1962).

Results in the present study are in agreement with different orders reported in literature with respect to NaOH using different catalysts. Zang et al. (2007) reported order 0.13 for NaOH and Ni based catalyst.

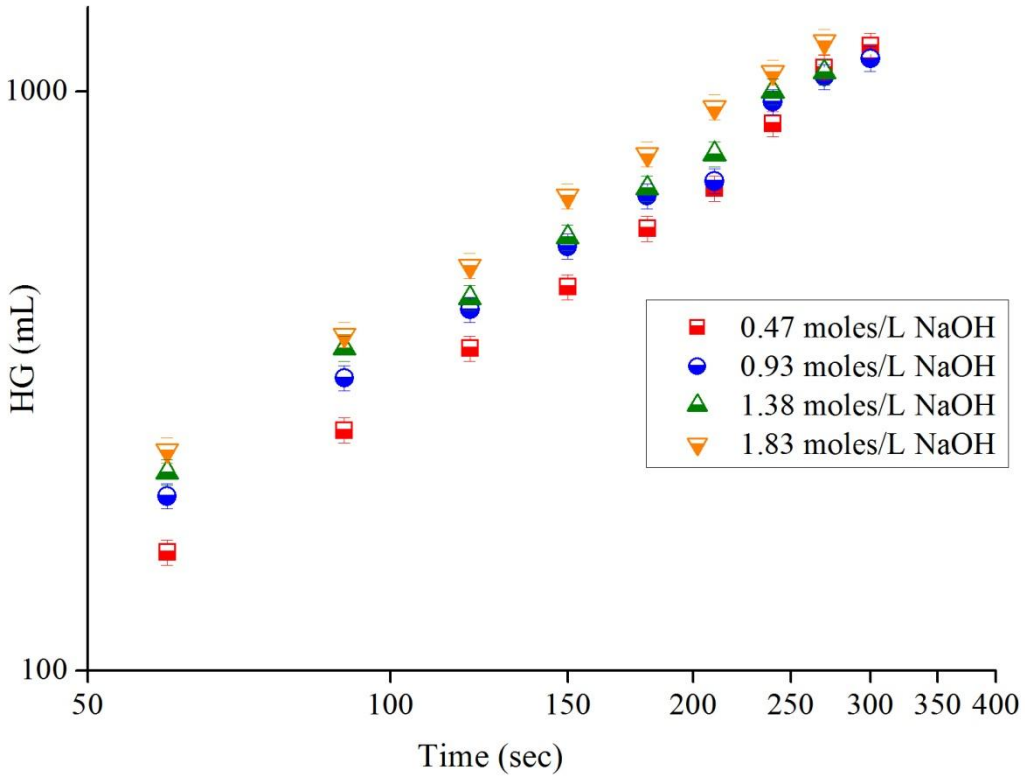

Figure 6.8 (a): Hydrogen generation with time at different NaOH concentrations

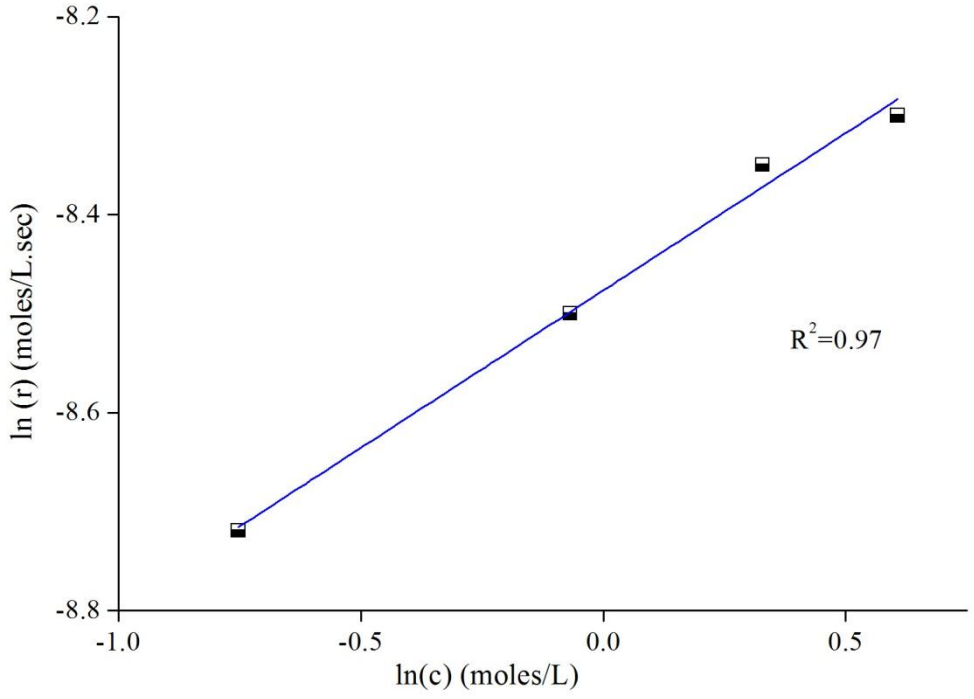

Figure 6.8 (b): Hydrogen generation rate as function of NaOH concentration

Demirci and Garin (2008) investigated negative order (-0.35) for NaOH with Ru-promoted sulphated zirconia catalyst. Metin and Ozkar (2009) used polymer-stabilized cobalt nanoclusters(0) and found variation in order of the hydrolysis reaction with and without stabilizer (NaOH) in the solution. First order kinetics is reported in aqueous solution and zero order in basic solution. As discussed in chapter 4, Fernandes et al. (2009) stated that the order is 0.12 with (Co-P-B) based catalyst. Present results reported 0.15 as order for NaOH with $CoCl_2$ as catalyst and γ-Al_2O_3 as catalyst promoter.

The rate equation with respect to the order of individual components, affecting the overall order is given as equation 6.7.

$$r_{H_2} = k_{overall}[NaBH_4]^1[Al_2O_3]^{0.5}[CoCl_2]^{1.5}[NaOH]^{0.15} \quad (6.7)$$

Effect of temperature on HGR

Temperature is an important parameter that affects the kinetics of the system drastically. Thus to observe change in kinetics of the present system with change in temperature, HGR is investigated at different temperatures and at constant $NaBH_4$ (1.25 moles/L), NaOH (1.4 moles/L), $CoCl_2$ (0.02 moles/L) and Al_2O_3 (0.09 moles/L) concentrations. Slope of volume of the HG versus time graph gives the rate at each temperature (303, 313, 323 and 333 K). $k_{overall}$ is calculated at different temperatures. The activation energy is calculated according to equation 6.8 (Fogler, 2000),

$$\ln(k_{overall}) = \ln(A) - \frac{E}{RT} \quad (6.8)$$

Here A is pre exponential factor (units of $k_{overall}$), E is apparent activation energy in (kJ/moles), R is 8.314 J/moles.K, T is absolute temperature (in Kelvin) and $k_{overall}$ is over all rate constant at each temperature with units $(sec)^{-1}(L/moles)^{2.15}$.

Different k values against temperature are shown in Table 6.1. ln ($k_{overall}$) versus (1/T) is plotted, as shown in Figure 6.9, to calculate the apparent activation energy for the present system.

The apparent activation energy calculated for the present system is 29 kJ/moles and the value of A is 18.62×10^8 $(sec)^{-1}(L/moles)^{2.15}$.

Table 6.1: Values of $k_{overall}$ at different temperatures

S. No.	T (K)	$k_{overall}$	(1/T)	ln ($k_{overall}$)
1.	293	16.310×10^3	0.0034	9.70
2.	303	23.523×10^3	0.0033	10.06
3.	313	35.340×10^3	0.0032	10.47
4.	323	47.120×10^3	0.0031	10.70

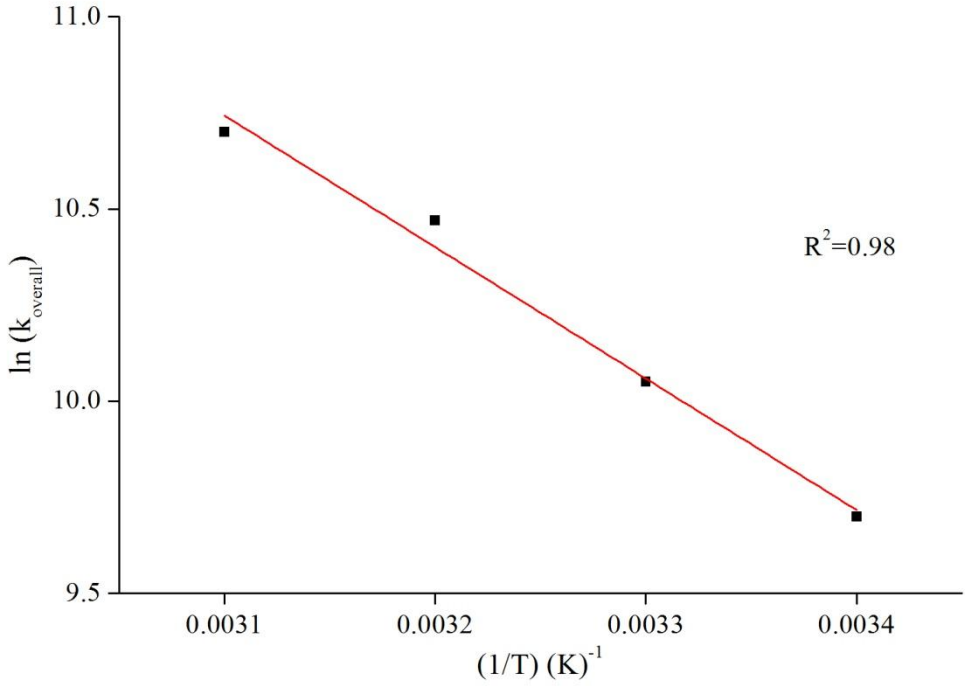

Figure 6.9: Arrhenius plot

Activation energy of this HG system is compared with activation energy of $NaBH_4/H_2O$ system without addition of alumina nanoparticles. It is observed that apparent activation energy reduces to the value of 29 kJ/moles from 44 kJ/moles as calculated in chapter 4. Thus alumina nanoparticles enhance the kinetics of the system.

Activation energy of 37.3 kJ/moles is reported by Shang and Chen (2006) for ruthenium supported on carbon as catalyst. Higher activation energy of 52 kJ/moles is observed by Zang et al. (2008) with Ni based catalyst and Demirci and Garin (2008) reported 76 kJ/moles for Ru-promoted sulphated zirconia catalyst. Activation energy of 34 kJ/moles is reported by Fernandes et.al (2009) for (Co-P-B) based catalyst. Metin and Ozkar (2009) obtained activation energy of 63±2 kJ/moles for aqueous medium and 37±2 kJ/moles for basic medium with cobalt(0) nanoclusters as catalyst.

Cakanyildirim and Guru (2010) reported activation energy of 132 kJ/moles and 78 kJ/moles at low and high temperatures, respectively. It is also interpreted form literature that activation energy varies likely with the type of catalyst system used, catalyst promoter, reaction experimental conditions and the chemical and physical properties of the components incorporated in the reaction. Factors that help in lowering activation energy are highly active γ-Al_2O_3 nanoparticles used as a promoter with $CoCl_2$ for hydrolysis of $NaBH_4$.

6.3. Characterization of residue from $NaBH_4/Al_2O_3/H_2O$ system with $CoCl_2$ as catalyst

The residue obtained from the optimum system consisting of $NaBH_4$ (1.26 moles/L), Al_2O_3 (0.12 moles/L), NaOH (0.93 moles/L), and (0.02 moles/L) $CoCl_2$ aqueous solution is analyzed. The residue obtained at the end of the reaction is grey colored solid powder and it is characterized using EDS, XRD and FTIR. Elemental composition is determined by the quantitative analysis of the surface by EDS.

EDS analysis

As shown in Table 6.2, residue consists of boron with maximum percentage followed by oxygen and aluminium and with the least percentage of cobalt and chlorine.

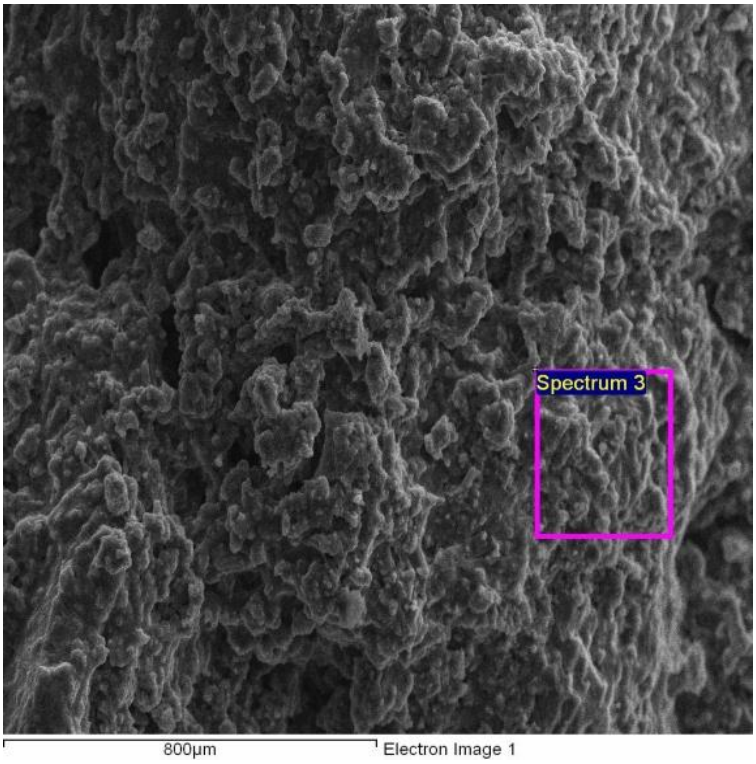

Figure 6.10(a): Sectioned area of residual material for EDS analysis

Elemental composition of one section observed by EDS is shown in Figure 6.10(a). It is estimated as Al (0.07 wt %), B (72.19 wt %), Cl (0.06 wt %), Co (0.07 wt %), Na (4.47 wt %) and O (23.14 wt %).

Similarly, results observed for section 2 are shown in Figure 6.10(b) with Al (0.12 wt %), B (74.24 wt %), Cl (0.09 wt %), Co (0.04 wt %), Na (4.26 wt %) and O (21 wt %).

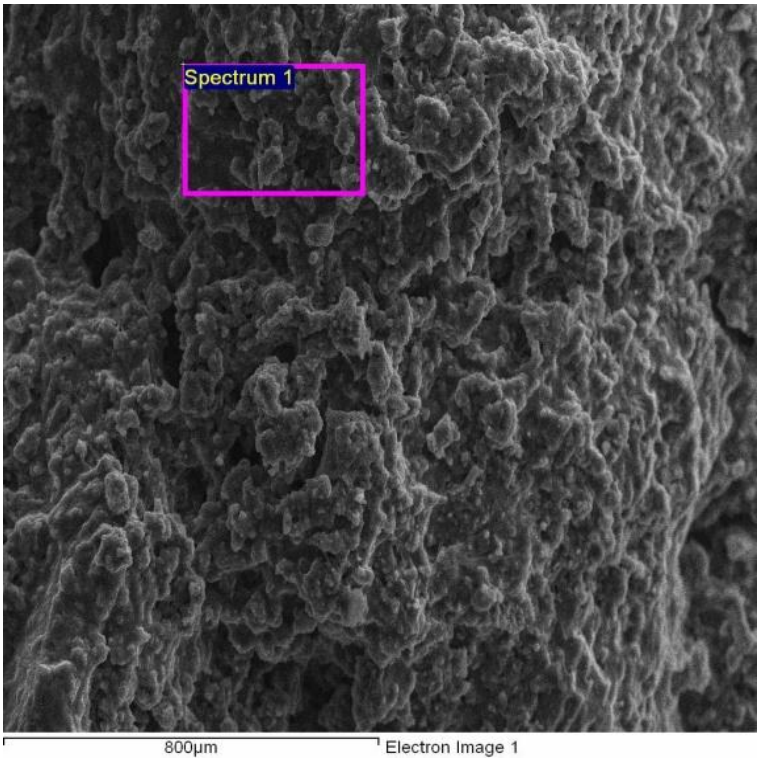

Figure 6.10(b): Sectioned area of residual material for EDS analysis

Table 6.2: EDS analysis of residual material

Element	Sectioned area in Figure 4(a)		Sectioned area in Figure 4(b)	
	Weight (%)	Atomic (wt %)	Weight (%)	Atomic (wt%)
B	72.19	80.22	74.24	81.8
Na	4.47	2.34	4.26	2.21
Al	0.07	0.03	0.12	0.05
Cl	0.06	0.02	0.09	0.03
Co	0.07	0.01	0.04	0.01
O	23.14	17.32	21.25	15.82

XRD analysis

XRD pattern of the residue is shown in Figure 6.11. Residue consists of polymeric sodium aluminates as the major components, for example $Na_2Al_{22}O_{34}$ (ICDD No.072-1406) and $NaAl_{11}O_{17}$ (ICDD No. 01-079-2288).

As shown in chemical reaction 5.3 in chapter 5, hydrolysis of Al in the solution increases overall HGR of the system, this is due to the formation of polymeric sodium aluminates confirmed from XRD analysis.

It is also observed that reaction 5.4 could be promoted by the formation of activated Co/Al complex like $CoAl_2O_4$ (ICDD No. 082-2251) in the solution. Therefore, as discussed in previous section, the formation of Na/Al and Co/Al species which plays the supplementary role in hydrogen generation is confirmed by XRD results.

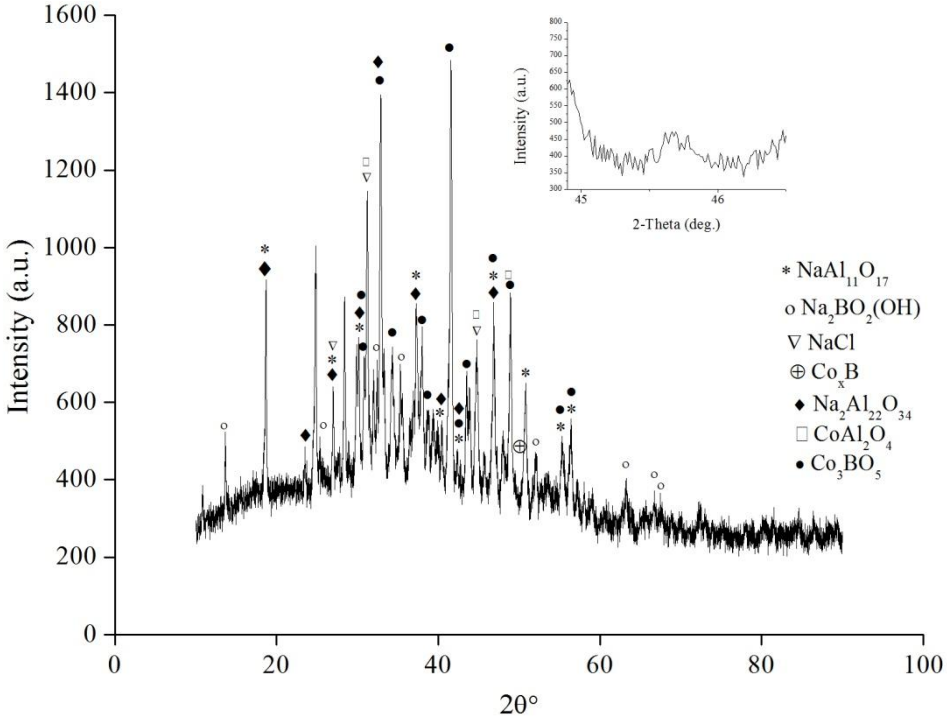

Figure 6.11: XRD analysis of residue

Presence of $Na_2BO_2(OH)$ (ICDD No. 037-0173) is also predicted by XRD results which is a result of formation of $NaBH_4$ hydrolysis byproduct $NaBO_2.H_2O$ (Soler et al., 2009). This observation concludes that Al and $NaBH_4$ hydrolysis reaction is enhanced by formation of NaOH based reactions 5.5 and 5.6. Due to the reduction of cobalt chloride with borohydride ions, NaCl (ICDD No. 01-071-3742) is formed as shown in reaction 4.1.

Formation of Co_3BO_5 (ICDD No. 085-1736) compound is the result of Co^{2+} ions reacting with $NaBO_2$ (George et al., 1993). Peak around $2\theta = 45°$ is shown in inset graph in Figure 6.11 that gives diffracted peaks. This indicates the amorphous structure of the material and presence of Co_xB compounds (Demirci and Miele, 2010).

FTIR analysis

FTIR analysis is carried for residue and it is observed that B-O deformation peaks (669, 735 and 846 cm^{-1}) shown in Figure 6.12 is an indication of the formation of Co_3BO_5 compound. Al-O stretching (914 cm^{-1}) and B-O stretching (1084 cm^{-1}) peaks predicts the formation of aluminates in the solution. B-O-H (1169 and 1282 cm^{-1}) peaks infer the formation of sodium metaborate based byproducts (Hannauer et al., 2011).

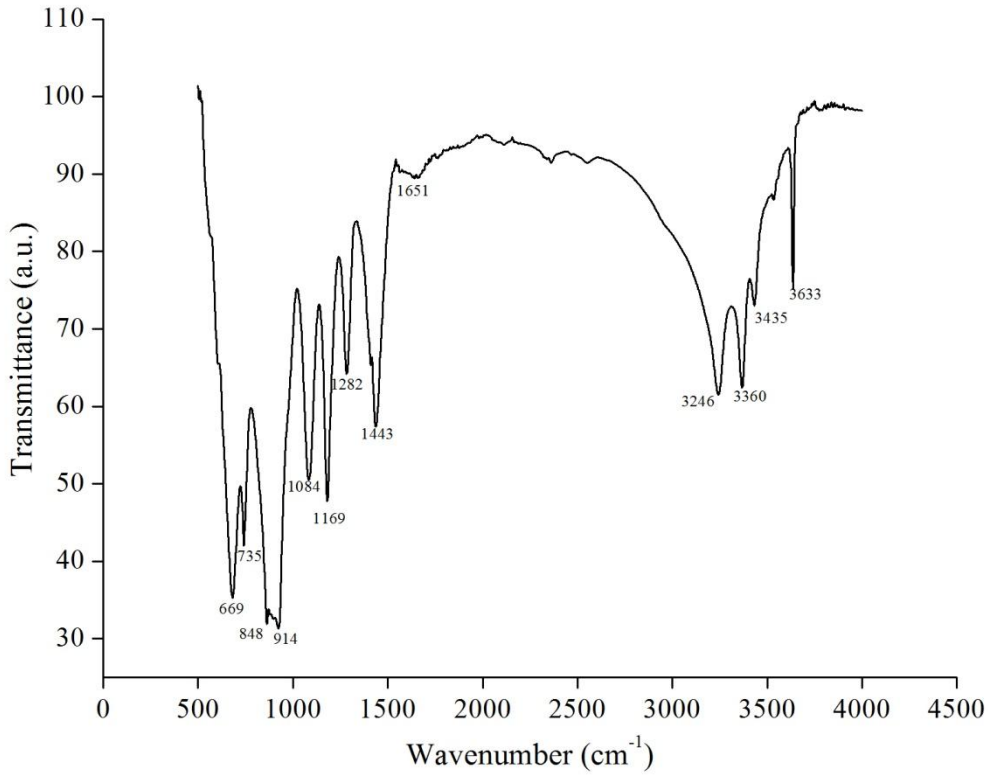

Figure 6.12: FTIR analysis of residue

Deformation and adsorption bands from 3200 to 3700 cm^{-1} envisage O-H stretching that reveal the formation of aluminium hydroxides (Xuelian et al., 2009). The B-H stretching band region almost completely disappeared that is form 2000 to 2300 cm^{-1}. Thus it could be concluded form this result that presence of Al_2O_3 nanoparticles in the system causes complete conversion of $NaBH_4$ (Dai et al., 2011).

6.4. Theoretical and experimental hydrogen capacities

For optimizing this HG system, maximum HG efficiencies are calculated at different mass ratios of $Al_2O_3/NaBH_4$. Hydrogen generation is dependent on the composition of various components of the system and to optimize the composition, mass ratios of $Al_2O_3/NaBH_4$ are examined. Efficiency of $NaBH_4/H_2O$ with $CoCl_2$ catalyst is calculated in section 4.5 in chapter 4. On similar terms, efficiency of $NaBH_4/Al_2O_3/H_2O$ with $CoCl_2$ is calculated using equations 2.11, 4.35 and 4.36.

The calculations are performed at constant $CoCl_2$ and NaOH concentrations. Theoretical and experimental hydrogen densities and efficiency of $NaBH_4/Al_2O_3$ system at different mass ratios of $Al_2O_3/NaBH_4$ are summarized in Table 6.3. Variation in the component ratio varies the efficiency of the system for maximum hydrogen yield. Here concentration of Al_2O_3 nanoparticles is kept constant and $NaBH_4$ is varied. Very high efficiency of 99.34% is achieved at mass ratio of 0.09:0.7 for $Al_2O_3/NaBH_4$.

Table 6.3: Theoretical and experimental H_2 densities

S. No.	Al_2O_3(g):$NaBH_4$(g)	H_2 Density (wt %)		Efficiency (%)
		Theoretical	Experimental	
1.	0.09 : 0.4	10.76	10.48	97.3
2.	0.09 : 0.5	10.76	10.56	98.14
3.	0.09 : 0.6	10.76	10.62	98.69
4.	0.09 : 0.7	10.76	10.69	99.34

The efficiency is compared with the efficiency of $NaBH_4/H_2O$ system; it is observed that there is a massive difference in the overall efficiencies of both the systems. It is also observed that difference in theoretical and experimental capacities is less as compared to the system without addition of alumina nanoparticles.

Above studies append novelty in the field of solid state HG systems by addition of alumina nanoparticles. Each factor that affects the overall rate of reaction is studied and kinetics of the system is investigated using power law kinetic model. This model describes the change in rate of reaction with concentration very minutely and change in HGR could be predicted. The property of power law kinetic model that does not follow any assumption, adds advantage to the research in this area.

To the best of knowledge kinetic studies with addition of alumina nanoparticles in the system is not reported so far in the literature. Efficiency of 99.34% is high enough to describe the effectiveness of the $NaBH_4/H_2O$ based system with alumina nanoparticles as a promoter and $CoCl_2$ as a catalyst. Thus, this HG system is highly proficient to be used in practical application for hydrogen generation and storage.

CHAPTER 7

Conclusions and future scope of work

7.1. Conclusions

The present work is a comprehensive study of two different HG systems ($NaBH_4$/γ-Al_2O_3 nanoparticles/H_2O & $NaBH_4$/H_2O) including optimization of catalyst, operating parameters followed by kinetic studies and analysis of residue obtained of both the HG systems.

- Slow and poor kinetics is observed without addition of catalyst for $NaBH_4$ hydrolysis reaction. Maximum hydrogen generation rate observed is 5.8 moles/L.sec for 1.75 moles/L $NaBH_4$. Therefore, a catalyst is required to improve the kinetics of reaction.

- On comparison with various platinum and ruthenium based catalysts that are not suitable for long term use due to the cost issues, cobalt chloride hexahydrate ($CoCl_2.6H_2O$) is chosen as a most efficient and low cost catalyst for $NaBH_4$/H_2O system. Moreover, strong cationic charge on cobalt and high solubility of chlorine increases the reactivity of $CoCl_2$ for $NaBH_4$ hydrolysis as compared to other Co based salts. At 1.75 moles/L of $NaBH_4$ the maximum hydrogen generation rate observed after addition of catalyst is 13.8 moles/L.sec.

- It is investigated that reaction rate of NaB_{H4} hydrolysis increases with increase in reactant ($NaBH_4$), stabilizer (NaOH) and catalyst ($CoCl_2.6H_2O$) concentration. Power law kinetic model is extensively used to study the kinetics due to its distinct advantages over other kinetic models (zero order, first order, second order Langmuir-Hinshelwood model and Michaelis & Menton model). Activation energy investigated for this system is 46 kJ/moles.

- Hydrogen generation densities of this system are calculated and it is observed that there is a variation between theoretical and experimental densities. For example, at 0.7 g of $NaBH_4$ experimental hydrogen density of 7.9 wt% and theoretical hydrogen density of 10.8 wt% is observed with efficiency of 73%. This observation adds limitation to $NaBH_4$/H_2O based HG system with $CoCl_2$ as catalyst for its practical application due to the difference in theoretical and experimental hydrogen storage densities.

- Therefore, the concept of dual-solid fuel is applied to this system to enhance hydrogen storage densities. Various catalyst promoting materials like γ-Al_2O_3 nanoparticles, γ-Al_2O_3 particles, CNT, MMT clay, SiO_2, zeolite and zirconia sand are compared with respect to hydrogen generation rate (HGR). Maximum HGR obtained is 19.47 moles/L.sec for $NaBH_4$ (1.26 moles/L)/Al_2O_3 nanoparticles (0.12 moles/L)/H_2O and $CoCl_2.6H_2O$ (0.02 moles/L) as catalyst at room temperature and atmospheric pressure. Therefore, Al_2O_3 nanparticles (20 nm) is selected as catalyst promoter for $NaBH_4$/ H_2O based HG system.

- Various catalysts like $CoCl_2.6H_2O$, $CoSO_4.7H_2O$, $(CH_3COO)_2Co.4H_2O$, $Co(NO_3)_2.H_2O$, $CdSO_4$, $CuSO_4.5H_2O$ are evaluated in terms of HG and HGR for $NaBH_4$/γ-Al_2O_3 nanoparticles/H_2O based HG system. Maximum HGR is observed for $CoCl_2.6H_2O$ at $NaBH_4$ (1.26 moles/L)/Al_2O_3 nanoparticles (0.12 moles/L)/H_2O and catalyst (0.02 moles/L) at room temperature and atmospheric pressure.

- Comparative studies are also performed between γ-Al_2O_3 (100-200 μm) and γ-Al_2O_3 (20 nm) to observe the change in HG with particle size. Higher HG is observed with γ-Al_2O_3 having particle size of 20 nm than γ-Al_2O_3 having particle size of 100-200 μm.

- Kinetic studies are performed by change in concentration of $NaBH_4$, γ-Al_2O_3 nanoparticles, $CoCl_2$ and NaOH. Activation energy calculated for this system is 29 kJ/moles. Thus, addition of alumina nanoparticles decreases activation energy of $NaBH_4$/H_2O based HG system.

- Theoretical hydrogen density of 10.76 wt% and experimental hydrogen density of 10.69 wt% is observed at mass ratio of 0.09 : 0.7 for Al_2O_3 : $NaBH_4$ with efficiency of 99.34%. Therefore, addition of alumina nanoparticles decreases the difference in theoretical and experimental HG densities, additionally improving the efficiency of $NaBH_4$ based HG system to be used in practical applications.

- The residue obtained from the optimum system consisting of $NaBH_4$ (1.26 moles/L), Al_2O_3 (0.12 moles/L), NaOH (0.93 moles/L), and (0.02 moles/L) $CoCl_2$ aqueous solution is analyzed. It is characterized using EDS, XRD and FTIR techniques to predict the possible reactions that could occur between different reactants. EDS confirmed maximum percentage of boron in the residue. XRD and FTIR results concluded that adsorbance of Na^+ and Co^+ ions occurred on alumina surface that resulted in the formation of sodium and cobalt aluminates in the solution.

- As compared with conventional $NaBH_4/H_2O$ based hydrogen storage systems and on account of HGR, activation energy and efficiency, $NaBH_4/\gamma\text{-}Al_2O_3$ nanoparticles/H_2O based HG system with $CoCl_2$ as catalyst is more competent and therefore, it can be considered as a proficient system to be used in practical fuel cell applications for hydrogen generation and storage applications.

7.2. Future scope of work

1. Hydrogen generation from pure $NaBH_4$ could be also be used for future work.
2. Recycling of the residue material needs to be studied for further improving the efficiency of this system.
3. Modelling and simulation techniques may be applied to the present system to study change in HGR at higher concentrations of components.
4. Designing this system with appropriate fuel cell technology for its implementation.

REFERENCES

Ahmad A.K., Hwang H.T. and Varma A., NbF_5 additive improves hydrogen release from magnesium borohydride, International Journal of Hydrogen Energy, 37, 17671 (2012).

Aiello R, Sharp J.H and Matthews M.A., Production of hydrogen from chemical hydrides via hydrolysis with steam, International Journal of Hydrogen Energy, 24, 1123 (1999).

Akdim O., Demirci U.B., Muller D. and Miele P., Cobalt(II) salts, performing materials for generating hydrogen from sodium borohyride, International Journal of Hydrogen Energy, 34, 2631 (2009).

Akdim O., Demrici U.B. and Mieli P., Deactivation and reactivation of cobalt in hydrolysis of sodium borohydride, International Journal of Hydrogen Energy, 36, 13669 (2011).

Akdim O., Demirci U.B., and Miele P., Highly efficient acid-treated cobalt catalyst for hydrogen generation from $NaBH_4$ hydrolysis, International Journal of Hydrogen Energy, 34, 4780 (2009 b).

Akdim O., Demirci U.B. and Miele P., More reactive cobalt chloride in the hydrolysis of sodium borohydride, International Journal of Hydrogen Energy, 34, 9444 (2009 a).

Alfonso E.Y.M., Beaird A.M., Davis T.A. and Matthews M.A., Hydrogen generation from chemical hydrides, Industrial and Engineering Chemistry Research, 48, 3703 (2009).

Amendola S.C., Sharp-Goldman S.L., Janjua M.S., Kelly M.T., Petillo P.J. and Binder M., An ultrasafe hydrogen gas generator: aqueous, alkaline borohydride solutions and Ru Catalyst, Journal of Power Sources, 85, 186 (2000 a).

Amendola S.C., Sharp-Goldman S.L., Janjua M.S., Spencer N.C., Kelly M.T. and Petillo P.J., A safe, portable, hydrogen gas generator using aqueous borohydride solution and Ru Catalyst, International Journal of Hydrogen Energy, 25, 96 (2000 b).

Amendola S.C., Sharp-Goldman S.L., Saleem J.M., Kelly M.T., Petillo P.J. and Binder M. An ultrasafe hydrogen generator: aqueous, alkaline borohydride solutions and Ru catalyst, Journal of Power Sources, 85, 186 (2000).

Apelblat A. and Manzurola E., Solubilities of magnesium, calcium, barium, cobalt, nickel, copper, and zinc acetates in water from T = (278.15 to 348.15) K, Journal of Chemical Thermodynamics, 31, 1347 (1999).

Arkhipov S.M., Lithium borohydride, Methods Synth Chem Reagents Prep, 16, 27 (1967).

Arzac G.M., Rojas T.C. and Fernandez A., Boron compounds as stabilizers of a complex microstructure in a CoB based catalyst for $NaBH_4$ hydrolysis, Chem Cat Chem, 3, 1313 (2011).

Birch M. E, Toni A., Eberenz R., Chai M., Andrews R., Hatfield R. L., Properties that influence the specific surface areas of carbon nanotubes and nanofibers Annals of Occupational Hygiene, 57, 1148(2013).

Bogdanovic B. and Schwickardi M., Ti-doped alkali metal aluminum hydrides as potential novel reversible hydrogen storage materials, Journal of Alloys Compounds, 1, 253 (1997).

Bogdanovic B., Brand R.A., Marjanovic A., Schwickardi M. and Tolle J., Metal-doped sodium aluminium hydrides as potential new hydrogen storage materials, Journal of Alloys Compounds, 302, 36 (2000).

Boss P.A.M., Becker C.A., Anderson G.W. and Wiedemeier B.J., Feasibility studies of the $NaBH_4/H_2O$ hydrolysis to generate hydrogen gas to inflate lighter than air (LTA) vehicles, Industrial and Engineering Chemical Research, 54, 7714 (2015).

Brunelle, J.P., Preparation of catalysts by metallic complex adsorption on mineral oxides, Pure and Applied Chemistry, 50, 1211 (1978).

Buchner R, Hefter G, May P.M. and Sipos P., Dielectric relaxation of dilute aqueous NaOH, $NaB(OH)_4$, $NaAl(OH)_4$, Journal of Physical Chemistry B, 103, 11186 (1999).

Cakanyildirim C. and Guru M., Supported $CoCl_2$ catalyst for $NaBH_4$ dehydrogenation, Renewable Energy, 35, 839 (2010).

Chandra D., Intermetallics for hydrogen storage, in solid state hydrogen storage, Materials and Chemistry, Woodhead Publishing Limited, UK, Chapter 12, 317 (2008).

Chen P., Xiong Z., Luo J., Lin J. and Tan K.L., Interaction of hydrogen with metal nitrides and imides, Nature, 420, 302 (2002).

Dai H.B., Guang L.M., Kang X.D. and Wang P., Hydrogen generation from coupling reactions of sodium borohydride and aluminum powder with aqueous solution of cobalt chloride, Catalysis Today, 170 , 50 (2011 a)

Dai H.B., Liang Y., Wang P. and Cheng H.M., Amorphous cobalt boron nickel foam as an effective catalyst for hydrogen generation from alkaline sodium borohydride solution, Journal of Power Sources 177, 17 (2008).

Dai H.B., Ma G.B., Xia H.J. and Wang P., Combined usage of sodium borohydride and aluminum powder for high-performance hydrogen generation, Fuel Cells, 11, 424 (2011 b).

Davis R.E, Kibby C.L. and Swain C.G, An inverse hydrogen isotope effect in the hydrolysis of sodium borohydride, Journal of American Chemical Society, 82, 5950 (1960).

Davis R.E., Bromels E. and Kibby C.L., Borohydrides III hydrolysis of sodium borohydride in aqueous solution, Journal of American Chemical Society, 84, 885 (1962).

Davis R.E., Swain C.G., General acid catalysis of the hydrolysis of sodium borohydride, Journal of American Chemical Society, 82, 5949 (1960).

Demirci U.B. and Garin F., Kinetics of Ru-promoted sulphated zirconia catalyzed hydrogen generation by hydrolysis of sodium tetra hydroborate, Journal of Molecular Catalysis: Chemical, 279, 57 (2008).

Demirci U.B. and Miele P., Sodium borohydride versus ammonia borane, in hydrogen storage and direct fuel cell applications, Energy and Environmental Science, 2, 627 (2009).

Demirci U.B., Akdim O., Hannauer J., Chamoun R. and Miele P., Cobalt, a reactive metal releasing hydrogen from sodium borohydride: A short review and research perspective, Science China Chemistry, 53, 1870 (2010).

Demirci U.B. and Miele P., Cobalt-based catalysts for the hydrolysis of $NaBH_4$ and NH_3BH_3, Physical Chemistry Chemical Physics, 16, 6872 (2014).

Demirci U.B. and Miele P., Cobalt in $NaBH_4$ hydrolysis, Physical Chemistry Chemical Physics, 12, 14651 (2010).

Demirci U.B., Akdim O., Hannauer J., Chamoun R. and Miele P., Cobalt, a reactive metal releasing hydrogen from sodium borohydride: A short review and research perspective, Science China Chemistry, 53, 1870 (2010).

Dillon A.C and Heben M.J., Hydrogen storage using carbon absorbents: past present and future, Applied Physics A, 72, 133 (2001).

Ding X. L., Yuan X., Jia C. and Ma Z. F, Hydrogen generation from catalytic hydrolysis of sodium borohydride solution using Cobalt Copper Boride (Co-Cu-B) catalysts, International Journal of Hydrogen Energy 35, 11007 (2010).

Eberle U., Felderhoff M. and Schuth T., Chemical and physical solutions for hydrogen storage, Angewandte Chemie International Edition, 48, 6608 (2009).

Fakioglu E., Yurum Y. and Veziroglu T.N., A review of hydrogen storage systems based on boron and its compounds, International Journal of Hydrogen Energy, 29, 1371 (2004).

Fan M.Q., Wang Y., Tang R., Chen D., Liu W., Tian G.L., Lv C.J. and Shu K.Y., Hydrogen generation from Al/$NaBH_4$ hydrolysis promoted by Co nanoparticles and $NaAlO_2$ solution, Renewable Energy, 60, 637 (2013).

Fernandes R., Patel N., Miotello A. and Filippi M., Studies on catalytic behavior of Co–Ni–B in hydrogen production by hydrolysis of $NaBH_4$, Journal of Molecular Catalysis A: Chemical 298, 1 (2009).

Fogler H.S., Elements of Chemical Reaction Engineering, 3rd edition. Englewood Cliffs, NJ: Prentice Hall, 2000.

George N.G., Kenneth J.K., Christopher M.S. and George C.H., Borohydride reduction of cobalt ions in water, chemistry leading to nano-scale metal, boride or borate particles, Langmuir, 9, 162 (1993).

Glavee G.N., Klabunde K.J., Sorensen C.M. and Hadjapanayis G.C., Borohydride reductions of metal ions, A new understanding of the chemistry leading to nano-scale particles of metals, borides, and metal borates, Langmuir, 8, 773 (1993).

Graetz J., Metastable metal hydrides for hydrogen storage, ISRN Materials Science, 2012, 8 (2012).

Grenman, H., Salmi, T., Murzin, D.Y. and Mensah J.A., The dissolution kinetics of gibbsite in sodium hydroxide at ambient pressure, Industrial and Engineering Chemistry Research, 49, 2600 (2010).

Guella, G., Zanchetta C., Patton B. and Miotello A., New insights on the mechanism of palladium-catalyzed hydrolysis of sodium borohydride from ^{11}B NMR measurements, The Journal of Physical Chemistry B, 110, 17024 (2006).

Gutbier H. and Hohne K., Process for the generation of hydrogen, U.S. Patent 3932600, 1976.

Hannauer J., Demirci U.B., Geantet C., Herrmann J.M. and Miele P., Enhanced hydrogen release by catalyzed hydrolysis of sodium borohydride–ammonia borane mixtures: a solution-state (11)B NMR study, Physical Chemistry Chemical Physics,13, 3809 (2011).

Harder S., Hydrogen storage in magnesium hydride, the molecular approach, Angewandte Chemie International Edition, 50, 4156 (2011).

Holbrook K.A. and Twist P.J., Hydrolysis of the borohydride ion catalysed by metal-boron alloys, Journal of Chemical Society (A), 4, 890 (1971).

Hordeski M.F., Alternative fuel sources in hydrogen and fuel cells: advances in transportation and power, Fairmont Press, United States, Chapter 3, 75 (2008).

Hou Z.F., First-principles investigation of $Mg(AlH_4)_2$ complex hydride, Journal of Power Sources, 159, 111 (2006).

Hu, Y.H., Ruckenstein, E., H_2 storage in Li_3N, temperature programmed hydrogenation and dehydrogenation, Industrial and Engineering Chemistry Research, 42, 5135 (2003).

Ingersoll J.C., Mani N., Thenmozhihal J.C. and Muthaiah A., Catalytic hydrolysis of sodium borohydride by a novel nickel-cobalt-boride catalyst, Journal of Power Sources, 173, 450 (2007).

Jang J.W., Shim J.H., Cho Y.W. and Lee B.J., Thermodynamic calculation of LiH_2, Li_3AlH_6, $2LiAlH_4$ reactions, Journal of Alloys Compound, 420, 286 (2006).

Jensen C.M and Takara S., Catalytically enhanced systems for hydrogen storage, Proceedings of Hydrogen Program Review, 1 (2000).

Jensen C.M. and Gross K.J., Development of catalytically enhanced sodium aluminum hydride as a hydrogen storage material, Applied Physics A, 72, 213 (2001).

Jianbo L., Yong F., Hua P., Meiqiang F., Liangliang W. and Jun Y., Controllable hydrogen generation performance from $Al/NaBH_4$ composite activated by La metal and $CoCl_2$ salt in pure water, Journal of Rare Earths, 30, 548 (2012).

Kanturk A, Sari M. and Poskin S., Synthesis, crystal structure and dehydration kinetics of $NaB(OH)_4.2H_2O$, Korean Journal of Chemical Engineering, 25, 1331 (2008).

Kim J.H., Jin S.A., Shim J.H. and Cho Y.W., Thermal decomposition behavior of calcium borohydride $Ca(BH_4)_2$, Journal of Alloys Compounds, 461, 20 (2008).

Klanchar M. and Lloyd C.L., Compact hydrogen generating systems based on chemical sources for low and high power applications, Proceedings of the 39th Power Sources Conference, 188 (2000).

Klanchar M., Hughes T.G. and Gruber P., Attaining DOE hydrogen storage goals with chemical hydrides, 15th Hydrogen Annual Conference, National Hydrogen Association, Washington D. C, 2004.

Kojima Y, Kawai Y, Kimbara M, Nakanishi H and Matsumoto S. Hydrogen generation by hydrolysis reaction of lithium borohydride, International Journal of Hydrogen Energy, 29, 1213 (2007).

Komova O.V., Simagina V.I., Netskina O.V., Kellerman D.G., Ishchenko A.V. and Rudina N.A., $LiCoO_2$-based catalysts for generation of hydrogen gas from sodium borohydride solutions, Catalysis Today, 138, 3 (2008).

Kosmulski M., pH-dependent surface charging and points of zero charge. IV. Update and new approach, Journal of Colloid and Interface Science 337, 439(2009).

Levy A., Brown J.B. and Lyons C.J., Catalyzed hydrolysis of sodium borohydride, Industrial & Engineering Chemistry Research, 52, 211 (1960).

Ley M.B., Jepsen L.H., Lee Y.S., Cho Y.W., Colbe J.B.V., Dornheim M., Rokni M., Jensen J.O., Sloth, M., Filinchuk, Y., Jorgensen, J.E., Besenbacher F. and Jensen T.R., Complex hydrides for hydrogen storage-new perspectives, Materials Today, 17, 122 (2014).

Li H.W., Yan Y., Orimo S., Zuttel A. and Jensen M.C., Review: Recent progress in metal borohydrides for hydrogen storage, Energies, 4, 185 (2011).

Lide D.R., Handbook of Chemistry and Physics, 84th ed. CRC Press, (2004).

Liu B.H. and Li Z.P., A review: hydrogen generation from borohydride hydrolysis reaction, Journal of Power Sources 187, 527 (2009).

Liu B.H., Li Z.P. and Suda S., Nickel and cobalt based catalysts for hydrogen generation by hydrolysis of borohydride, Journal of Alloys and Compounds, 415, 288 (2006).

Mao J., Guo Z., Poh C.K., Ranjbar A., Guo Y., Yu X. and Liu H., Study on the dehydrogenation kinetics and thermodynamics of $Ca(BH_4)_2$, Journal of Alloys Compounds., 500, 200 (2010).

Manna J., Roy B., Sharma P., Efficient hydrogen generation from sodium borohydride hydrolysis using silica sulfuric acid catalyst, Journal of Power Sources, 275, 727(2015).

Marrero A.E.Y., Beaird A.M., Thomas A.D. and Matthews M.A., Hydrogen generation from chemical hydrides, Industrial & Engineering Chemistry Research, 48, 3703 (2009).

McNaught D. and Wilkinson A., IUPAC Compendium of Chemical Terminology (the "Gold Book") Blackwell Scientific Publications, Second Edition, 1997.

Metin O. and Ozkar S., Hydrogen generation from the hydrolysis of ammonia-borane and sodium borohydride using water-soluble polymer-stabilized cobalt(0) nanoclusters catalyst, Energy and Fuels, 23, 3517 (2009).

Mitrofanova R.P., Mokahilov Y.I. and Maltseva N.N., Stepwise gas liberation in the thermal decomposition of $LiBH_4$, Russian Journal of Inorganic Chemistry, 34, 2207 (1989).

Miwa K., Aoki M., Noritake T., Ohba N., Nakamori Y., Towata S., Zuttel A., Orimo S., Thermodynamical stability of calcium borohydride, $Ca(BH_4)_2$, Physical Review B, 74, 122 (2006).

Moussa G., Moury R., Demirci U.B., Sener T. and Miele P., Boron-based hydrides for chemical hydrogen storage, International Journal of Energy Research, 37, 825 (2013).

Muir S.S and Yao X., Progress in sodium borohydride as a hydrogen storage material: Development of hydrolysis catalysts and reaction system, International Journal of Hydrogen Energy, 36, 5983 (2011).

Murooka S., Tomoda K., Hoshi N., Haruna J., Cao M., Yoshizaki A. and Hirata K., Consideration on fundamental characteristic of hydrogen generator system fueled by $NaBH_4$ for fuel cell hybrid electric vehicle, IEEE International Electric Vehicle Conference, 2012.

Ozkar S and Zahmakiran M., Hydrogen generation from hydrolysis of sodium borohydride using Ru(0) nano-clusters as catalyst, Journal of Alloys and Compounds, 404, 728 (2005).

Parida K. M., Amaresh C., Das P.J. and Sahu N., Synthesis and characterization of nano-sized porous gamma-alumina by control precipitation method, Materials Chemistry and Physics, 113, 244(2009).

Patel N., Fernandes R. and Miotello A., Hydrogen generation by hydrolysis of $NaBH_4$ with efficient Co-P-B catalyst: a kinetic study, Journal of Power Sources, 188, 411 (2009).

Patel N., Patton B., Zanchetta C., Fernandes R., Guella G. and Miotello A., Pd/C powder and thin film catalyst for the hydrogen production by hydrolysis of sodium borohydride, International Journal of Hydrogen Energy, 33, 287 (2008).

Pecsok R., Polarographic studies on the oxidation and hydrolysis of sodium borohydride, Journal of American Chemical Society, 75, 2862 (1953).

Pitcher G.K. and Kavarnos, G.J., A test assembly for hydrogen production by the hydrolysis of solid lithium hydride, Journal of the International Association for Hydrogen Energy, 575 (1997).

Rajoria R. K., Prasad B., Mishra I. M. and Wasewar K. L., Adsorption of benzaldehyde on granular activated carbon: kinetics, equilibrium and thermodynamics, Chemical and Biochemical Engineering**,** 22, 219(2007).

Retnamma R., Novais A.Q. and Rangel C. M., Kinetics of hydrolysis of sodium borohydride for hydrogen production in fuel cell application: A review, International Journal of Hydrogen energy, 36, 9772 (2011).

Ritter J.A., Ebner A.D., Wang J. and Zidan R., Implementing a hydrogen economy, Materials Today, 6, 18 (2003).

Ronnebro, Development of group II borohydrides as hydrogen storage materials," Current Opinion in Solid State Material Science, 15, 44 (2011).

Sakintuna B., Darkrim F.L. and Hirscher H., Metal hydride materials for solid hydrogen storage: a review, International Journal of Hydrogen Energy, 32, 1121 (2007).

Schlesinger H.I., Brown H.C., Finholt A.E., Gilbreath J.R., Hoekstra H.R. and Hyde E.K., Sodium borohydride, its hydrolysis and use as a reducing agent and in the generation of, hydrogen, Journal of American Chemical Society, 75, 215 (1953).

Shang Y. and Chen R., Semi empirical hydrogen generation model using concentrated sodium borohydride solution, Energy and Fuels, 20, 2149 (2006).

Shashikala K., 15 Hydrogen storage materials, Functional Materials, 607 (2012).

Shu L., Liang W. L., Jun Y., Qiang S. W. and Qiang F. M., 2012, Hydrogen generation from coupling reactions of Al Li /$NaBH_4$ mixture in water activated by Ni powder, Transactions of Nonferrous Metals Society of China., 22, 1140 (2012).

Smith E., Hydrogen generation by means of the aluminium/water reaction, Journal of Hydronautics, 6, 106 (1972).

Snow G.D., Nano particles for hydrogen storage, transportation, and distribution. Patent No.: US 6,589,312 BI 2003.

Soler L., Candela A.M., Macanas J., Munoz M. and Casado J., In situ generation of hydrogen from water by aluminium corrosion in solutions of sodium aluminate, Journal of Power Sources, 192, 21 (2009).

Soler L., Macanas J., Munoz M. and Casado J., Synergistic hydrogen generation from aluminium, aluminium alloys and sodium borohydride in aqueous solutions, International Journal of Hydrogen Energy, 32, 4702 (2007).

Soler, L., Candela, A.M., Macanas, J., Munoz, M. and Casado, J., In situ generation of hydrogen from water by aluminium corrosion in solutions of sodium aluminate, Journal of Power Sources, 192, 21 (2009).

Sposito G., The Environmental Chemistry of Aluminum, Lewis publishers, (1996).

Thomas L., Gert, R; Douglas G., Luigi C., Francois R., Peter G. and Christoph K., Requirements on measurements for the implementation of the EC definition of the term nanomaterial, JRC reference reports, 2012.

Vajo J.J., Skeith S.L. and Mertens F., Reversible storage of hydrogen in destabilized $LiBH_4$, Journal of Physical Chemistry B, 9, 3719 (2005).

Vyas R. K., Shashi, Kuamr S., Determination of micro-pore volume and surface area of zeolite molecular sieves surface area of zeolite molecules sieves by D-R and D- A equation. A comparative study, Indian Journal of Chemical Technology, 11, 704(2004).

Walter J.C., Zurawski A, Montgomery D, Thornburg M and Revankar S. Sodium borohydride hydrolysis kinetics comparison for nickel, cobalt and ruthenium boride catalysts, Journal of Power Sources, 179, 335 (2008).

Wang L.L., Graham D.D., Robertson I.M. and Johnson D.D., On the reversibility of hydrogen-storage reactions in $Ca(BH_4)_2$: Characterization via experiment and theory, Journal of Physical Chemistry C, 113, 96 (2009).

Wang L., Li Z., Zhang P., Wang G. and Xie G., Hydrogen generation from alkaline NaBH4 solution using Co-Ni-Mo-P/g-Al_2O_3 catalysts , International Journal of Hydrogen Energy, 41, 146 (2016).

Wang Y., Zhou L.T., Yuan H., Shen W.H., Tang R., Fan M.Q. and Shu K.Y., Hydrogen generation from the reaction of Al-7.5wt% Li-25wt% Co/$NaBH_4$ powder and pure water, International Journal of Electrochemical Science, 8, 9764 (2013).

Xu D., Dai P., Guo Q. and Yue X., Improved hydrogen generation from alkaline $NaBH_4$ solution using cobalt catalyst supported on modified activated carbon, International Journal of Hydrogen Energy, 33, 7371 (2008).

Xuelian D.U., Yanqin W., Xinghua S. and Jiangong Li., Influences of pH value on the microstructure and phase transformation of aluminum hydroxide, Powder Technology, 192, 40 (2009).

Ye W., Zhang H., Xua D., Maa L. and Yi B., Hydrogen generation utilizing alkaline sodium borohydride solution and supported cobalt catalyst, Journal of Power Sources, 164, 544 (2007).

Ying W., Hydrogen Storage via Sodium Borohydride: Current Status, Barriers and R&D Roadmap, Presentation presented at GECP-Stanford University, April 14−15, 2003.

Zahmakiran M. and Ozkar S., Zeolite-confined ruthenium(0) nano-clusters catalyst: record catalytic activity, reusability, and lifetime in hydrogen generation from hydrolysis of sodium borohydride, Langmuir, 27, 266 (2009).

Zahmakiran M. and Ozkar M., Water dispersible acetate stabilized ruthenium(0) nano-clusters as catalyst for hydrogen generation from the hydrolysis of sodium borohydride, Journal of Molecular Catalysis A, 258, 95 (2006).

Zaluski L., Zaluska A. and Strom J. O., Hydrogenation properties of complex alkali metal hydrides fabricated by mechano-chemical synthesis, Journal of Alloys Compounds, 290, 71 (1999).

Zhang Q, Wu Y, Sun X. and Ortega J., Kinetics of catalytic hydrolysis of stabilized sodium borohydride solutions, Industrial and Engineering Chemistry Research, 46, 1120 (2007).

Zhuang D.W., Kang Q., Muir S.S., Yao X., Dai H.B., Ma G.L. and Wang P., 2013, Evaluation of cobalt-molybdenum-boron catalyst for hydrogen generation of alkaline sodium borohydride solution-aluminum powder system, Journal of Power Sources, 224, 304 (2013).

Zuttel A., Wenger P., Rentsch S. and Sudan P., $LiBH_4$ A new hydrogen storage material, Journal of Power Sources, 118, 1 (2003).

PUBLICATIONS

Peer-Reviewed (SCI) Journals

- **Arshdeep Kaur**, D. Gangacharyulu, P. K.Bajpai, "Kinetic studies on $NaBH_4/H_2O$ hydrogen storage system with $CoCl_2$ as catalyst," Bulgarian Chemical Communications, Volume 48, Number 2 (pp. 295 – 301) 2016.

- **Arshdeep Kaur**, D. Gangacharyulu, P.K. Bajpai, "Catalytic hydrogen generation from $NaBH_4/H_2O$ system: effects of catalyst and promoters," Brazilian Journal of Chemical Engineering, Volume 34, Number 4, October – December 2017.

Communicated

- **Arshdeep Kaur**, D. Gangacharyulu, P.K. Bajpai, "Kinetic studies on hydrogen generation from $NaBH_4/Al_2O_3$ nanoparticles/H_2O system with $CoCl_2$ as catalyst," International Journal of Hydrogen Energy. **(Communicated)**

Conference Publications (International)

- **Arshdeep Kaur**, D. Gangacharyulu, P.K. Bajpai, Hydrogen generation from $NaBH_4/Al_2O_3$ nanoparticles/H_2O with $CoCl_2$ as catalyst, IEEE 10th Conference on Industrial Electronics and Applications (ICIEA) **(Auckland, New Zealand)**, 761, 2015.

- **Arshdeep Kaur**, D. Gangacharyulu, P.K. Bajpai, Kinetics studies of hydrolysis reaction of cobalt chloride catalyst on hydrogen generation from sodium borohydride, 4^{th} International Conference on Advances in Energy Research (**IIT Bombay)**, 2013.